Functional analysis of putative adenosine recycling enzymes in *Arabidopsis thaliana*

by

Katja Engel

A thesis
presented to the University of Waterloo
in fulfillment of the
thesis requirement for the degree of
Master of Science
in
Biology

Waterloo, Ontario, Canada, 2009

AUTHOR'S DECLARATION

I hereby declare that I am the sole author of this thesis. This is a true copy of the thesis, including any required final revisions, as accepted by my examiners.

I understand that my thesis may be made electronically available to the public.

ABSTRACT

Adenosine (Ado) salvage is essential in plant development. The lack of Ado kinase activity (ADK) in *Arabidopsis thaliana adk1 adk2* double mutants results in embryonic lethality; reduction of ADK expression causes a pleiotropic phenotype due to the accumulation of Ado inhibiting transmethylation activities. The phenotype of ADK mutants shows that this enzyme plays a critical role in Ado salvage but the functional significance of the other putative Ado recycling enzymes Ado deaminase (ADA) and Ado nucleosidase (ADN) in *Arabidopsis thaliana* have yet to be elucidated.

ADA catalyzes the irreversible deamination of Ado to inosine. The locus At4g04880 (*AtADA*) of *A. thaliana* is annotated as encoding a putative ADA, based on its amino acid sequence similarity and the presence of important, conserved catalytic residues. However, indirect and direct spectrophotometric activity assays of the recombinant enzyme demonstrated that the gene product of this locus does not possess ADA activity; complementation experiments to test for the functionality of the *AtADA* product in *A. thaliana* and *E. coli* confirmed its lack of ADA activity. Instead, phylogenetic analysis revealed that AtADA belongs to the group of ADA-like (ADAL) proteins, a group closely related to ADAs that to date have not been shown to have ADA activity. AtADA is no exception as it also lacks ADA activity based on the *in vivo* and *in vitro* experiments outlined in this thesis. Thus, the locus At4g04880 should be re-annotated as ADAL. The question of the function of AtADAL cannot be answered as of yet; in general, the knockout of ADA gene product demonstrated that At4g04880 is not essential for Arabidopsis growth. Since no further ADA-related genes exist in the genome of Arabidopsis it is concluded that ADA activity is not present in this plant.

ADN catalyzes the conversion of purine and pyrimidine ribosides to their corresponding bases; although it prefers Ado as a substrate it also acts on cytokinins. The activity of this enzyme has been described in several plant species

but no corresponding genes have been identified to date. The genome of Arabidopsis was screened for ADN genes using an inosine-uridine nucleoside hydrolase sequence from the protozoa *Crithidia fasciculata*. Two genes, annotated as *ADN1* and *ADN2* were identified and their gene products were studied using a spectrophotometric assay. The substrate spectrum of ADN2 includes both purine and pyrimidine nucleosides but it prefers to utilize uridine. Thus, ADN2 is proposed to be involved in the purine and pyrimidine salvage in Arabidopsis but predominantly in uridine recycling. Recombinant ADN1 did not show activity on any of the tested substrates. Even though the *in vivo* role of both ADNs is still uncertain, due to their lack or low activity on Ado there may yet be the *ADN* gene in the Arabidopsis genome which likely acts on both adenosine and cytokinin ribosides.

ACKNOWLEDGEMENTS

First of all, I would like to express my deepest gratitude to my supervisor Dr. Barbara Moffatt for her guidance, encouragement and advice throughout this study. I have learned a lot. Thank you.

Thanks to my committee members Dr. Simon Chuong (University of Waterloo, Waterloo, Ontario, Canada) and Dr. Matthew Smith (Wilfrid Laurier University, Waterloo, Ontario, Canada) for their support during my project.

I am thankful to my colleagues and members of Barbara Moffatts lab; especially to Tony Facciuolo, Ishari Waduwara, Yong Li, Sanghyun Lee and Sarah Schoor. It was my pleasure to work with you.

Thanks to my German collaborators Dr. Klaus von Schwartzenberg and Hanna Turcinov (University of Hamburg, Germany); I very much enjoyed working with you on this project.

Thanks to Makoto Yanagisawa, Terry (Shiu Cheung) Lung and Johny Bozdarov; it was fun to TA and work with you.

I am deeply grateful to my friends who supported me during my time of study especially to Barbara Güttler, Daniela Kiekebusch, Saskia Bolle and Brian Garcia.

Finally, I would like to take this opportunity to express my profound gratitude to my parents and grandparents for their confidence in me and their continuous and unconditional support during my study here in Canada, even though the distance was not easy for them…

TABLE OF CONTENTS

LIST OF FIGURES

LIST OF TABLES

LIST OF ABBREVIATIONS

ADA	adenosine deaminase
ADAL	adenosine deaminase-like
Ade	adenine
ADE	adenine deaminase
ADGF	adenosine deaminase-related growth factor
ADK	adenosine kinase
ADN	adenosine nucleosidase
Ado	adenosine
amiRNA	artificial microRNA
AMP	adenosine monophosphate
AMPD	adenosine monophosphate deaminase
CK	cytokinin
CV	column volume
DAP	2,6-diaminopurine
DEPC	diethylpyrocarbonate
dH_2O	deionized water
dNTP	deoxynucleotide triphosphates
DTNB	5, 5-dithiobis(2-nitrobenzoic acid)
EGFP	enhanced green fluorescent protein
GFP	green fluorescent protein
Gua	guanosine
GUS	β-glucuronidase
Hcy	homocysteine
IMP	inosine monophosphate
Ino	inosine

IU-NH	inosine-uridine nucleoside hydrolase
LB	Luria-Bertani
MBP	maltose binding protein
MS	Murashige and Skoog
MTase	methyl transferase
NH	nucleoside hydrolase
OD_{600}	optical density at 600 nm wavelength
O/N	over night
ORF	open reading frame
PCR	polymerase chain reaction
RNA	Ribonucleic acid
RT	room temperature
RT-PCR	reverse transcription PCR
PVDF	polyvinylidene difluoride
sADK	sense silencing of ADK
SAH	*S*-adenosyl-L-homocysteine
SAHH	*S*-adenosyl-L-homocysteine hydrolase
SAM	*S*-adenosyl-L-methionine
SCID	severe combined immunodeficiency
TNB	2-nitro-5-thiobenzoic acid
UMP	Uridine 5'-monophosphate
Uri	uridine
UTR	untranslated region

Chapter 1

INTRODUCTION

1.1 ARABIDOPSIS THALIANA

Arabidopsis thaliana is a small flowering plant that is widely used to study the cellular and molecular biology of plants. Arabidopsis is a member of the mustard family, Brassicaceae, which includes species such as cabbage and radish, that is native of the northern hemisphere (Alberts *et al.,* 2005). A mature Arabidopsis plant has a basal rosette of 6-12 leaves and a primary shoot of up to 30 cm in height. Arabidopsis offers important advantages for research particularly for genetic and molecular analyses because of its small genome (5 chromosomes, 125 Mb) which was sequenced completely by the Arabidopsis Genome Initiative (2000).

Out of ca. 26,000 gene products identified, approximately 30 % could not be assigned to a specific function (Arabidopsis Genome Initiative, 2000). Varieties of approaches are used to collect information about the function of genes. Insertional mutagenesis has been extensively used to obtain knockout mutants that help to assign biological function to unknown gene products (Radhamony *et al.,* 2005). Through investigations of the phenotype linked with the mutation the function of the gene can be deduced.

Further advantages of Arabidopsis are its efficient transformation via *Agrobacterium tumefaciens* infection, its inexpensive cultivation in controlled environments and its short life cycle of about 6 weeks, from germination to maturity.

The research described in this thesis uses Arabidopsis to investigate the functional significance of the putative adenosine recycling enzymes, adenosine deaminase and adenosine nucleosidase. Three metabolic pathways in Arabidopsis generate adenosine as a product: 1) *S*-adenosyl-L-methionine (SAM) dependent methylation cycle, 2) the salvage pathway of purine nucleotides and 3) cytokinin (CK) degradation. These metabolic pathways and the important enzymes involved in each, will be introduced in the following sections.

1.2 METHYL CYCLE

Many biochemical reactions in plants involve the transfer of methyl groups; *S*-adenosyl-L-methionine (SAM) is the principal methyl donor for these reactions (Cantoni, 1975). The transfer of methyl groups from SAM plays a role in a range of cellular activities including DNA methylation, gene regulation, protein modification, as well as the synthesis of hundreds of metabolites including biotin, nicotinamine and ethylene (Moffatt and Weretilnyk, 2001).

When the methyl group of SAM is transferred by a methyltransferase (MTase) to an acceptor, a molecule of *S*-adenosyl-L-homocysteine (SAH) is produced as a by-product (Figure 1). As SAH is a strong inhibitor of SAM-dependent MTases, it has to be removed to maintain methyl recycling and MTase activities (Moffatt and Weretilnyk, 2001). To do so, SAH hydrolase (SAHH, EC 3.3.1.1; Enzyme 4 in Figure 1) converts SAH into adenosine (Ado) and homocysteine (Hcy); *in vivo* this reversible reaction is directed towards SAH hydrolysis by removal of the products Ado and Hcy. Ado deaminase (ADA, EC 3.5.4.4; Enzyme 2 in Figure 1), Ado kinase (ADK, EC 2.7.1.20; Enzyme 1 in Figure 1) and Ado nucleosidase (ADN, EC 3.2.2.7; Enzyme 3 in Figure 1) catalyze different reactions that metabolize Ado. In plants Ado salvage is primarily mediated by ADK (Dancer *et al.,* 1997; Moffatt *et al.,* 2002); the roles of ADA and ADN have not yet been defined, nor have their contributions to plant development been elucidated. The research in this thesis was designed to address these issues.

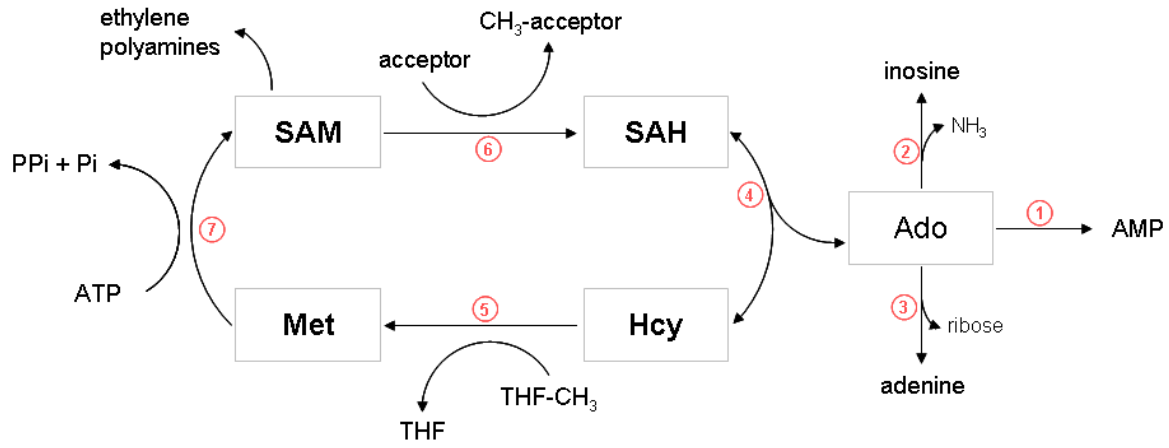

Figure 1 – Activated methyl cycle and adenosine salvage. *S*-adenosyl-L-methionine (SAM) is the donor of methyl groups in the transmethylation cycle shown. Methyltransferases (6) generate *S*-adenosylhomocysteine (SAH) during transmethylation. SAH hydrolase (4) converts SAH into adenosine (Ado) and homocysteine (Hcy). The forward reaction of this reversible process is supported by removal of Ado and Hcy. Ado is removed from the cycle by the action of ADK (1), ADA (2) or ADN (3); Hcy is metabolized by methionine synthase (5). SAM is regenerated by SAM synthetase (7).

1.3 Purine and Pyrimidine Salvage

Purine and pyrimidine nucleotides are important compounds in metabolic pathways and essential for plant development (Zrenner *et al.,* 2006). Ado recycling enzymes described in the previous section play an important role in the salvage of purines. The *de novo* biosynthesis of purine and pyrimidine nucleotides involves multiple enzymatic steps, several of which require the hydrolysis of ATP or GTP. All organisms, including plants have developed salvage pathways to recycle bases and nucleosides at low metabolic cost (Zrenner et al., 2006).

Relevant Ado metabolizing enzymes are ADA (enzyme 5 in Figure 2), ADK (enzyme 4 in Figure 2) and ADN (enzyme 1 in Figure 2). Ado can be recycled to adenine (Ade) nucleotides but also can be converted to inosine (Ino) nucleotides (Figure 2). In animals the recycling of Ado to Ino is primarily catalyzed by Ado

deaminase (ADA) but this enzyme activity is not thought to be present in plants (Moffatt and Ashihara, 2002). No ADA enzyme activity could be found in plant extracts i.e. *Catharanthus roseus* (Yabuki and Ashihara, 1991) or *Solanum tuberosum* tubers (Katahira and Ashihara, 2006). The conversion of Ado to Ino can be alternatively catalyzed by AMP deaminase (enzyme 6 in Figure 2), converting Ado monophosphate (AMP) to Ino monophosphate (IMP). Subsequently, IMP can be converted into Ino or xanthine; the latter enters the purine degradation pathway.

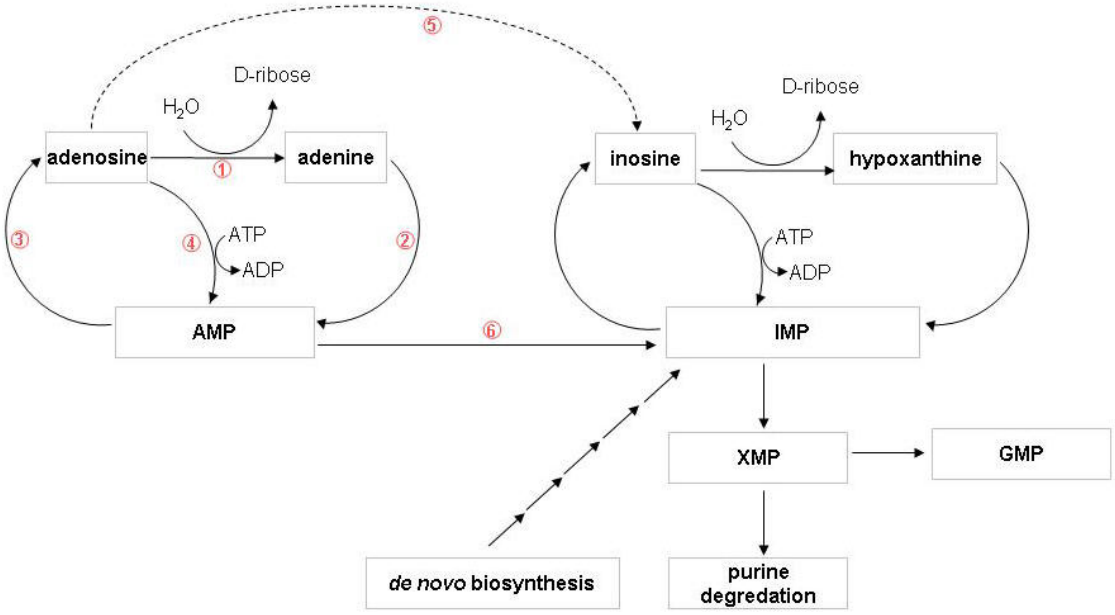

Figure 2 – Purine bases, nucleosides and nucleotides can be recycled via the purine salvage pathway. Animals primarily recycle adenosine to inosine by adenosine deaminase (5); plants primarily recycle adenosine by adenosine kinase (4). Adenosine monophosphate (AMP) deaminase (6) converts AMP to IMP that is further converted to xanthine monophosphate (XMP). XMP enters the purine degradation pathway. Other enzymes seen in the cycle are: adenosine nucleosidase (1), adenine phosphoribosyltransferase (2) and 5'-nucleotidase (3).

ADN contributes to purine salvage in many organisms, it catalyses the irreversible hydrolysis of Ado to Ade and ribose (Figure 2). This enzyme activity has

been demonstrated in crude extracts or partially purified preparations of several plants, including barley (Guranowski and Schneider, 1977) and wheat (Chen and Kristopeit, 1981). However, a gene coding for ADN has not been identified yet.

In Figure 3 is shown the pyrimidine salvage pathway with a focus on uridine (Uri). Uridine 5'-monophosphate (UMP) is the product of *de novo* pyrimidine biosynthesis. UMP can be recycled to the base uracil and the nucleoside uridine (Figure 3). The first enzyme that was characterized in the Arabidopsis pyrimidine salvage pathway was the bi-functional uridine kinase/ uracil phosphoribosyltransferase (Islam *et al.,* 2007). Uridine kinase activity was found in

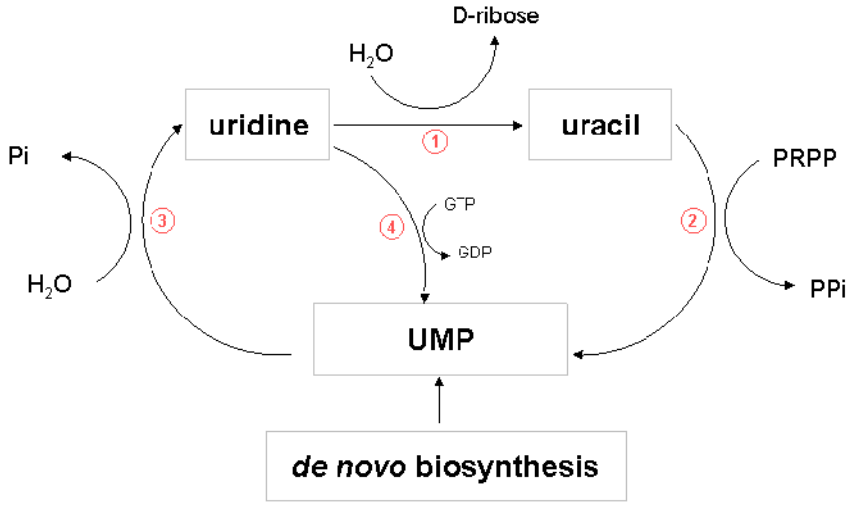

Figure 3 – Uridine salvage pathway. Uridine 5'-monophosphate (UMP) is the end product of the *de novo* pyrimidine biosynthesis; it can be recycled via uracil and uridine involving following enzymes: Uridine-nucleosidase (1), uridine kinase/ uracil phosphoribosyltransferase (2), 5'-nucleotidase (3), uridine-monophosphokinase (4).

the N-terminal region of the gene and uracil phosphoribosyltransferase activity was found in the C-terminal region. The pyrimidine specific 5'-nucleotidase of the Arabidopsis salvage pathway has not yet been cloned or characterized. A gene coding for Uri nucleosidase was identified and the protein product was recently characterized by Jung *et al.* (2009).

Details of the putative adenosine recycling enzymes ADA and ADN and subjects relevant to this research will be described in the following sections.

1.4 Adenosine Kinase in *Arabidopsis thaliana*

ADK catalyzes the phosphorylation of Ado to AMP (Figure 1, enzyme 1) and has an important role in maintaining the methylation cycle in plants (Moffatt and Weretilnyk, 2001). Mutant plants with reduced ADK enzyme activity show a severe phenotype compared to wild type; the lack of Ado recycling and the accumulation of Ado leads to methylation defects. Hypomethylation of pectin was reported in ADK silencing mutants (Moffatt *et al.,* 2002) as well as up to 25 % less methylated cytosine in genomic DNA (Engel, Diploma thesis). The two ADK isoforms identified in *A. thaliana*, ADK 1 (locus At3g09820) and ADK 2 (locus At5g63400), are very similar, sharing 92 % amino acid identity (89 % nucleotide identity) (Moffatt *et al.,* 2000). Both genes encode functional enzymes that are capable of utilizing both Ado and CK ribosides as substrates (Moffatt *et al.,* 2000).

In order to investigate the role of ADK in *A. thaliana*, plant lines with reduced ADK activity (sADK lines) were created. Due to sense silencing, the ADK activity in these sADK lines range from seven to 70 % of that found in the wild type; lower levels of residual ADK activity correlate with a more severe phenotype (Moffatt *et al.,* 2002). The ADK-deficient lines are characterized by wrinkled leaves, clustered inflorescences and reduced primary shoot height; a complete loss of the primary shoot is observed in cases of extremely reduced ADK activity. Plants with more than 50 % residual ADK activity show normal wild-type morphology (Moffatt *et al.,* 2002). ADK transcript and protein is abundant in all major organs, but the abundance decreases as the plant matures i.e. more ADK transcript and protein can be found in younger leaves than in older; ADK also decreases as siliques mature (Pereira *et al.,* 2007). ADK protein levels in different organs are consistent with other enzymes involved in the methylation cycle such as SAHH, SAM synthetase and a SAM-dependent methyltransferase.

1.5 Adenosine Deaminase in *Arabidopsis thaliana*

As mentioned earlier, ADA catalyzes the irreversible deamination of Ado to Ino (see Figure 1, Enzyme 2) as well as 2′-deoxyadenosine to 2′-deoxyinosine. ADA activity has been documented in extracts of bacteria, invertebrates and vertebrates (Cristalli *et al.,* 2001) but this enzyme activity is not proposed to be present in plants. In mammalian cells, the loss of ADA enzyme activity causes severe combined immunodeficiency (SCID) due to the accumulation of toxic metabolites in the purine salvage pathway (Fischer, 2000). ADA has been shown to require no cofactor but a zinc ion is included in the active site pocket (Frick *et al.,* 1987). The crystal structure of mouse ADA bound to 1-deazaadenosine confirmed the presence of a zinc-activated water molecule in the active site (Wilson and Quiocho, 1993).

Locus At4g04880 of *A. thaliana* is annotated as a putative Ado/AMP deaminase (electronic annotation, Genbank) and its protein product was demonstrated to have ADA activity by an *in vitro* SAHH activity assay which is dependent on ADA activity to draw the reaction in the hydrolysis direction (Sherri Fry, 499 report). Unfortunately, this experimental result did not prove to be repeatable. As an *in vivo* test for the functionality of the ADA gene product, the cDNA corresponding to the gene At4g04880 was isolated from *A. thaliana* and overexpressed in an ADK-silenced plant line with a severe phenotype (16 % residual ADK activity). The resulting transgenic plants (sADK 9-1 35S::ADA) appeared phenotypically normal indicating a complementation of ADK activity by the transgene, suggesting that the locus At4g04880 encodes a functional ADA activity. One part of my thesis research sought to verify this conclusion and to elucidate the identity of At4g04880 as ADA.

1.6 Adenosine Deaminase in *E. coli*

Adenosine deaminase is present in *E. coli* cells and catalyzes the conversion of Ado to Ino (enzyme 5 in Figure 2). ADA activity is not essential for the growth of *E. coli* and the deletion of ADA gene is not lethal. Even though ADK activity (enzyme

4 in Figure 2) has not been found in *E. coli* (referenced in Petersen and Moller, 2001) the activity of Ado nucleosidase and Ade phosphoribosyltransferase (enzymes 1 and 2 in Figure 2) can by-pass ADA deficiency.

As previously stated, ADA deficiency in mammals causes immunodeficiency. More than 50 ADA mutations are known in humans (Arredondo-Vega *et al.,* 1998) causing severe combined immunodeficiency, late evolving immunodeficiency, or "partial" ADA deficiency with no phenotype. Relating the genotype to a phenotype is difficult because: 1) often only one allele is mutated and 2) determination of residual ADA activity is problematic due to tissue availability and low ADA activity in all phenotypes (Arredondo-Vega *et al.,* 1998). Therefore, ADA-deleted *E. coli* strains have been a useful tool to determine ADA activity of cloned and overexpressed human ADAs, by complementation. *E. coli* SØ3834 is a multiple auxotroph (rpsL, Δadd-uid-man, metB, guaA, uraA::Tn10) with a deletion of the bacterial ADA gene; on minimal medium, it requires guanosine (Gua) to grow (Hove-Jensen and Nygaard, 1989). This Gua requirement can be satisfied by 2,6-diaminopurine (DAP) if a plasmid coding for a functional ADA is introduced into the strain (Chang *et al.,* 1991). The synthesis of Gua from DAP is illustrated in Figure 4. This convenient complementation system in *E. coli* SØ3834 will be used to test the ADA identity of locus At4g04880 (Section 1.5).

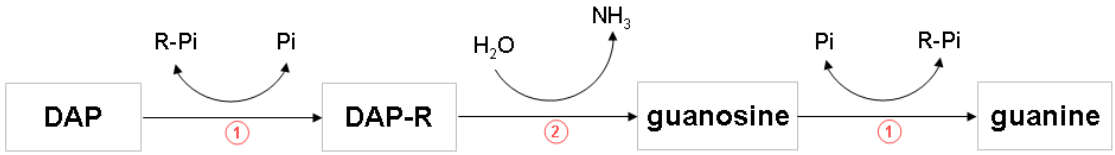

Figure 4 – Synthesis of guanosine and guanine from 2,6-diaminopurine (DAP). DAP is converted to guanine by the activity of two enzymes: 1) purine nucleoside phosphorylase, 2) adenosine deaminase. The SØ3834 mutant requires guanine to grow. DAP can satisfy the guanine needs if a functional adenosine deaminase is provided. Figure adapted from (Chang *et al.,* 1991).

1.7 Evolutionary Conserved Amino Acids in Adenosine Deaminase-Related Proteins

ADA from mammals and bacteria are well characterized because of the importance of understanding ADA deficiency and SCID in humans. Important residues for the catalytic function of the ADA have been identified by several studies and are outlined in Table 1. The amino acid alignment of mammalian and *E. coli* ADA shows high overall similarities but only four regions of four or more contiguous highly conserved amino acids (Chang *et al.,* 1991).

Table 1 – Important residues for the catalytic function of ADA.

Residues	Catalytic function	Reference
His 15 His 17 His 214 Asp 295	Zinc binding	(Wilson *et al.,* 1991) (Chang *et al.,* 1991) (Maier *et al.,* 2005)
His 17 Gly 184 Glu 217 His 238 Asp 296	Donating or accepting hydrogen bonds	
Ser 265 – His 238	Salt link	

Ade deaminase (ADE) catalyzes the deamination of Ade to hypoxanthine (Figure 2), a similar hydrolytic deamination as that catalyzed by ADA. Also, AMP deaminase (AMPD) which converts AMP to IMP (Figure 2) uses a similar mode of enzymatic reaction as that of ADA. A third group of ADA-related proteins are the adenosine deaminase-related growth factors (ADGFs). ADGFs have been identified in invertebrates and vertebrates and ADA activity was demonstrated for some ADGF members (Maier *et al.,* 2005). In vertebrates ADGF is also known as cat eye syndrome critical region protein (CECR1). Cat eye syndrome is a rare human disorder characterized by, among other symptoms, defects of the eyes (Schinzel *et*

al., 1981). As demonstrated in *Drosophila,* ADGFs stimulate mitogenic activity that is correlated with ADA activity (Zurovec *et al.,* 2002). The genome of *Drosophila* contains six ADGFs; two of them possess ADA activity and are demonstrated to act as mitogenic, whereas a third ADGF investigated lacked enzymatic activity and was not mitogenic. It was evident that ADGFs require catalytic activity for their stimulation of cell proliferation by depleting extracellular Ado (Zurovec *et al.,* 2002).

A phylogenetic study demonstrated sequence similarities between ADA, ADGF, ADE and AMPD families (Maier *et al.,* 2005) and revealed conserved regions among and within these enzyme groups. Plant sequences were not included in this study since only one plant gene was available at the time (H. McDermid, personal communication). This analysis revealed a new family of ADA-related proteins, termed ADA-like enzymes (ADAL). These proteins are closely related to ADAs and even though ADAL along with ADGF possess all the required catalytic residues for ADA activity, no ADAL member has been shown to process this activity (Maier *et al.,* 2005). A further characteristic of ADA and ADAL subfamilies is that no signal peptide was predicted whereas some of the ADGFs were predicted to have a signal peptide. ADALs were identified in several organisms i.e. mammals, insects and bacteria (Maier *et al.,* 2005). Recently, ADAL transcripts were shown to be present in different tissues of zebrafish, predominantly in kidney and liver (Rosemberg *et al.,* 2007), although no ADA activity could be detected. The function of ADAL proteins remains unknown. The other ADA-related enzymes ADA, ADGF, ADE and AMPD are also abundant in mammals, insects and bacteria, suggesting a very fine-tuning of Ado/Ade levels in these organisms (Rosemberg *et al.,* 2008).

The phylogenetic analysis from Maier *et al.* (2005) revealed that some ADA-related genes have been incorrectly labelled as classic ADAs. *Drosophila melanogaster* ADA is a member of the ADALs, while some other insect ADAs belong in the ADGF subfamily. As stated earlier, the locus At4g04880 of Arabidopsis has been computationally annotated as a putative ADA/AMPD. Another part of my thesis

research sought to reveal the identity of this locus using a phylogenetic analysis that included all available plant sequences.

1.8 CYTOKININS

In general, cytokinins stimulate cell division; they are involved in plant growth and development such as root proliferation and apical dominance (Werner *et al.,* 2003); they are highest in abundance in roots and shoots where they exist in the low nM concentration (Schmuelling, 2004). CKs are Ade molecules with an N^6 side chain and occur in different forms such as: the free base; a nucleoside and a nucleotide and can be rapidly interconverted between these forms. The structure of the N^6 side chain classifies CKs as isoprenoid or aromatic; structure and conformation of the side chain influences their biological activity (Schmuelling 2004).

Several enzymes of the plant Ado salvage pathway can catalyze the interconversion of CKs, such as Ade phosphorybosyltransferase (Moffatt *et al.,* 1994) and ADK (von Schwartzenberg *et al.,* 1998). The regulatory mechanism of intracellular CK activity involves reversible hydrolysis of the CK ribosides to CK bases, which are the most active forms of CKs. This reaction is thought to be catalyzed by Ado nucleosidase but a corresponding gene has not yet been identified (Hirose *et al.,* 2008). A CK-specific phosphoribohydrolase encoded by the *LONELY GUY* (*LOG)* genes has been described recently in rice; they convert CK nucleotides directly to the corresponding bases (Kurakawa *et al.,* 2007) thus contributing to the level of “active” cytokinins in plants.

1.9 ADENOSINE NUCLEOSIDASE IN *ARABIDOPSIS THALIANA*

As mentioned previously, ADN catalyses the irreversible hydrolysis of Ado to Ade and ribose (Enzyme 3 in Figure 1). This enzyme activity has been demonstrated in crude extracts or partially purified preparations of several plants but a gene coding for ADN has not been identified.

Inosine-uridine preferring nucleoside hydrolase (IU-NH; EC 3.2.2.1) was first identified and geneticly and structurally characterized in protozoan (Gopaul *et al.,*

1996). The enzyme catalyzes the hydrolysis of all purine and pyrimidine nucleosides into their corresponding ribose and base forms, preferring Ino and Uri as substrates. This enzyme is particularly important for parasitic organisms, since they are deficient in *de novo* synthesis of purines and salvage the host's purine nucleosides. A histidine residue has been shown to be important for the catalytic mechanism for this enzyme activity, by acting as a proton donor. A highly conserved amino acid sequence in the N-terminal region of the enzyme contains four aspartates (DXDXXXDD) that are a hallmark of nucleoside hydrolase activity (Versées and Steyaert, 2003).

One aspect of this research involved searching for ADN genes and enzyme activity in Arabidopsis. The genome was screened for putative ADNs using a known IU-nucleoside hydrolase sequence from *Crithidia fasciculata*. Candidate genes were investigated, their gene products were studied and their role in plant development examined using T-DNA insertion lines.

1.10 THE *ARABIDOPSIS THALIANA* MUTANT *CYM*

The Arabidopsis mutant *cym* (cytokinin metabolism) was identified in a population of plants treated with the chemical mutagen ethyl-methane sulfonate (Auer, 1999). The mutant is resistant to CK ribosides and has reduced Ado nucleosidase activity based on radiochemical assays of crude plant extracts (Auer, 1999). Compared to wild-type protein extracts, *cym* mutant extracts have only 50 % activity on isopentenyladenine riboside and 68 % on Ado. CK nucleotides and nucleosides accumulated in shoot tissue but in root the CK levels were similar to the wild type (Auer, Nordstrom, Sandberg, unpublished data.) The *cym* mutation was reported to be located on chromosome 2 of Arabidopsis based on preliminary mapping data (Auer, 2002) but a corresponding gene was never identified (C. Auer, personal communication). *ADN2* is hypothezised to be the gene for the location of the mutation due to its close proximity to the mapped region. ADN2 is annotated as an IU-NH (Section 1.9); a mutation in this gene is likely to account for the *cym*

phenotype described above. One part of this research sought to investigate *ADN2* as the gene carrying the *cym* mutation.

1.11 Aim of Thesis Research

It is evident that organisms may contain several enzymes acting on Ado, reflecting the need to maintain strict control over this metabolite. The consequences of Ado accumulation are illustrated by the SCID in humans or the pleiotropic phenotype of *Arabidopsis thaliana* mutants. Relatively few of the Ado recycling enzyme activities have been characterized in plants. This thesis research sought to identify whether two principal Ado metabolizing enzymes, ADN and ADA are present in Arabidopsis and if so, what is their functional significance in plant development.

Chapter 2

MATERIAL AND METHODS

2.1 CHEMICALS

Chemicals used in this research were ACS grade or of higher quality; they were purchased from Sigma-Aldrich, Bioshop or BioBasic unless otherwise indicated.

2.2 PLANT MATERIAL AND PLANT GROWTH

2.2.1 PLANT MATERIAL

In order to understand the role of ADA and ADN in plant development several mutants were used in this research. *A. thaliana* ecotype Columbia is the genetic background of all mutant lines used and was used as control for all the experiments outlined. An overview of all mutant plant lines used is provided in Table 2. T-DNA insertion lines were obtained from the The Arabidopsis Stock Center (Alonso *et al.,* 2003); these lines were stable in their morphology and development throughout generations. The flanking sequences of the T-DNA insertion were identified and the presence of the transgene was verified by PCR analysis. Each was backcrossed twice with wild-type Columbia before phenotypic analysis. Lines deficient in ADK activity (sADK 9-1) were generated by overexpression of an ADK1 transgene (Moffatt *et al.,* 2002). amiADK lines were created by Sanghyun Lee by introduction of an artificial micro (ami) RNA construct specific for ADK genes into wild-type Arabidopsis. The phenotype of the sADK 9-1 mutants ranged in their severity: the plants were not phenotypically uniform due to inconsistent silencing of ADK gene expression (Table 2). The more deficient mutants were visually identified and selected at 2-3 weeks based on the waviness of their leaves and general size.

Phenotypic variations were also observed throughout the progeny of amiADK plants; more deficient mutants were selected at 2-3 weeks.

A heterozygous masp::ADA amiADK transgenic line was also produced. The masp::ADA expression construct was created by S. Lee (Moffatt Lab) based on the vector pSAT3.masP.MCS.masT (Chung *et al.,* 2005). This construct was introduced into the amiADK background described above to test whether it would complement ADK deficiency.

Homozygous *cym* seeds were provided by Carol Auer (University of Connecticut, Department of Plant Science, USA). The phenotypic analysis described in this thesis was performed on following plant population: *cym* #3 planted November 26, 1999, seeds collected February 1, 2000. Original *cym* seeds obtained 1998 did not germinate and were not available for analysis.

Table 2 – Overview of mutant plant lines used in this research.

Gene	Locus	Plant Line	Description	Phenotype	Marker	H[1]
***ADK* 1** ***ADK* 2**	At3g09820 At5g03300	**sADK 9-1**	ADK1 cDNA in sense orientation expressed from CaMV 35S promoter	wrinkled leaves, clustered fluorescence, reduced primary shoot height; residual ADK activity 16 %	Kan	✓
		amiADK 7-7	artificial miRNA expressed from CaMV 35S promoter; targets both ADK isoforms	bushy, small shoots, reduced rosette width, wrinkled leaves; residual ADK activity 5-7 %	Bar	✓
ADA	At4g04880	***ada* 1-1**	T-DNA insert in 8th exon of *ADA* SALK _010573	WT phenotype	-	✓
		***ada* 1-2**	T-DNA insert in 5th exon of *ADA* SALK _144851	WT phenotype	-	✓
		masp::ADA	ADA cDNA in sense orientation under control of mannopine synthase promoter	WT phenotype	Bar	-
		35S::ADA	ADA cDNA in	WT phenotype	Bar	-

			sense orientation under control of CaMV 35S promoter			
ADN 1	At1g05620	***adn* 1-1**	T-DNA insert in 6th intron of *ADN1* SALK _128723	WT phenotype	-	✓
***ADN* 2**	At2g36310	***adn* 2-1**	T-DNA insert in 2nd exon of *ADN2* SALK _083120	WT phenotype	-	✓
ND[2]	ND[2]	***cym***	ethylmethane sulfonate induced mutant	pale green leaves; red stem base, fasciation, altered phyllotaxy	-	✓
Double mutants		**sADK 9-1 *ada* 1-1**	double mutant obtained by genetic cross	phenotype is more severe than sADK 9-1 parent; residual ADK activity reduced from 16 to 7 %	-	✓
		***adn* 1 *adn* 2**	double mutant obtained by genetic cross	phenotype like WT under long-day growth conditions	-	✓
		sADK 9-1 35S::ADA	Double mutant obtained by introducing 35S::ADA construct into the genome of sADK 9-1 plants via *A. tumefaciens*	phenotype like WT; no over-expression of ADA; ADK activity increased	Bar	-

1 – Homozygous, 2 – Not defined

2.3 PLANTING *ARABIDOPSIS THALIANA* AND GROWTH CONDITIONS

Depending on required plant quantity, selection method or experimental requirements, seeds were either planted on soil (1500 cm² flats) or germinated on Murashige and Skoog (MS) agar plates (15 cm^2). MS media was used in half strength, containing half the macro- and micronutrients as described by Murashige and Skoog (1962) and vitamins (Gamborg *et al.,* 1968).

2.3.1 Planting on Soil

Seeds from *A. thaliana* were suspended in 0.1 % (w/v) agar and stored at 4°C in the dark for 48 h to allow seed stratification. Flats were filled with a 1:2 soil mix of Sunshine LC1 Mix and Sunshine LG3 Germination Mix (SunGro, Canada Ltd). The soil was thoroughly wetted at first with warm water followed by cold water and left to drain for 5 min. Next, seeds were dispersed on the wet soil using a Pasteur pipette. The flats were covered with a transparent lid and transferred to the growth chamber. Seeds were germinated and grown under long day conditions with a dark/light cycle of 8/16 h (140 $\mu mol \bullet m^{-2} \bullet s^{-1}$ photosynthetically active radiation [PAR]) at 18°C/22°C. For the short-day growth conditions, plants were maintained in a 16/8 h dark/light cycle with the same temperature and light intensity.

The transparent lid was removed when plants developed their first true leaves. Plants were watered until they reached full maturity after approximately 6 weeks. Watering was stopped when siliques started browning and plants were left to dry.

2.3.2 Planting on Murashige and Skoog Basal Media

Plants were grown on ½ MS medium. The pH was adjusted to 5.7 using 0.1 M KOH prior addition of 0.8 % (w/v) agar (Sigma) and subsequently autoclaved for 30 min at 120 °C. Approximately 25 ml media were poured into sterile Petri dishes (15 cm^2) and seeds sterilized with chlorine gas (Clough and Bent, 1998) were applied to the surface of the solidified media. Plates were stored at 4°C in the dark for 48 h to allow seed stratification and subsequently shifted to the growth chamber under continuous light, 21 °C and 50 $\mu mol \bullet m^{-2} \bullet s^{-1}$ PAR If desired, plants were transplanted on soil at two weeks of age and grown to maturity.

2.4 DNA AND RNA METHODS

2.4.1 GENOMIC DNA EXTRACTION

The following protocol was used for the isolation of plant genomic DNA suitable for PCR analysis (Edwards *et al.,* 1991). DNA was extracted from *A. thaliana* rosette leaves using the following extraction buffer: 200 mM Tris-HCl pH 7.5, 250 mM NaCl, 25 mM EDTA and 0.5 % (w/v) sodium dodecyl sulfate (SDS).

Approximately 10 mg healthy leaf tissue, collected by punching the leaf with the microfuge cap, was transferred to a 1.5 ml microfuge tube, prefilled with 50 µl extraction buffer. Tissue was macerated with a plastic grinder, 350 µl extraction buffer was added and the tube was vortexed for 5 seconds. The sample was centrifuged at 15,000 rpm for 5 min and 300 µl of supernatant were transferred to a new microfuge tube, prefilled with 300 µl isopropanol. The mixture was inverted and incubated at RT for 2 min and then centrifuged for 5 min at 15,000 rpm. The DNA pellet was recovered, vacuum-dried and resuspended in 100 µl 10 mM Tris-HCl ph 8.5. The DNA was stored at -20 °C. Generally 1 µl of extracted DNA was used for a PCR.

2.4.2 PLASMID DNA ISOLATION

The EZ-10 Spin Column Plasmid DNA Miniprep Kit (Bio Basic) was used for the extraction of plasmid DNA from 4 ml overnight (O/N) cultures of *E. coli* DH5α. The procedure was followed as outlined by the manufacturer (BioBasic). All solutions used were provided by the manufacturer, all centrifugation steps were performed using an Eppendorf bench top centrifuge at 4°C.

2.4.3 RNA EXTRACTION

RNA was extracted from *adn* mutant lines and wild type to determine the ADN1 and ADN2 transcript abundance in the T-DNA lines. Four to five fully-expanded rosette leaves of 3 to 4 week-old-plants were ground in liquid nitrogen and transferred to an Eppendorf tube prefilled with 1 ml of TriPure Isolation Reagent

(Roche). The mixture was vortexed for 10 seconds and incubated at room temperature (RT) for at least 5 min. After adding 200 µl of chloroform, the sample was vortexed for 15 seconds und incubated at RT for 10 min. Subsequently the sample was centrifuged for 15 min at 13,000 g at 4° C. The aqueous phase (500 µl) was transferred to a new microfuge tube prefilled with 500 µl isopropanol. The contents of the tube were mixed by inversion and incubated at RT for 5 min following which the mixture was centrifuged for 10 min at 13,000 g. The RNA pellet was washed with 1 ml of 75 % ethanol (prepared in deionized water (dH_2O) treated with diethylpyrocarbonate (DEPC)) and centrifuged for 5 min at 13,000 g. The air-dried pellet was resuspended in 30 µl of DEPC treated dH_20 and incubated at 60° C for 10 min. The average yield was 15 µg. All RNA was stored at -80 °C.

2.4.4 cDNA Synthesis

Two µg of total RNA was treated with DNAse in 10 µl total volume using RNase-free H_20, 10x Turbo DNase buffer (Ambion), 2 U Turbo DNAse I (Ambion). The mixture was incubated for 1 h at 37°C; subsequently DNase inactivation reagent (Ambion) was added and incubated for 2 min at RT. The mixture was centrifuged for 2 min 14,000 g at 4 °C and the supernatant was used subsequently for cDNA synthesis. To 10 µl of this RNA solution, 1 µl 100 µM anchor-T-primer ($T_{20}G$, $T_{20}C$, $T_{20}A$), 1 µl 10 mM deoxynucleotide triphosphates (dNTPs) were added and incubated for 10 min at 70°C. The mixture was transferred to ice after which 4 µl 5x first strand buffer (Invitrogen), 2 µl 0.1 M DTT (Invitrogen) were added and preincubated for 2 min at 42°C. Subsequently 100 U SuperScript II (Invitrogen) were added and the reaction mix was incubated for 50 min at 42 °C. The resulting cDNA was diluted 1:10 with PCR- H_20 (ultrapure H_20, autoclaved and UV-light treated) and tested for intactness by amplification of the actin cDNA.

2.4.5 DNA and RNA Quantification

Nucleic acids were quantified using a NanoDrop Spectrometer (Thermo Scientific). For measurement 1.5 µl sample was applied to the spectrophotometer.

2.4.6 DNA Sequencing and Analysis

Sequencing was performed by the dideoxynucleotide chain termination method (Sanger), using sequence-specific primers. DNA samples were prepared in the required concentration and volumes and analyzed by TCAG DNA Sequencing Facility (Centre for Applied Genomics, Hospital for Sick Children, Toronto, Ontario, Canada). Sequences were analysed using SeqMan™II Analysis software (DNASTAR, version 5.00).

2.5 Cloning of DNA Constructs

2.5.1 Creating Expression Vector for ADA-Complementation

The open reading frame (ORF) of the *A. thaliana* locus At4g04880 was amplified from a full-length cDNA clone (U24331, ABRC) using proof-reading Taq polymerase (Phusion High-Fidelity DNA Polymerase, Finnzymes). PCR was performed as described in Section 2.6.1. PCR primers were designed to insert a *Nde*I-recognition site at 5'-end and a *Hind*III-recognition site at 3'-end of the ADA ORF (primer 17 and 18 in Table 6). Using these recognition sites the ORF was ligated into pMAL-c4e (New England Biolabs). Digestion of the vector with *Nde*I and *Hind*III releases the 1.2 kb maltose-binding protein gene fragment. The resulting recombinant plasmid was named pAtADA. In this construct, the expression of ADA is controlled by the strong, constitutive Ptac promoter.

The *E. coli* Ado deaminase was used as positive control in the complementation experiment. The ORF was amplified from genomic DNA of *E. coli* DH5α using proof-reading Taq polymerase. PCR-primers inserted a *Nde*I-recognition site at 5'-end and a *Pst*I-recognition site at 3'-end of the add ORF (primer 15 and 16 in Table 6). Using the restriction enzyme recognition sites the ORF was ligated into pMAL-c4e substituting the maltose binding protein gene as described above. Since the *E. coli* strain DH5α is a K12 derivative, the resulting vector was named pK12ADA.

The vector pMAL-c4e was used as a negative control in the complementation experiments; this vector encodes the maltose binding protein (MBP), to simplify the nomenclature this plasmid will be named pMBP for this reason.

2.5.2 Creating an ADN- EGFP- Fusion Vector

The ADN ORFs (ADN 1 and ADN 2) were amplified from cDNA templates using proof-reading Taq polymerase (as described above). Primers were designed to insert a *Nco*I-recognition sites at both the 5'-and at 3'-ends of each ADN sequences and the stop codon was removed. For ADN1 amplification primer 1 and 2 from Table 6 and for ADN2 amplification primer 3 and 4 from Table 6 were used. Using the *Nco*I-recognition sites the ORF was ligated into a modified pCambia-3301 (www.Cambia.org; β-glucuronidase (GUS) gene replaced by a green fluorescent protein (GFP) gene by Yong Li (Moffatt Lab); unpublished). The binary vector and PCR product were digested with *Nco*I and their subsequent ligation fused the ADN ORFs to the enhanced green fluorescent protein (EGFP). The resulting binary vectors were named ADN 1-EGFP and ADN 2-EGFP, respectively. The expression of ADN-EGFP fusion proteins from these constructs was controlled by the constitutive CaMV 35S promoter.

2.5.3 Creating an ADN- 2xGFP- Fusion Vector

Both, ADN 1 and ADN 2 ORFs were amplified as described in Section 2.5.1 using the same primers as described above. Each ORF was inserted into the multiple cloning site of a modified pSAT6 vector (Tzfira *et al.,* 2005); EGFP gene replaced by two GFP genes by S. Lee (Moffatt Lab)) thereby fusing the double-GFP to the N-terminus of ADN. A 82 kd fusion protein of ADN and 2xGFP was created. In a second cloning step, the expression cassette of pSAT6-ADN-2xGFP was ligated into the binary vector pPZP-RCS2-bar using the homing endonuclease *PI-Psp*I. The resulting vector was named pPZP-ADN-2xGFP. The expression of ADN-2xGFP fusion-protein was controlled by the constitutive CaMV 35S promoter.

2.5.4 Creating an ADN- Strep-Tag - Fusion Vector

The ADN ORFs (ADN 1 and ADN 2) were amplified as described in Section 2.5.1 using a *Nco*I-recognition site to insert the ORFs into the multiple cloning site of pXNS2pat-N1 (C. P. Witte, unpublished). The primer pair 1, 13 (Table 6) was used to amplify ADN1 and the primer pair 3, 14 was used for ADN2. The reverse primer was designed to introduce the *Nco*I site without eliminating the stop codon. The construction fuses a 21 amino acid long StrepII-tag to the N-terminus of each ADN. The resulting vectors were named pADN1-NStrep and ADN2-NStrep, respectively. The expression of these ADN-NStrep fusion-proteins was controlled by the constitutive CaMV 35S promoter.

2.5.5 Creating an ADN 1 – Profinity eXact Fusion Vector

The ORF of ADN1 was amplified from a cDNA template using the primer pair 1,10 (Table 6) introducing a 5'-*Nco*I recognition site and a 3'-*Not*I-recognition site. The ligation of ADN1 into pPAL7 (BioRad) resulted in a N-terminal fusion to the Profinity eXact tag. The resulting vector was named pPAL-ADN1. The expression of the fusion protein was controlled by a T7 promoter. Elution of purified recombinant protein from the affinity column resulted in a native ADN1 protein with only three additional amino acids on the N-terminus.

2.5.6 Creating an ADN- Histidine-Tag Fusion Vector

As described above the ORF of both ADNs (ADN 1 and ADN 2) were amplified from a cDNA template. The primers were designed to insert a 5'-*Nde*I recognition site and a 3'-*Not*I-recognition site on each ADN ORF (for ADN1 primer 9, 10; for ADN2 primer 11, 12 from Table 6). Using these recognition sites the ORF was ligated into the multiple cloning site of pET-28a(+) resulting in an N-terminal fusion to a 6xHis tag. The resulting vectors were named pADN1-NHis and pADN2-NHis, respectively. The expression of these ADN-NHis fusion-proteins was controlled by a T7 promoter.

Table 3 – Overview of DNA constructs

Construct	Expression promoter	Affinity tag	Tag location	Use
ADN1-NHis	T7	6 His	N-terminal	Recombinant ADN activity assay
ADN2-NHis	T7	6 His	N-terminal	
ADN1-NStrep	T7	Step-tag-II	N-terminal	"Native" ADN activity assay
ADN2-NStrep	T7	Step-tag-II	N-terminal	
ADN1-tagless	T7	Profinity eXact	N-terminal	Recombinant ADN activity assay
ADN 1-EGFP	CaMV 35S	-	N-terminal	Localisation experiment
ADN 2-EGFP	CaMV 35S	-	N-terminal	
ADN2-2xGFP	CaMV 35S	-	N-terminal	
pK12ADA	P_{tac}	-	-	ADA complementation
pAtADA	P_{tac}	-	-	

2.6 POLYMERASE CHAIN REACTION (PCR)

2.6.1 HIGH FIDELITY PCR

For amplification of the ORF of interest from a cDNA template, a proof-reading Taq-polymerase (Phusion High-Fidelity DNA Polymerase, Finnzymes) was used in the following reaction mix and the product was amplified using the cycle profile as indicated in Table 5.

Table 4 – Reaction mix for high fidelity PCR

Contents	Stock Concentration	Volume [µl]
cDNA template	1-10 ng	1
HF Buffer	5 x	10
Fw primer	10 µM	2.5
Rev primer	10 µM	2.5
dNTPs	10 mM	1.0
Phusion Polymerase	2 u/µl	0.5
PCR H_2O	-	32.5

Table 5 – Cycle profile for high fidelity PCR

Temperature [°C]	Time	Cycles
98	30 seconds	1
98	10 seconds	28
55-60*[1]	20 seconds	
72	20 seconds	
72	7 min	1
4	∞	1

*[1] Annealing temperature for respective primer see Table 6. For Phusion Polymerase an annealing temperature of Tm+3 °C was used.

Table 6 – Overview of primer used

No	Primer name	Primer sequence	Tm
1	05620 F	AACCATGGCGATAGGAGACCGC	58
2	05620 R	AACCATGGTAGACTCCATAAGCCTATCCAT	58
3	36310 F	AACCATGGATTGTGGTATGGAGAAT	58
4	36310 R	AACCATGGTTGGCTTCATCAGCTTTGC	58
5	128340 LP	TCCTCAAACCTGGTTCACATC	58
6	128340 RP	CAGCTTGATCCAGAGTTTTCG	58
7	083120 LP	AGGAGCTGAGAGTTTCAAGGG	58
8	083120 RP	ATGAACTATCGCGTTTGATGG	58
9	ADN1 FW	AAAACATATGGCGATAGGAGACCGC	55
10	ADN1 RWb	AAAGCGGCCGCTTAAGACTCCATAAG	55
11	ADN2 FW	AAAACATATGGATTGTGGTATGGAGAATTG	55
12	ADN2 RWb	AAAAGCGGCCGCTTATGGCTTCATC	55
13	ADN1 *Nco*I RW	AAACCATGGTTAAGACTCCATAAGCCTATCC	55
14	ADN2 *Nco*I RW	AAACCATGGTTATGGCTTCATCAGCTTTG	55
15	ADA-K12 FW	AAACATATGATTGATACCACCCTGCC	55
16	ADA-K12 RW	AAACTGCAGTTACTTCGCGGCGAC	55
17	fwdADApet	GGAATTCCATATGGAATGGATACAATCACTGCCC	60
18	revADApet	CCCAAGCTTCTAAACGT	60
19	ADN1.2-FW	AAAACATATGGCGATATTCGTAGC	55
20	actin 2F	CCGATGGTGAGGATATTCAGCC	58
21	actin 2R	TGTCACGGACAATTTCCCGTTCTGC	58
22	LBa1	TGGTTCACGTAGTGGGCCATCG	55
23	LBb1.3	ATTTTGCCGATTTCGGAAC	55

2.6.2 COLONY- PCR

In order to identify bacterial cells with a desired plasmid a “colony-PCR” was performed. A toothpick of a single colony was used to dilute bacterial cells in a PCR microfuge, prefilled with 10µl sterile dH_2O; five µl were removed from the microfuge tube and spotted onto a new agar plate. The PCR was performed using homemade Taq polymerase (Yong Li, Moffatt Lab) and 10x Buffer (500 mM KCl, 100 mM Tris-HCl, pH 8.3, 15 mM MgSO4, 0.1 % Triton X-100, 0.1 % Tween 20). The PCR was performed as described in Table 9. The following PCR mix was used for all reactions:

Table 7 – Reaction mix for colony-PCR

Contents	Stock Concentration	Volume [µl]
Bacterial cell suspension	-	5
Buffer	10 x	2.5
Fw primer	10 µM	0.5
Rev primer	10 µM	0.5
dNTPs	10 mM	0.5
Enzyme	-	1.0
PCR H_2O	-	15.0

2.6.3 ANALYTICAL PCR

Plant genotyping was done by PCR using gene-specific primers for the target transgenes (see Table 6). Homemade Taq polymerase and 10x Buffer was used as described above. Genomic DNA was isolated as described in Section 2.4.1 and 1 µl of DNA was used in following PCR mix and product was amplified using the indicated cycle profile.

Table 8 – Reaction mix for control PCR

Contents	Stock Concentration	Volume [µl]
DNA	-	1
Buffer	10 x	2.5
Fw primer	10 µM	0.5
Rev primer	10 µM	0.5
dNTPs	10 mM	0.5
Enzyme Mix	-	1.0
PCR H_2O	-	19.0

Table 9 – Cycle profile for control PCR

Temperature [°C]	Time	Cycles
94	4 min	1
94	15 seconds	35
57-60*	20 seconds	
72	1 min per 1kb	
72	7 min	1
4	∞	1

* Annealing temperature for respective primer see Table 6

2.6.4 SEMI-QUANTITATIVE REVERSE TRANSCRIPTION PCR

The exponential phase of amplification was determined for actin, ADN1, ADN2 using wild-type cDNA. A PCR master mix was prepared including wild-type cDNA but no primer. The master mix was split into 8 aliquots and primers were added individually. Aliquots were removed from the PCR cycler at the indicated cycle numbers and resolved by electrophoresis through a 1 % (w/v) agarose gel. The PCR products were quantitated using Alpha Innotech software (AlphaEaseFC

version 6.0.0, SpotDenso Analysis Tool). Cycle number was plotted against the log of the intensity value and a straight line indicated the exponential phase of amplification.

Semi-quantitative reverse transcription-PCR (RT-PCR) was performed at the determined cycle number (Table 11) for all plant lines. The actin PCR was run simultaneously to assure equal cDNA loading for all samples. Equal loading of all samples required emperical trial and error adjustment.

Table 10 – Cycle profile for reverse-transcription PCR.

Temperature [°C]	Time	Cycles
94	2 min	1
94	15 seconds	30*[1]
55	20 seconds	
72	1 min	
72	7 min	1
4	∞	1

*[1]number of cycles see Table 11

Table 11 – Primer pairs and cycle numbers for RT- PCR.

Primer*[2]	Gene	Cycles for RT-PCR
Actin 2F/R	*Actin2*	24
05620 F/R	*ADN1*	30
ADN1.2 F/05620 R	*ADN1*	32
36310 F/R	*ADN2*	30

*[2]primer sequences are described in Table 6.

2.7 Restriction Digestion of PCR Products and Vectors

In order to digest double-stranded DNAs for cloning, the restriction endonucleases *Hind*III, *Nco*I, *Nde*I and PstI (Fermentas) were used. These enzymes generate sticky-end DNA fragments of four nucleotides. For cloning the ADN ORF

from pSAT6-2xGFP into pPZP-RCS2-bar the homing endonuclease PI-*PspI* was used. This enzyme does not have a stringently defined recognition sequence (New England Biolabs). All restriction digests were performed in the recommended buffers. A preparative digest was performed in a 100 µl volume with 1 µg DNA, 1 u of enzyme and incubated at recommended temperature for at least two hours. An analytical digest was performed in a 20 µl volume with approximately 300 ng Miniprep-DNA and 0.5 u enzyme incubated at recommended temperature for 1 h.

2.8 Agarose Gel Electrophoresis

DNA fragments were separated using 1.0 % (w/v) agarose gels in 1x Tris-acetate-EDTA buffer (1 L of 10x buffer contains: 48.4 g Tris-base, 11.4 ml glacial acetic acid, 9.3 g EDTA). Ethidium bromide was added to the gel to a final concentration of 10 µg/µl. For loading, samples were mixed with 5x glycerol-dye-EDTA loading buffer (5 ml glycerol, 3.3 ml 0.2 M EDTA, 0.85 ml 1 % (w/v) bromophenol blue, 0.85 ml xylene cyanol). DNA was separated at 80-100 V for 20 to 40 min. Ethidium bromide (fluorescent dye) intercalated in the DNA and the detection of DNA was performed using a UV transilluminator.

2.9 Purification of DNA Fragments from Agarose Gel

In order to purify a DNA fragment from an ethidium bromide-stained agarose gel the QIAquick Gel Extraction Kit (Qiagen) was used. The procedure was followed as outlined by the manufacturer. All solutions used were provided from Qiagen, all centrifugation steps were performed using an Eppendorf bench top centrifuge at 4°C.

2.10 DNA Dephosphorylation and Ligation

To increase ligation efficiency terminal phosphate groups were removed from 5'-end of the restricted vector DNA using Alkaline Phosphatase (Roche). This step was performed using an enzyme isolated from northern shrimps (*Pandalus borealis*)

since a complete and irreversible heat inactivation at 65°C was feasible. The reaction was performed following the instructions of the manufacturer.

In order to ligate DNA fragments the NEB Quick ligation kit was used for 10 min ligation step. Enzymatic reactions were performed as outlined by the manufacturer.

2.11 Plant and Bacterial Cell Transformation

2.11.1 Preparation of Heat-Shock Competent *E. coli*

This protocol is an adaptation of procedure described in Hanahan (1985); it was used to prepare heat-shock competent *E. coli* DH5α, BL21(DE3), BL21-CodonPlus(DE3)-RIPL (Novagen) and SØ3834 (Chang *et al.,* 1991). The cells were stored at -80°C for up to one year without losing their high transformation efficiency. The following steps were performed: (1) cells were grown O/N in 5 ml Luria-Bertani (LB) media (10 g tryptone, 5 g yeast extract, 5 g NaCl per litre H_20) at 37°C with shaking at 220 rpm; (2) 2 ml of the O/N culture was added to 100 ml LB-medium and incubated at 37°C, with shaking; (3) when the culture reached the optical density at 600 nm (OD_{600}) of 0.4-0.6 the cells were harvested in pre-chilled tubes by centrifugation at 3000 g for 5 min at 4 °C; (4) the pellet was gently resuspended in 0.4 V of ice-cold sterile Tfb I (30 mM KOAc, 100 mM RbCl, 10 mM $CaCl_2$, 50 mM $MnCl_2$, 15 % glycerol, pH 5.8) and incubated on ice for 5 min followed by centrifugation at 3000 g for 5 min at 4°C; (5) the pellet was gently resuspended in 0.04 V ice-cold Tfb II (10 mM MOPS, 75 mM $CaCl_2$, 10 mM RbCl, 15 % glycerol, pH 6.5) and incubated on ice for 15 min; (6) the cells were aliquoted (100 µl) into prechilled microfuge tubes on dry ice and stored at -80 °C.

2.11.2 Heat-Shock Transformation of Bacterial Cells

For the introduction of purified plasmid DNA or ligation products into bacterial cells, heat-shock competent cells were used. Aliquots of competent cells were removed from -80°C and placed on ice for thawing. To 50 µl competent cells 80 ng

of plasmid DNA or 5 µl of ligation mix were pipetted, mixed and incubated on ice for 20 min. Subsequently cells were incubated at 42 °C for 45 seconds and quickly chilled on ice for 2 min. LB-media (500 µl) was added to the cells and incubated for 1 h at 37°C, 220 rpm. Cells were spin down at 8000 g for 1 min, resuspended in approximately 100 µl LB and transferred to agar plates supplemented with appropriate antibiotic and grown O/N at 37°C.

2.11.3 Transformation of *Arabidopsis thaliana* Using *Agrobacterium tumefaciens* (Floral Dip Method)

Plant transformation was performed using a modified method described by Clough and Bent (1998). Young, healthy plants of about 4-weeks-old containing a large number of immature floral buds and only few developed siliques were used for this method. *Agrobacterium tumefaciens* strain GV3101 carrying the binary plasmid of interest was grown in a LB media at 28°C, 220 rpm. The medium was supplemented with gentamycin (25 µg/ ml), rifamycin (25 µg/ ml) and the suitable antibiotic for selection of the binary plasmid of interest. A liquid culture (200 ml) was started by inoculation with 1 ml of a saturated O/N culture and grown for 15-20 h at 28°C. Cells were harvested by centrifugation at 5,500 rpm for 10 min at 4°C and resuspended in dipping medium (5 % (w/v) sucrose, 0.05 % Silwet L-77) to a final OD_{600} of 0.8. The inoculation solution was added to a sterilized aluminium tray, plants were inverted, and above-ground tissue was moistened with solution by gentle agitation for 2-3 seconds. Dipped plants were placed under a plastic dome and left in low light conditions for 24 h before being returned to the growth chamber. Plants were watered and grown until siliques were fully developed. Seeds were harvested from mature brown dry siliques and selected for positive transformants as described in the following section.

2.11.4 GLUFOSINATE AMMONIUM (BASTA) SELECTION OF *ARABIDOPSIS THALIANA*

All binary constructs used in this research carry the *bar* gene of *Streptomyces hygroscopicus*, which encodes phosphinothricin acyl transferase; plants expressing this enzyme are able to inactivate glufosinate ammonium and can grow in presence of the herbicide (40 mg/ L). Seeds of putative transformed plants were planted on soil as described in Section 2.3.1. Following the development of the first true leaves the treatment with an herbicide was started. A 0.067 % solution of herbicide ("WipeOut", Wilson Laboratories, Ontario) was sprayed on plants daily, for one week. Within 48 h sensitive plants showed yellowing of leaves and died within 7 days. Positive transformed plants tolerant to the herbicide were grown to maturity.

2.11.5 AGRO-INFILTRATION

This procedure was used for transient expression of GFP-fused proteins in leaves of tobacco *Nicotiana benthamiana*. Infiltration of tobacco *Nicotiana benthamiana* was performed using a 3-week-old seedlings (4-leaf stage). *Agrobacterium tumefaciens* strain GV3101 carrying the binary plasmid of interest was grown in LB at 28°C, 220 rpm, supplemented with gentamycin (25 µg/ ml), rifamycin (25 µg/ ml) and the suitable antibiotic for selection of the binary plasmid. A 50 ml liquid culture was started by inoculation with 0.5 ml of an saturated O/N culture and supplemented with 20 µM acetosyringone (Fluka) and grown for 15-20 h. Cells were harvested by centrifugation at 5,500 rpm for 10 min at 4°C. In addition a culture of *Agrobacterium tumefaciens* carrying a plasmid encoding the p19 protein of the *Tomato bushy stunt virus* was grown as described above using kanamycin (50 µg/ ml), tetracycline (5 µg/ ml) and rifamycin (25 µg/ ml) in the media. Both strains were combined in one centrifuge bottle and harvested as described above. The volume of each culture harvested was determined so that the cells could be resuspended in infiltration medium (10 mM $MgCl_2$, 10 mM MES, pH 7.5, 100 µM acetosyringone) resulting in a final OD_{600} of 1.0 for the strain carrying P19 and 0.5

for the second strain used. The resuspended cells were incubated at RT for 2 h. Infiltration was performed using a 3 ml syringe without needle. The syringe was pressed on the underside of the leaf while a simultaneous counterpressure was applied to the other side and the infiltration solution was injected into the airspaces of the leaf. Plants were left under low light conditions for 24 h before being returned to the growth chamber. The expression of GFP was monitored 3-7 days after infiltration under a confocal laser scanning microscope. The upper side of the leaves were examined for fluorescence, which lasted about three to four days. The co-infiltration of p19 enhanced the transient expression of the target protein (Voinnet *et al.,* 2003).

2.12 Activity Assays

2.12.1 Detection of ADK Activity

2.12.1.1 Extraction of Plant Proteins

In order to extract proteins from rosette leaves 100 mg tissue was collected, placed in a pre-chilled conical glass homogenizer and 200 µl Super Buffer (5 mM DTT, 50 mM HEPES, pH 7.2, 1 mM EDTA, pH 8.0, 50 mM citric acid, pH 4.2, 10 mM boric acid, pH 6, 20 mM sodium-metabisulfate, 4 % (w/v) polyvinylpolypyrolidone (Bio Basic #9003-39-8; MW 40,000) were added. The tissue was ground thoroughly. This crude extract was centrifuged two times, for 2 min each time, at 14,000 rpm at 4 °C. Subsequently small molecules including purines, nucleosides and nucleotides were removed from the cleared crude extract using gel filtration. The filtration column was prepared by adding 1.2 ml of swollen Sephadex G25 (in 50 mM HEPES buffer, pH 7.2) to a 1.5 ml microfuge tube with a partially pierced bottom (performed with 20 gauge needle). “Microfuge columns” were placed in 13x100 mm glass test tubes and the excess buffer was removed by centrifugation at maximum speed in a tabletop centrifuge (IEC Model HN-S) for 15 seconds (no brake) at RT. The column was transferred to a new test tube and 150 µL of crude extract was applied and was

spun for 15 seconds. The eluate was collected in microfuge tubes and stored at 4 °C. Protein extracts were used for analysis the same day or were stored at -20 °C with 20 % glycerol.

2.12.1.2 Measurement of Protein Concentration

The assay of ADK activity requires a specific protein concentration range it was necessary to determine the protein concentration of the crude leaf extracts. This was determined using the BioRad protein assay reagent following the manufacturer's instructions. Glycerol (final concentration 10 %) was added to the sample prior to the protein concentration measurement, Bio-Rad Protein Assay Dye Reagent was used in a 1:4 dilution. A protein standard curve was prepared using a concentration of 2 to 10 µg/ ml bovine serum albumin, in duplicates. The protein samples were assayed in duplicates as well, typically in a 1:500 dilution. The absorbance of samples and standards was measured at 595 nm, after 5 min incubation at RT. The bovine serum albumin standard slope was used to determine the concentration of the samples. Subsequently the protein concentration of each sample was adjusted to 0.1mg/ ml using Super buffer.

2.12.1.3 [^{3}H] –ADK Assay

The ADK assay measures the conversion of radioactive [2,8-^{3}H] Ado to Ado monophosphate (AMP) (Moffatt *et al.,* 2000). The assays of ADK activity were performed using desalted crude protein extracts prepared as described in Section 2.12.1.1. The reaction took place in a 30°C waterbath for 5 min and was stopped with 1 mL of ice-cold stop buffer (0.05 M NaOAc, 2.0 mM K_2HPO_4, pH 5.0). AMP was precipitated using ice-cold 0.5 M $LaCl_3$. The precipitate was collected by vacuum filtration through a glass fiber filter with a pore size of 1.2 µm. The filter was immersed in Cytoscint (MP Biomedicals) and radioactivity was quantified by liquid scintillation counting (Beckmann LS 1701).

2.12.2 Detection of ADN Activity

Nucleoside hydrolases catalyse the irreversible hydrolysis of nucleosides to their corresponding base and ribose. Two different enzyme assays were used to quantitate nucleoside hydrolase activity. The spectrophotemetric assay followed the decrease in absorbance of the substrate provided whereas the colorimetric assay measured the formation of the ribose product. The first assay was used to determine the kinetic parameters of the enzymatic reaction whereas the second assay was used to verify the mode of reaction performed by the enzyme.

2.12.2.1 Spectrophotometric Assay

The 1 ml reaction mixture contained the nucleoside at the desired concentration in 50 mM Hepes, pH 7.2. The reaction was initiated by adding the enzyme (5 to 10 µg) and the increase or decrease in absorbance was recorded at the appropriate wavelength (Table 12). The conversion of a 1 mM solution of nucleoside resulted in a change in absorbance as outlined in Table 12. The molar extinction coefficient was used to determine the activity of the enzyme. The specific activity for uridine is calculated as following:

$$specific\ activity = \frac{\Delta A_{280nm} / \min}{\Delta \varepsilon_{280nm} * [E]} = \left[\frac{\mu mol}{\min * mg} \right] \quad (1)$$

where ΔA_{280nm} is the delta absorbance per minute at 280 nm wavelength, $\Delta \varepsilon_{280nm}$ is the delta millimolar extinction coefficient for uridine at 280 nm and [*E*] is the enzyme concentration in milligram.

To determine the temperature and pH profile of ADN 2 Uri was used as substrate. For the temperature profile the reaction mix as described above was used. Following buffer systems were used to cover the pH range of 3.5 to 9.5: 50 mM acetate, 50 mM MES, 50mM Tris-HCl, adjusted to the desired pH with HCl or NaOH. The molar extinction coefficient is not a linear function of the pH and does

vary over a pH range (Parkin *et al.,* 1991). The molar extinction coefficient for each pH was not determined in this research.

Table 12 – Wavelength and delta millimolar extinction coefficient for substrates used in the spectrophotometric assay.

Substrate	λ [nm]	$\Delta\varepsilon^*$ [$mM^{-1}cm^{-1}$]	Reference
Adenosine	276	-1.4	(Parkin, 1996)
Cytidine	280	3.42	(Liang *et al.,* 2008)
Guanosine	308	0.16	(Parkin, 1996)
Inosine	280	-0.92	(Parkin *et al.,* 1991)
Thymidine	265	-1.7	(Hansen and Dandanell, 2005)
Uridine	280	-1.8	(Hansen and Dandanell, 2005)

*$\Delta\varepsilon$ = delta millimolar extinction coefficient

2.12.2.2 COLORIMETRIC ASSAY

Nucleoside hydrolase activity was determined by monitoring the formation of a reducing sugar at 37 °C from a 1 mM substrate in 50 mM Hepes, pH 7.2. The assay volume was 1 ml. After 20 min incubation the reaction was stopped by the addition of 0.3 ml termination reagent (4 % (w/v) Na_2C0_3, 1.6 % (w/v) glycine, 0.045 %(w/v) $CuS0_4$) followed by 0.3 ml of 0.12 % (w/v) neocuproine (Fluka). Subsequently, the colour was developed at 95°C for 10 min and the absorbance was measured at 450 nm. A ribose standard curve was used to determine the sample concentration.

2.12.3 Detection of ADA Activity

2.12.3.1 Colorimetric Assay

The enzymatic activity of SAHH was assayed spectrophotometrically in the hydrolytic direction using *S*-adenosylhomocysteine (SAH) as a substrate (Wolfson *et al.,* 1986); Ado and L-homocysteine (Hcy) are the products of this reaction. The conversion of 5, 5-dithiobis(2-nitrobenzoic acid) (DTNB or Ellman's reagent) to 2-nitro-5-thiobenzoic acid (TNB) by Hcy is measured at 412 nm and 30°C. The extinction coefficient of 13,600M^{-1} cm^{-1} for TNB is used to calculate the amount of L-homocysteine formed. The addition of ADA (Roche) ensured that the reaction catalyzed by SAHH proceeded in the hydrolytic direction. Two blanks were conducted: (1) contained all components except SAHH enzyme, (2) contained all components including SAHH, except the ADA enzyme. This assay was used to test the activity of the plant ADA by substituting the commercial enzyme.

Plant enzyme was obtained by recombinant expression of the At4g04880 ORF in *E. coli* BL21-CodonPlus(DE3)-RIPL (Stratagen) as described in Section 2.14. A 6x histidine-tag was fused to the C-terminus of the ORF and was used as a source of the recombinant plant enzyme. This expression vector (p778) was constructed by Sherri Fry (Moffatt Lab).

2.12.3.2 Spectrophotometric Assay

The 1 ml reaction mixture contained Ado at the desired concentration in 50 mM Tris-HCl, pH 7.2 and 37 °C. The reaction was initiated by adding recombinant plant ADA (source see Section 2.12.3.1) and decrease in absorbance was recorded at 265 nm due to conversion of Ado to Ino. The conversion of a 1 mM Ado resulted in a -8.4 change in absorbance (Kaplan, 1955). This molar extinction coefficient was used to determine the activity of the enzyme:

$$enzyme\ activity = \frac{\Delta A_{265nm} / \min}{\Delta \varepsilon_{265nm}} \quad (2)$$

$$enzyme\ activity = \frac{\Delta A_{265nm} / \min}{-8.4 mM^{-1} * cm^{-1}} = \frac{\Delta A_{265nm} * mM}{-8.4 * \min} \quad (3)$$

where ΔA_{265nm} is the delta absorbance per minute at 265 nm wavelength and $\Delta\varepsilon_{265nm}$ is the delta millimolar extinction coefficient for adenosine at 265 nm.

Alternatively, the ADA activity was monitored at 240 nm wavelength detecting the increase of Ino concentration. The enzyme activity was determined using the delta molar extinction coefficient of 7.2 mM^{-1} cm^{-1} (Pospisilova *et al.,* 2008).

The enzyme assay described above was also used to determine the ADA activity in *E. coli* crude extracts. *E. coli* harbouring the constructs for ADA complementation (see Section 2.5.1) was grown in 10 ml 2xYT medium containing appropriate antibiotics and supplemented with 100 µM IPTG or no IPTG. After growing O/N at 37 °C, cells were pelleted and resuspended in 200 ul buffer [10 mM Tris pH 8.2, 50 µM EDTA, 2 mM $CaCl_2$]. The cells were lysed by sonication, cell debris was removed by centrifugation and supernatant was collected. The total protein content was determined using Bradford. The ADA activity assay was initiated by adding 2 µg total protein to the reaction mixture described above.

2.12.3.3 ADA COMPLEMENTATION IN SØ3834

The construction of the vectors used in this experiment was described in Section 2.5.1. The vectors were transformed into SØ3834 using the heat shock method (see Section 2.11.2). Positive transformants were selected on LB plates supplemented with 50 µg/ml ampicilin; in addition, the mutant strain SØ3834 carried tetracycline (5 µg/ml) resistance. The protein expression was under the control of the tac-promoter, a strong but leaky *E. coli* hybrid promoter (de Boer *et al.,* 1983). A starter culture was inoculated with a single colony recovered from selective media and grown O/N at 37°C and 200-220 rpm in LB with appropriate antibiotic. Culture

tubes (18 x 150 mm) containing 10 ml of minimal medium [contained per L: 13.6 g KH_2PO_4, 2 g $(NH_4)_2SO_4$, $FeSO_4$ pH 7.2, 50 mg methionine, 2 ml glycerol, 0.2 g $MgSO_4$, 0.01 g $CaCl_2$, 1 mg thiamine] supplemented with 20 mg/L DAP and appropriate antibiotic were inoculated with 10 µl of the O/N culture. IPTG was added to the culture tubes of a concentration between 0 mM and 5 mM and grown O/N at 37°C, 175 rpm. After O/N incubation, the growth of each culture was estimated by measuring the OD_{600}.

2.13 Measurement of ADA and ADN Abundance in Plants

2.13.1 Immunoblot

Proteins were extracted as described in Section 2.12.1.1 using 50 mM HEPES, pH 7.2 in a 1:2 ratio tissue vs. buffer. Typically, 150 mg rosette leaf tissue was used for each extraction. Cleared supernatant was used for protein determination using the Bradford method (see Section 2.12.1.2). Each sample was mixed 1:5 with 5x SDS loading buffer [60 mM Tris-HCl, pH 6.8, 25 % glycerol, 2 % (w/v) SDS, 0.1 % (w/v) bromophenol blue, 5 % 2-mercaptoethanol], boiled for 5 min at 95 °C and 20 µg total protein was loaded per lane along with prestained protein marker (low MW range; Fermentas). The samples were applied to a 1.5 mm thick SDS polyacrylamide gel consisting of 5 % stacking, 12.5 % separating prepared with a 10 well comb. The samples were electrophoresed in 1x SDS running buffer [25 mM Tris base, pH 8.3, 192 mM glycine, 0.1 % (w/v) SDS] at 80 V for 20 min followed by 120 V. Samples were run depending on desired separation grade.

Prior to the transfer of the proteins onto a polyvinylidene difluoride (PVDF) western blotting membrane (Roche) the gel was soaked in Bjerrum and Schafer-Neilson transfer buffer (48 mM Tris, 38 mM glycine, 20 % methanol, 0.0375 % (w/v) SDS) two times for 15 min. Proteins were transferred using a BioRad Semi-dry Transblotter following the manufacturer's instructions. Transfer was performed at a constant voltage of 20V for 45 min. Once the transfer was completed, the membrane was stained temporarily with 0.2 % (w/v) Ponceau S prepared in 3 % trichloroacetic

acid for 2 min to verify equal loading of samples and successful transfer. After obtaining an image of the Ponceau-stained membrane the colour was washed off using PBS-T (1 % (w/v) dry milk powder, 0.3 % Tween 20 in phosphate-buffered saline (PBS) (1 L PBS contained: 8 g NaCl, 0.2 g KCl, 1.44 g Na_2HPO_4, 0.24 g KH_2PO_4, pH to 7.4). Subsequently the membrane was blocked for 30 seconds with polyvinyl alcohol (0.1 % (w/v) PVA; Sigma P8136; MW 30-70 000) and quickly washed in dH_20 followed by 5 min in PBS-T. Next, the membrane was incubated with the desired primary antibody in PBS-T at the appropriate dilution (Table 13) for 2 h at RT, with gentle shaking.

Table 13 – List of antibodies used in this research.

Antibody	Raised in	Raised against	Grade	Dilution factor
ADA[#]	Rabbit	ADA*	Crude serum	500
ADN[#]	Rabbit	ADN 2*	Crude serum	500
SAHH	Rabbit	SAHH 1*	Crude serum	3,000
ADK	Rabbit	ADK 1*	Affinity purified	5,000
Anti-Rabbit-IgG Peroxidase conjugated[+]	Goat	-	Affinity purified	10,000

[+]Jackson ImmunoResearch Laboratories; *full length cDNA from *Arabidopsis thaliana* was expressed in *E. coli* and affinity purified prior application in antibody production; [#] produced in this research

Membranes were washed 3x in PBS-T for 10 min each and subsequently incubated in secondary antibody for 1 hr at RT, with gentle shaking. Membrane was washed 3x in PBS-T for 10 min before developed using enhanced chemiluminescence detection [100 mM Tris-HCl pH 8.8, 1.25 mM luminol, 2 mM 4-iodophenylboronic acid, 5.3 mM hydrogenperoxide] (Haan and Behrmann, 2007). Chemiluminescence was detected using the DNR BIS303PC Bio-Imaging System (version 3.0.3).

2.14 Large-Scale Protein Expression

All expression vectors used in this thesis were dependent on T7 RNA polymerase expression. For high-level protein production the desired plasmid was transformed in BL21(DE3) or BL21-CodonPlus(DE3)-RIPL cells (Stratagene). A starter culture was inoculated with a single colony recovered from selective media, in LB with appropriate antibiotic and grown O/N at 37°C and 200-220 rpm. The large-scale culture [2xYT media [16 g Tryptone, 10 g Yeast Extract, 5 g NaCl, pH 7.0] supplemented with 0.6 % glycerol and appropriate antibiotic] was inoculated with 1/100th of the O/N culture and grown in a 1L baffled flask at 37°C, at 175 rpm. When an OD_{600} of 1.0 was reached the culture was shifted to RT and grown for 1 h, by which cells typically reached an OD_{600} of 1.5 to 2.0. Subsequently expression was induced by the addition of 100 µM IPTG and growth was continued at RT for 15 to 20 h at 180 rpm. Cells were harvested by centrifugation at 3000 g for 10 min at 4 °C using an Eppendorf tabletop centrifuge. Cell pellets were stored at -20 °C until purification.

2.15 Protein Purification Using Affinity Chromatography

2.15.1 Purification of Recombinant Protein from *E. coli*

All purification steps were carried out at 4 °C. Cell pellets were thawed and resuspended in one volume of lysis buffer (Table 14) per one gram of cell pellet. Cell lysis was preceded by 40 seconds sonication (power level 5, 12 watts, Sonic Dismembrator 100, Fisher Scientific) on ice followed by a 20 second break; each cycle was repeated 5 times. Cell debris and insoluble material was removed by centrifugation at 12,000 g for 20 min. Subsequently the supernatant was filtered through a 0.45 µm filter (Millipore). The supernatant was passed through the appropriate affinity column using gravity flow. Wash and elution steps were carried out as outlined by the manufacturer; see Table 14 for details. Samples were taken at each step to monitor the success of the purification. Samples were mixed 1:5 with 5x SDS loading buffer [60 mM Tris-HCl, pH 6.8, 25 % glycerol, 2 % (w/v) SDS,

0.1 % (w/v) bromophenol blue, 5 % 2-mercaptoethanol] and boiled at 95 °C for 5 min. Approximately 50 µl cell debris obtained after sonication and centrifugation as described above was mixed with 50 µl 5x SDS loading buffer and 25 µl 1x SDS running buffer [25 mM Tris base, pH 8.3, 192 mM glycine, 0.1 % (w/v) SDS] and boiled for 30 min at 95 °C. All samples were separated by migration through a 12.5 % SDS-polyacrylamide gel at 200 V until the dye reached the end of the gel. Fractions with purified protein were identified, pooled and dialysed against 50 mM HEPES, pH 7.2. The average volume of 4 ml protein solution was dialysed against 1 L buffer for 2 hour and fresh 1 L buffer O/N. Protein concentration was determined using the Bradford assay (see Section 2.12.1.2). Protein was stored at -80 °C after adding 10 % glycerol. The ADN2 protein was also lyophilized and stored at 4°C; the protein was still active after 6 month of storage.

Table 14 – Composition of buffers used for affinity purification.

Ni-NTA His bind resin (Novagen)		**Usage**
2x lysis buffer	0.04 mM Tris, pH 7.9, 1 M NaCl, 10 mM imidazole, 1 mg/ml lysozyme	1 ml per mg cell pellet
Binding buffer	0.02 mM Tris, pH 7.9, 0.5 M NaCl, 5 mM imidazole	10 column volumes (CV)
Wash buffer	0.02 mM Tris, pH 7.9, 0.5 M NaCl, 30 mM imidazole	5 CV
Elution buffer	0.02 mM Tris, pH 7.9, 0.5 M NaCl, 250 mM imidazole	5x 1ml
Profinity eXact resin (BioRad)		**Usage**
Lysis buffer and Wash buffer	0.1 M sodium phosphate, pH 7.2	1 ml per mg cell pellet
Elution buffer	0.1 M sodium phosphate, pH 7.2, 0.1 M sodium fluoride	3x 1ml
Strep tactin superflow agarose (Novagen)		**Usage**
Extraction buffer	100 mM Tris, pH 8.0, 150 mM NaCl, 1 mM EDTA, 10 mM DTT, 0.5 % Triton-X-100, 10 ug/ml avidin, 1 mM PMSF, 1 protease inhibitor tablet	2 ml per mg tissue
Wash buffer	100 mM Tris, pH 8.0, 150 mM NaCl, 1 mM EDTA, 2 mM DTT, 0.05 % Triton-X-100	20 CV
Elution buffer	100 mM Tris, pH 8.0, 150 mM NaCl, 1 mM EDTA, 2 mM DTT, 0.05 % Triton-X-100, 2.5 mM desthiobiotin	4 CV

2.15.2 Purification of "Native" ADN Protein

Arabidopsis rosette leaf tissue (750 mg) was ground in liquid nitrogen and transferred in a 2.0 ml microfuge tube prefilled with extraction buffer (see Table 14). The mixture was vortexed 20 seconds and centrifuged for 15 min at 4°C and

20,000x g in an Eppendorf table top centrifuge. The supernatant was transferred into a new centrifuge tube prefilled with 50 µl Strep-Tactin Superflow Agarose (Novagen). The mixture was incubated by rotating for 30 min at 4°C and subsequently centrifuged for 20 s at 700x g. The beads were washed 3x with 1 ml wash-buffer (Table 14) each time. Bound protein was eluted with 2x 200 µl elution buffer (Table 14). Samples were analyzed by electrophoresis through a 12.5 % SDS gel as described in Section 2.15.1. Positive fractions were pooled and dialysed against 50 mM HEPES, pH 7.2 as described in Section 2.15.1. For activity assays, protein from a fresh preparation was used only or the protein was stored at 4 °C for a maximum of 3 days. For western blot analysis, protein was stored at -20 °C.

2.16 Subcellular Localization of ADN

Leaves of tobacco *Nicotiana benthamiana* were placed on a microscope slide and fixed lightly on the bottom with a drop of dH_2O. The tissue was viewed using a Zeiss LSM 510 Meta Confocal microscope. Samples were excited at 488 nm and emission was detected at 509 nm for EGFP and 650 nm for chlorophyll autofluorescence.

2.17 Gene Discovery, Sequence Collection and Characterization

The Basic Local Alignment Search Tool (BLAST) version 2.0 on the National Center for Biotechnology Information (NCBI) server (http://blast.ncbi.nlm.nih.gov/Blast.cgi) was used to screen the genome of *Arabidopsis thaliana* for putative ADNs. Screens using the amino acid sequence of *Crithidia fasciculata* as query were performed using the "*Arabidopsis thaliana* RefSeq protein" database. Putative nucleoside hydrolase identity was verified using visual analysis of their alignments and the presence of the aspartic motif (DXDXXXDD) (1.9).

Nucleotide and amino acid sequence of *Arabidopsis thaliana* proteins ADN 1, ADN 2 and ADA were retrieved from the TAIR webpage (http://www.arabidopsis.org/).

The amino acid sequence similarity between different proteins was analyzed using NCBI "BLAST 2 sequences" (http://blast.ncbi.nlm.nih.gov/bl2seq/wblast2.cgi).

The Conserved Domain Architecture Retrieval Tool (CDART) from NCBI (http://www.ncbi.nlm.nih.gov/Structure/lexington/lexington.cgi) was used to identify conserved domains in proteins of interest.

The NetPhos software (http://www.cbs.dtu.dk/services/NetPhos/) was used to predict phosphorylation sites on serine, threonine or tyrosine residues of ADN1 or ADN2.

The AtProteome database (http://fgcz-atproteome.unizh.ch/index.php) was used to identify the proteome map for ADN1 and ADN2. Proteins in the database were identified using mass spectrometry in different organs of Arabidopsis; proteins were displayed with the number of distinct peptides with which the protein was identified and whether or not these peptides contained post-translational modifications (Baerenfaller *et al.,* 2008)

AtGenExpress Visualization Tool (http://jsp.weigelworld.org/expviz/expviz.jsp) was used to obtain transcript abundance information for *ADN1* and *ADN2* using existing microarray data.

2.18 Multiple Alignment and Phylogenetic Analysis

The identification of ADA-related amino acid sequences was performed in NCBI Blast searches of GenBank restricted to eukaryotic taxa, using the AtADA protein as query. The annotation of the received sequences were manually reviewed; proteins without annotations were excluded from the analysis. The alignment was performed using ClustalW program provided on the European Bioinformatics Institute (EBI) server (http://www.ebi.ac.uk/). A phylogenetic tree was constructed according to Neighbor-Joining method (Saitou and Nei, 1987) using

percentage identity with the Jalview program at the EBI server (Waterhouse *et al.,* 2009). The Jalview program was used to eliminate gaps in the alignment and to minimize the redundancy of sequences using a threshold of 95 %. The design of the tree was adjusted using FigTree software version 1.2.3 (http://tree.bio.ed.ac.uk/software/figtree/).

Chapter 3

RESULTS

3.1 THE IDENTITY OF At4g04880 (*AtADA*)

Locus At4g04880 of *A. thaliana* is annotated as encoding a putative ADA based on a computational prediction; the amino acid sequence contains most of the catalytic important sequences for ADA activity. This research sought to demonstrate ADA activity for this protein product by 1) *in vitro* activity assay of the recombinant enzyme using indirect colorimetric assay and direct spectrophotometric assay, 2) *in vivo* test for functionality of the AtADA gene product in *A. thaliana* and *E. coli*. Both sets of experiments demonstrated that AtADA does not process ADA activity but further investigations of the amino acid sequence suggests that the protein product encoded by this locus belongs to the novel group of ADA-like (ADAL) proteins.

3.1.1 *AtADA* T-DNA INSERTION LINES

In order to elucidate the function of *AtADA*, two T-DNA insertion lines were retrieved from the SALK-Institute collection: *ada1-1* and *ada1-2* (Table 2) which contain T-DNA insertions in exons of the *AtADA* (Figure 5A). Mutant line *ada1-2* was acquired near the end of the research and has not yet been examined in detail. Western blot analysis demonstrated the absence of AtADA in the *ada1-1* mutant protein extract (Figure 5B, n=3 independent biological replicates). This result indicates that *ada1-1* is a complete knockout of *AtADA*. The AtADA expression level in *ada1-2* mutant was not investigated to date. However, homozygous *ada1-1* and *ada1-2* T-DNA insertion mutants displayed a wild-type-like phenotype when grown under long-day and short-day growth conditions (data not shown) suggesting that *AtADA* is not essential for plant growth and development when grown under ideal conditions.

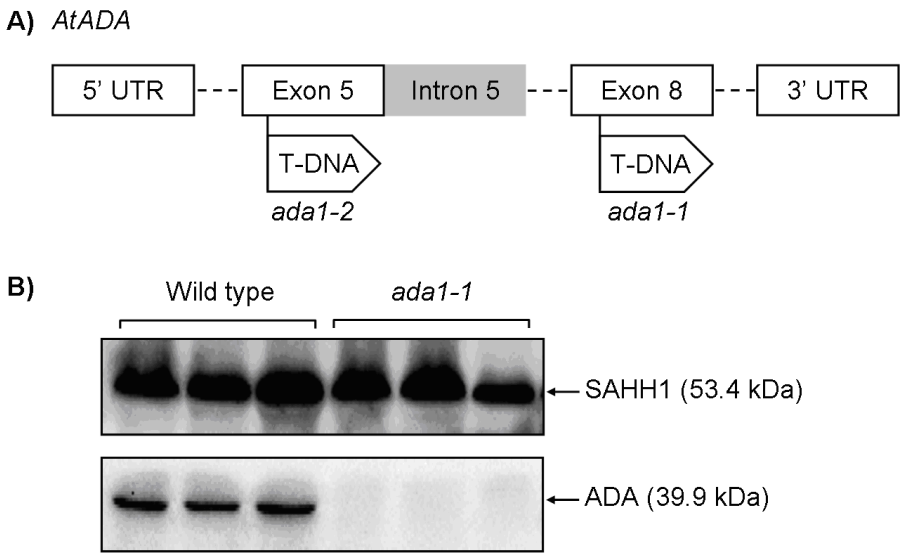

Figure 5 – Analysis of the T-DNA insertion allele in the *AtADA* gene (At4g04880) of *Arabidopsis thaliana*. A) A schematic of the *AtADA* gene and the location of the *ada1-1* and *ada1-2* T-DNA insertion alleles. The exact location of the T-DNA inserts is shown in Appendix A. B) Western blot analysis for expression of AtADA. Rosette leaf protein extracts (20 µg) from wild type (WT) and *ada1-1* were probed with polyclonal anti-AtADA antibody. Wild-type AtADA migrates at a molecular mass of 39.9 kDa. The AtADA polypeptide is absent in *ada1-1* extracts. Three replicates for WT and *ada1-1* were analyzed with the same result.

To test the hypothesis that *AtADA* encodes an ADA, the recombinant protein was tested for ADA activity using activity assays as described in the following sections. Furthermore, an *in planta* test for ADA functionality of the *AtADA* gene product in *A. thaliana* was conducted using *ada1-1* as a control (Section 3.1.3.1).

3.1.2 Detection of ADA Activity

ADA activity of the recombinant plant ADA (AtADA) was studied using two different activity assays as mentioned above. The protein used in the assays was expressed in *E. coli* and used as a crude extract or was purified using a C-terminal His-tag as described in Section 2.15.1. It was not possible to analyze the stability of purified AtADA enzyme under different storage conditions due to the lack of enzyme

activity; therefore the studies were done on fresh enzyme preparations. Enzyme was stored at 4 °C for a maximum of 7 days prior analysis.

3.1.2.1 Colorimetric Assay

To test the enzymatic activity of recombinant AtADA an indirect colorimetric assay was used based on the requirement for ADA in an assay of *S*-adenosylhomocysteine hydrolase (SAHH) (Section 2.12.3.1). SAHH catalyzes the reversible reaction of SAH into Ado and Hcy; the formation of TNB by Hcy was detected at 412 nm. When the assay was coupled with a functional ADA enzyme, the hydrolytic direction of the SAHH catalysis was ensured and the rate of TNB production was high. When using commercial grade calf intestinal ADA (Roche) the TNB production was 1.49 mM per min (Figure 6). When ADA was absent from the reaction mixture, the TNB production dropped to 0.38 mM per min (Figure 6). The lack of ADA activity changed the position of the reaction equilibrium towards the condensation reaction of SAHH, hence the hydrolysis reaction and TNB production was diminished. The addition of AtADA did not shift the equilibrium towards the hydrolysis reaction; the TNB production for the assay containing AtADA did not differ from the negative control assay without ADA (Figure 6).

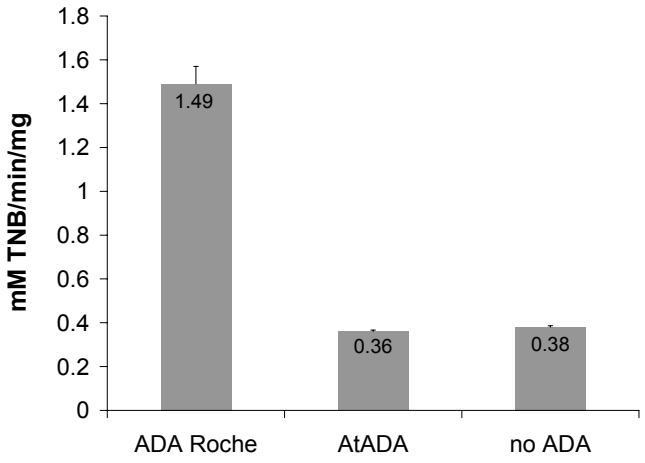

Figure 6 – Colorimetric assay for adenosine deaminase (ADA) activity. ADA activity was monitored indirectly in a continuous colorimetric assay at 412 nm detecting the increase of 2-nitro-5-thiobenzoic acid (TNB) concentration. When a functional calf intestinal ADA (ADA Roche) was added to the reaction 1.49 mM TNB per min was produced. In the absence of ADA in the reaction mixture TNB was produced but in a lower concentration. The addition of plant ADA (AtADA) did not lead to an increased TNB production different from the negative control. Five µg ADA protein was used in the assay. Data are expressed as mean ± standard deviation (*n* = 2).

3.1.2.2 SPECTROPHOTOMETRIC ASSAY

To test whether AtADA possesses ADA activity, an *in vivo* complementation test in *E. coli* was designed (Section 2.12.3.3). Successful complementation was determined by the growth promoting effect of the introduced plasmids coding for K12ADA or AtADA. The introduction of pMPB into *E. coli* served as a negative control in this experiment; the results are outlined in Section 3.1.2.3. These three complementation constructs were also used to check ADA activity in the lysate of SØ3834 and BL21(DE3) backgrounds using a spectrophotometric assay at 265 nm as described in Section 2.12.3.2.

It was expected that SØ3834 is deficient in ADA activity due to deletion of the gene, whereas in the host BL21(DE3) the ADA gene is intact and was assumed to

be functional. As shown in Figure 7, the negative control SØ3834pMBP did not show ADA activity whereas in BL21(DE3)pMBP a low enzyme activity was detected. This result was achieved for crude extracts obtained from cultures grown without IPTG or with 100 µM IPTG. The introduction of pAtADA did not lead to detectable ADA in SØ3834 cells and did not lead to an increase in the ADA activity in BL21(DE3) background for either growth condition.

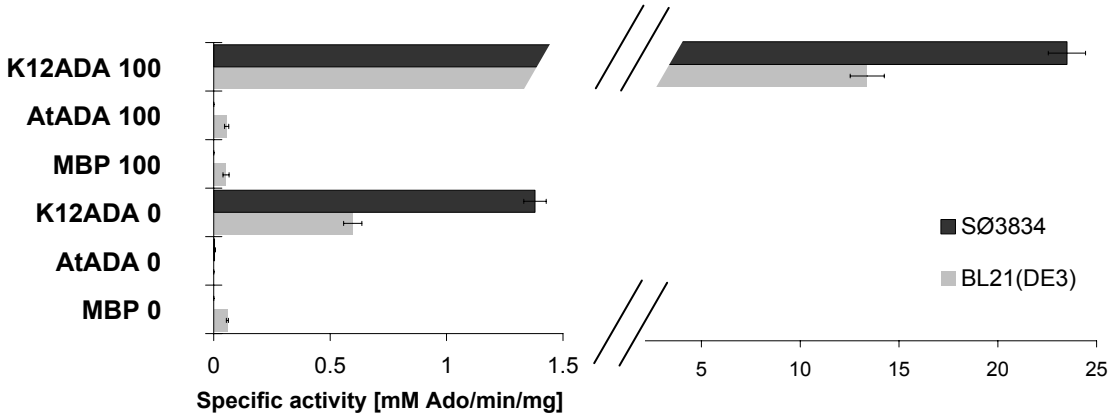

Figure 7 – ADA activity in *E. coli* crude extracts. Effect of tac::maltose binding protein (MBP), tac::*Arabidopsis thaliana* ADA (AtADA) and tac::*E. coli* K12 ADA (K12ADA) on the ADA activity of SØ3834 and BL21(DE3) lysate. Prior lysis, the cells were cultured for 17 h with either 0 or with 100 µM IPTG. Bars represent ± standard deviation (*n* = 2).

In contrast, the introduction of pK12ADA resulted in detectable ADA activity in SØ3834 crude extracts and an increase of ADA activity in BL21(DE3) when grown without IPTG (K12ADA 0, Figure 7). A further increase in ADA activity for both K12ADA lines was detected when the cultures were grown with 100 µM IPTG; the activity was increased 22-fold in BL21(DE3) and 17-fold in SØ3834 background.

The *E. coli* lysates used for the activity assays described above were separated in a 12.5 % SDS-PAGE and stained with Coomassie brilliant blue in an attempt to detect the K12ADA polypeptide. The expression of K12ADA (36.3 kDa) was easily detected in lysates of cells induced with 100 µM IPTG (lane 2 and 9, Figure 8); the polypeptide representing K12ADA protein is indicated with an arrow in

Figure 8. The high abundance of K12ADA protein in this crude extract correlates with the high ADA activity detected in the spectrophotometric assay (Figure 7).

K12ADA expression in cells grown without IPTG (lane 3 and 8, Figure 8) could not be detected on the SDS gel. The polypeptide profile detected in these lysates was indistinguishable to that of cells expressing MBP only (compare lanes 4 and 7). Either the K12ADA expression is below the detection limit of the Coomassie brilliant blue or the K12ADA polypeptide is masked by other proteins. Despite being unable to observe a K12ADA protein in the non-induced extract of either *E. coli* strain, ADA enzyme activity was detected in the spectrophotometric assay as shown in Figure 7 (K12ADA 0).

Lysates of *E. coli* strains carrying pAtADA did not show ADA activity in the spectrophotometric assay (Figure 7). The extracts were analyzed in a 12.5 % SDS-PAGE stained with Coomassie brilliant blue to verify the presence of the AtADA polypeptide and to eliminate the possibility that the lack of ADA activity was due to the lack of AtADA protein. In the lysates of non-induced cells no AtADA polypeptide was distinguishable (data not shown). IPTG induction of AtADA expression was associated with the presence of a new 39.9 kDa polypeptide (lane 5 and 6, Figure 8); AtADA was detected in the same abundance in the lysate of both *E. coli* strains used. In IPTG-induced lysates, AtADA and K12ADA were detectable in the SDS-PAGE but AtADA was less abundant than K12ADA.

No ADA activity was detected in the spectrophotometric assay of the lysate of SØ3834 cells expressing AtADA (Figure 7), nor was any enzyme activity above background found in BL21-CodonPlus(DE3)-RIPL. As mentioned earlier, the abundance of AtADA in the IPTG-induced lysate was lower than in the K12ADA lysate; increasing the amount of total protein used in the spectrophotometric assay to 50 μg did not lead to measureable ADA activity in SØ3834pAtADA (data not shown).

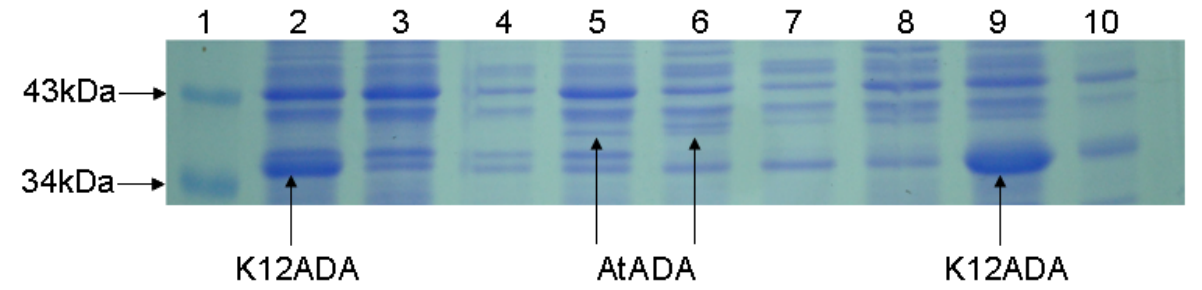

Figure 8 – Expression of K12ADA and AtADA. SDS-PAGE of SØ3834 (lane 6 to 9) and BL21-CodonPlus(DE3)-RIPL (lane 2 to 5, lane 10) lysates grown without IPTG (lane 3 and 8) or 100 µM IPTG (lane 2, 4 to 7, 9 and 10) harboring the ADA complementation constructs as follows: lane 2, 3, 8 to 10: pK12ADA; lane 5, 6: pAtADA; lane 4: pMBP. For SØ3834 lysates 25 µl were loaded onto the SDS-gel and 20 µl for BL21-CodonPlus(DE3)-RIPL lysates except in lane 10 only 5 µl was loaded. The complete SDS-PAGE picture can be seen in Appendix C.

As previously stated, AtADA expression was demonstrated by the presence of a 39.9 kDa polypeptide (lane 5 and 6, Figure 8) that was absent in the lysates of K12ADA and MBP. To verify the identity of the 39.9 kDa polypeptide and to ensure the functionality of the AtADA expression construct a western blot analysis was performed. The soluble protein fraction of BL21(DE3) lysates of all three complementation constructs were separated on 12.5 % SDS-PAGE and transferred to a PVDF membrane. The expression of MBP and K12ADA was strong and could be detected on the Ponceau stained membrane (panel B, Figure 9); both proteins were visible as distinct bands at the expected size (MBP: 50.9 kDa, K12ADA: 36.3 kDa). AtADA expression was low but detectable using western blot technique (panel A, Figure 9). The anti-AtADA antibody detected a distinct band in the lysate of BL21(DE3)pAtADA at the expected size for AtADA (39.9 kDa); a nonspecific polypeptide of approximately 34 kDa was detected in all extracts. Based on the Ponceau staining and the anti-AtADA western the expression level of all three constructs differed but all three plasmids were capable of expressing the transgene.

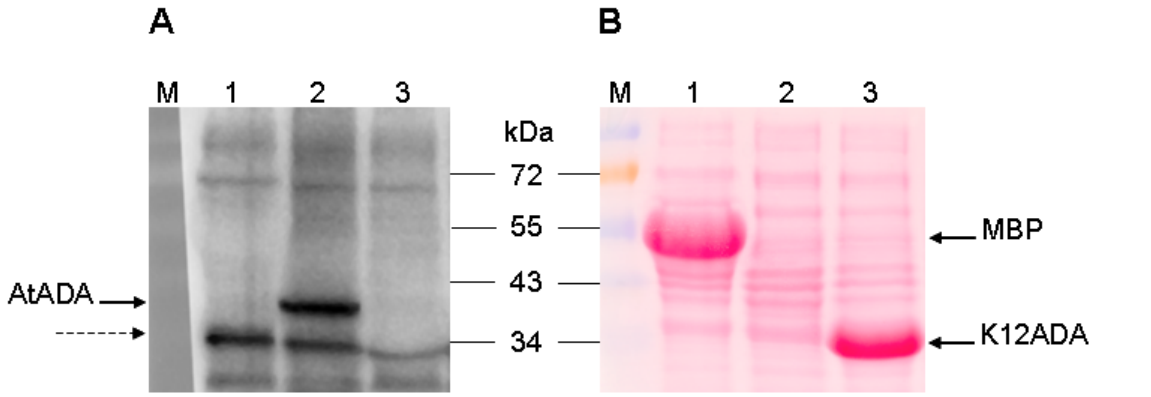

Figure 9 – Expression of ADA complementation constructs in BL21(DE3). Cells carrying pK12ADA (3), pAtADA (2) or pMBP (1) were induced with 100 µM IPTG at OD_{600}=0.5 and grown at 37 °C for 6 h. Cells were lysed and soluble fraction was separated on 12.5 % SDS PAGE and transferred to PVDF membrane. A) immunoblot stained with anti-AtADA antibody to show AtADA expression; dashed arrow marks polypeptide of strong but nonspecific antibody binding B) Ponceau-stained PVDF membrane visualizing maltose binding protein (MBP) and *E. coli* K12 adenosine deaminase (K12ADA) accumulation.

It was demonstrated above that the spectrophotometric assay can detect ADA activity in both BL21-CodonPlus(DE3)-RIPL and SØ3834 cell lysates; the use of SØ3834 cells was advantageous due to the absence of ADA background activity (K12ADA, Figure 7). The expression level of the plant ADA in *E. coli* was relatively low compared to the *E. coli* K12ADA (compare lanes 2 and 5 or lanes 6 and 9 in Figure 8), most likely due to a codon usage problem. If the specific activity of AtADA on Ado is much lower than that of K12ADA, the concentration of the enzyme in the lysate might not have been sufficient enough to be detected. To address this issue the recombinant plant ADA purified from *E. coli* (2.12.3.1) was used in higher concentration in the spectrophotometric assay. Ado was used as a substrate in two different concentrations: 65 µM and 200 µM. ADA activity was monitored at 240 nm wavelength detecting the increase of Ino concentration (2.12.3.2). The complete conversion of Ado to Ino by the recombinant ADA from the calf intestine (Roche) resulted in a change of absorbance of 0.26 for 65 µM Ado (graph A, Figure 10) and 0.76 for 200 µM Ado (graph D, Figure 10). For this control reaction 5 µg calf ADA

was used. The same amount of recombinant AtADA was used in the assay but no change in absorbance was observed (graph B, Figure 10); also, a five-fold increase of AtADA in the assay did not lead to a change in absorption over the time course (compare graph B and E, Figure 10). The addition of 25 µg AtADA caused a slight

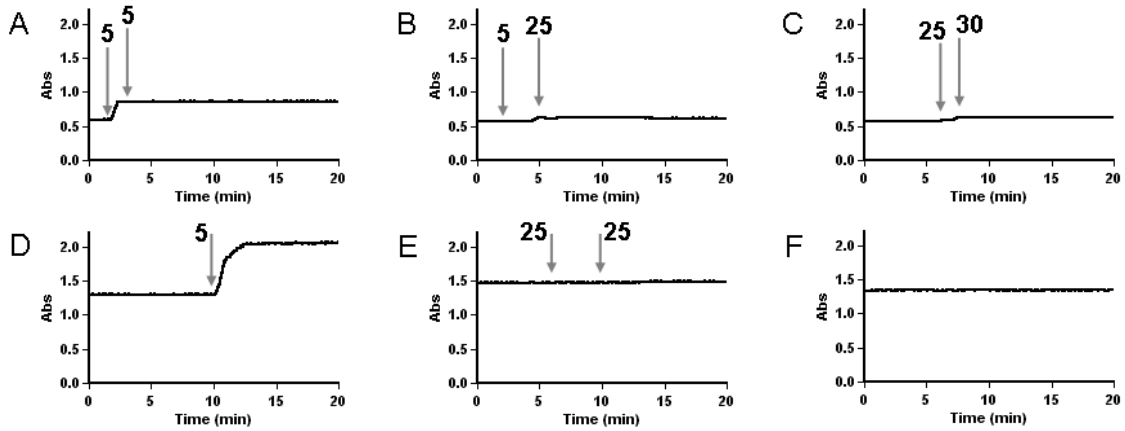

Figure 10 – Time course of adenosine deaminase (ADA) activity. ADA activity was monitored in a continuous spectrophotometric assay at 240 nm detecting the increase in inosine concentration. The substrate Ado was used at 65 µM (A, B, C) and 200 µM (D, E, F). The arrows in the graphs indicate the time when the enzyme was added to the reaction mixture; the numbers on the arrows indicate the amount of enzyme [µg] added. The following enzymes were used: A and D: recombinant calf ADA (Roche), B and E: recombinant plant ADA, C: recombinant plant Ado nucleosidase, F: no enzyme.

jump in the absorption at 240 nm (graph B, Figure 10) but this is most likely due to protein absorbance at this wavelength since there was no increase in absorbance over the time course of the experiment consistent with Ado hydrolysis. This conclusion was supported by the observation of a similar jump in absorption when 30 µg Ado nucleosidase (ADN) was added to the reaction mixture containing 65 µM Ado (graph C, Figure 10); Again, no change of absorption over the time course was detected. It was not tested if the addition of 30 µg BSA will cause the same jump in absorption. The fact that the conversion of Ado to Ade and ribose by ADN was not detectable at 240 nm demonstrates the specificity of the chosen wavelength for ADA activity. Thus neither the spectrophotometric nor the colorimetric assays provided

any evidence that the putative AtADA encoded by At4g04880 has ADA enzyme activity.

3.1.2.3 ADA COMPLEMENTATION IN SØ3834

E. coli SØ3834 is a multiple auxotroph with a deletion of the bacterial ADA gene; on minimal medium it requires Gua to grow but DAP can satisfy the Gua requirement if a plasmid coding for a functional ADA is introduced into the strain. Therefore, SØ3834 is a useful tool to determine ADA activity of cloned and overexpressed plant ADA by *in vivo* complementation (Section 1.6). Successful complementation was determined by the growth promoting effect of the introduced plasmid pAtADA. A plasmid coding for MBP was used as a negative control in this experiment. The introduction of a plasmid coding for the *E. coli* K12ADA is expected to complement ADA deficiency in SØ3834 and acted as a positive control (Section 2.12.3.3).

It was anticipated that the multiple auxotroph SØ3834 would not grow in minimal medium supplemented with DAP if no functional ADA was introduced. However, as shown in Figure 11 the SØ3834pMBP did grow in the minimal media but growth was significantly reduced compared to the strain carrying a functional *E. coli* ADA (K12ADA). There was leaky expression of K12ADA from the tac-promoter (non-induced condition, 0 µM IPTG) which promoted the growth of SØ3834 on the minimal medium; pK12ADA transformants grew to a 2.6-fold higher density as monitored by the OD_{600} of the culture, than did the pMBP transformants. pAtADA transformants did not show growth different from the negative control under non-induced conditions; SØ3834pAtADA grew to the same OD_{600} as SØ3834pMBP (0 µM IPTG, Figure 11). The low concentration of 5 µM IPTG elevated slightly the growth promoting effect of pK12ADA; the transformants grew to a 2.9 -fold higher OD_{600} than did the pMBP transformants. Again, pAtADA transformants did not differ in growth from the negative control (5 µM IPTG, Figure 11).

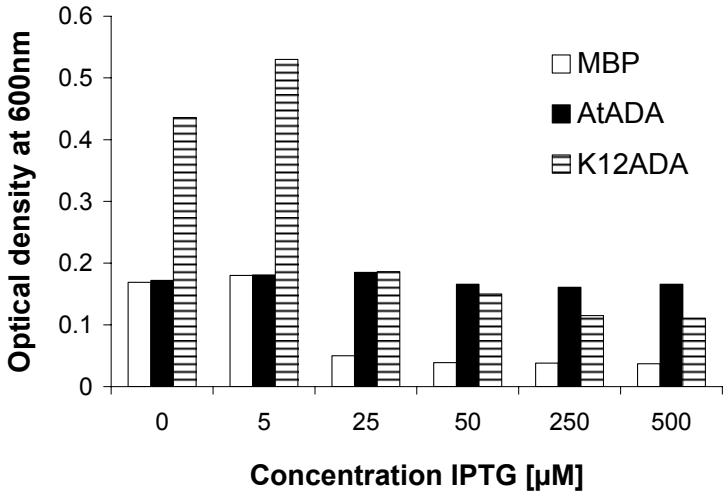

Figure 11 – Growth of SØ3834 in minimal media plus DAP. Effect of tac::maltose binding protein (MBP), tac::AtADA and tac::K12ADA on the growth of SØ3834 in minimal media supplemented with DAP. DAP can satisfy the guanosine requirement of SØ3834 if a functional ADA is introduced.

Interestingly, higher concentrations of IPTG (25 to 500 µM) caused decreased cell growth for SØ3834pK12ADA and SØ3834pMBP; culturing with 500 µM IPTG resulted in a drop of OD_{600} to 0.105 and 0.03, respectively. In contrast, the growth of SØ3834pAtADA did not change with increasing IPTG concentration. This suggested that overexpression of K12ADA or MBP might be inhibitory to *E. coli* and is consistent with the idea that AtADA was not being expressed in the same quantity in these strains.

3.1.3 Complementation of ADK Deficiency by AtADA

A final *in planta* test for ADA activity of the At4g04880 gene product was carried out. The AtADA cDNA was overexpressed in an ADK-silenced plant line with a severe phenotype (see Table 2) corresponding to 16 % residual ADK activity. Since the sADK lines are known to have higher concentrations of Ado leading to inhibition of MTases, the thought was that if At4g04880 encodes ADA activity it

should reduce the Ado concentration and alleviate some of the abnormal morphology of the sADK plants.

sADK 9-1 35S::ADA appeared phenotypically normal suggesting complementation of the ADK deficiency in sADK 9-1 plants by the At4g04880 cDNA expression. However, it must be excluded that the 35S promoter driving the expression of the putative AtADA was interfering with the activity of the 35S promoter expressing the ADK cDNA (which triggers ADK gene silencing). This type of *trans*-inactivation mediated by homology between 35S promoters on the T-DNAs has been documented previously by Daxinger *et al.,* (2008). These authors crossed 21 randomly chosen homozygous SALK lines with a line containing a 35S::β-glucuronidase (GUS) gene transgene; 11 of the lines showed silencing of the GUS gene in the F2 generation. Thus I conducted an ADK activity assay to exclude the possibility that the normal phenotype of sADK 9-1 35S::ADA plants was due to the loss of ADK silencing.

3.1.3.1 Radiochemical Assay of ADK activity in sADK 9-1 35S::ADA Leaf extracts

ADK activity was measured in desalted leaf crude extracts by the conversion of radioactive [2,8-^{3}H] Ado to AMP (Section 2.12.1.3) of sADK9-1 and sADK 9-1 35S::ADA plant lines and is presented as residual ADK activity compared to wild type in Figure 12. The lowest ADK activity was observed in sADK 9-1 plants with 7.25 % residual ADK activity. All transgenic sADK 9-1 35S::ADA plant lines contained an ADK activity of more than 80 % compared to wild type. Earlier analysis of the sADK lines showed that plants with more than approximately 50 % residual ADK activity have a normal phenotype (Moffatt *et al.,* 2002). Thus introduction of the AtADA overexpression construct driven by a CaMV35S promoter into the sADK 9-1 background caused an increase of ADK activity of about 70 % (Figure 12) explaining the wild-type phenotype of sADK 9-1 35S::ADA plants.

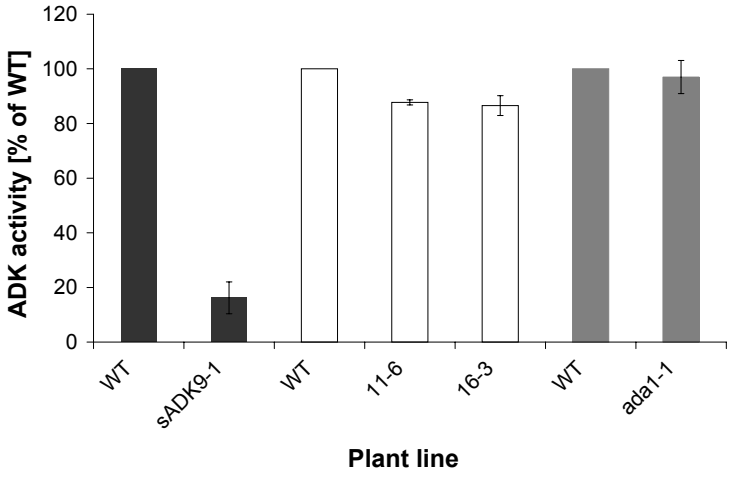

Figure 12 – ADK activity assay in sADK 9-1 35S::ADA plants. ADK activity was measured in desalted leaf crude extracts of the indicated plant lines and is expressed as percentage of wild-type activity (WT). Different colors indicate separate ADK assay runs. WT activity in nmol AMP/min/mg: black=3.61 (Engel, Diploma thesis), white=1.53, grey=1.42. Different transformants of sADK 9-1 carrying the 35S::ADA transgene (20-3, 11-6 and 16-3) were analyzed along with a T-DNA insertion mutant of At4g04880. Data are expressed as mean ± standard deviation (*n* = 2 for assay runs indicated with white or grey color, n=5 for black).

The interruption of the AtADA gene product in *ada* 1-1 plant lines did not lead to a change in ADK activity. Plants lacking the At4g04880 gene product had wild-type levels of ADK activity.

3.1.4 AT4G04880 ENCODES AN ADENOSINE DEAMINASE-LIKE PROTEIN

A phylogenetic study by Maier *et al.,* (2005) demonstrated sequence similarities between the ADA-related proteins ADA, ADE, AMPD and ADA-like enzymes and revealed conserved regions among and within these groups. This study did not include plant sequences. I carried out a phylogenetic analysis of eukaryotic ADA-related protein sequences to address whether At4g04880 encoded a protein belonging to one of these subfamilies.

Amino acid sequences used in this analysis were derived from the NCBI database (see Section 2.17) and are listed in Appendix B. The alignment of these 132 sequences was used to obtain the phylogenetic tree in Figure 14. Since the alignment of all sequences was very large, an alignment of reduced sequences is shown in Figure 13. Protein sequences used for the reduced alignment are listed in Table 15. All plant proteins included in this alignment are annotated either as putative ADA or as uncharacterized proteins.

Table 15 – Collection of ADA-related proteins used in the multiple alignment. Plant proteins annotated as ADA are marked with (*), uncharacterized proteins are marked with (°)

Protein name	Organism name	Common name	Protein accession
B9P4P9°	*Populus trichocarpa*	Western balsam poplar	B9P4P9
B9RXP2*	*Ricinus communis*	Castor bean	B9RXP2
A5C4M9°	*Vitis vinifera*	Grape	A5C4M9
Q8LPL7*	*Arabidopsis thaliana*	Mouse-ear cress	Q8LPL7
Q8H3U7*	*Oryza sativa subsp. japonica*	Rice	Q8H3U7
A3BN30°	*Oryza sativa subsp. japonica*	Rice	A3BN30
A2YPL0°	*Oryza sativa subsp. indica*	Rice	A2YPL0
B6TRX4*	*Zea mays*	Maize	B6TRX4
B4FH67°	*Zea mays*	Maize	B4FH67
A9TIL6°	*Physcomitrella patens subsp. patens*	Moss	A9TIL6
ADAL_HUMAN	*Homo sapiens*	Human	Q6DHV7
ADAL_PAPAN	*Papio anubis*	Baboon	A9X1B0
ADAL_BOVIN	*Bos taurus*	Bovine	Q0VC13
ADAL_MOUSE	*Mus musculus*	Mouse	Q80SY6
ADAL_DANRE	*Danio rerio*	Zebrafish	Q4V9P6
ADA_RAT	*Rattus norvegicus*	Rat	Q920P6
ADA_MOUSE	*Mus musculus*	Mouse	P03958
ADA_HUMAN	*Homo sapiens*	Human	P00813
ADA_DANRE	*Danio rerio*	Zebrafish	Q6DG22
ADA_ECOLI	*Escherichia coli*	Bacteria	P06134

The amino acid sequences of the retrieved proteins were compared and several conserved regions were found throughout the alignment (data not shown). The six most highly conserved regions of the alignment are shown in Figure 13; these

regions include important residues required for ADA activity i.e. His 15, His 17 and His 214 for zinc binding, Gly 184 Glu 217 His 238 Asp 296 for donating or accepting hydrogen bonds (Wilson *et al.,* 1991) (see Table 1). Amino acids conserved in all proteins are highlighted with a grey star underneath the alignment. Within the first conserved region shown in Figure 13, ADAL and plant proteins share three conserved amino acids; these amino acids are marked with a red star. Subsequently, in all conserved regions shown in Figure 13 plant proteins share many amino acids that define the ADAL subfamily (Figure 13, red stars) but not the ones that define the ADA subgroup (Figure 13, black stars).

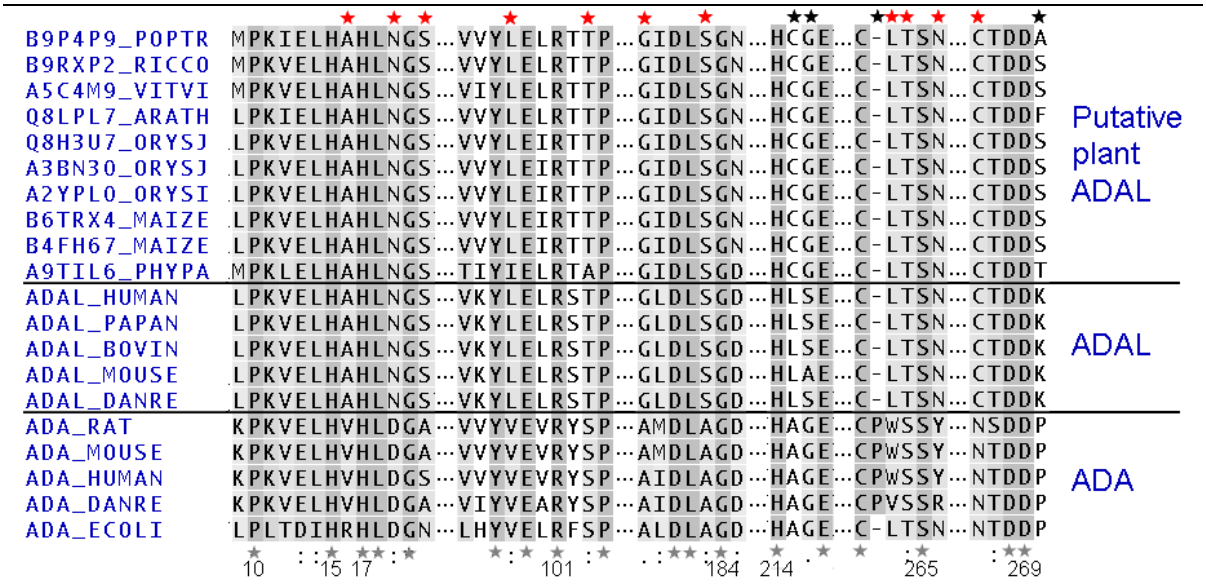

Figure 13 – Amino acid alignment of conserved domains among ADA and ADAL proteins. Grey stars indicate amino acids that are identical among all groups of proteins, red stars indicate amino acids conserved among ADAL proteins and black stars indicate amino acids conserved among ADA proteins. Species abbreviations are explained in Table 15. Horizontal lines represent margins between proposed groups of ADA-related proteins. Amino acids are numbered according to mouse ADA.

To determine the phylogenetic position of AtADA among the ADA-related subfamilies, a tree based on protein sequences from eukaryotes was constructed.

The phylogenetic analysis was performed using the alignment of all amino acid sequences listed in Appendix B. The alignment was performed using the ClustalW software on the EBI server and the phylogenetic tree was constructed according to Neighbor-Joining method (Saitou and Nei, 1987) using percentage identity (2.18). Jalview provided on the EBI server (2.18) was applied to minimize the redundancy of sequences using a threshold of 95 %. This threshold was not applied to the ADA-related sequences from human and baboon. As shown in Figure 14 the ADA, ADGF and the ADAL proteins clearly form three clusters but originate from a common ancestor. The cluster of classic ADA proteins is highlighted in red; it contains sequences annotated as ADA only. The cluster of ADAL (black and green) and ADGF (blue) contain a lot of proteins annotated as ADA or hypothetical proteins without annotation. The phylogenetic analysis from Maier *et al.* (2005) revealed that some ADA-related genes have been incorrectly labelled as classic ADAs and this I presume is the reason why so many putative ADAs are contained in the ADAL and ADGF cluster in Figure 14. Nevertheless, the ADAL and ADGF clusters in my analysis are defined by the position of already characterized proteins i.e. *Drosophila melanogaster* and *human* ADALs as well as *Danio rerio* and *Homo sapiens* ADGF/CECR1, respectively. The plant proteins included in the analysis formed a well defined cluster (highlighted with green in Figure 14) and are grouped within the ADAL subfamily. The sequences of four dicot plants cluster together as well as the three sequences of monocot plants maize, rice and sorghum. The ADA-related sequences from the moss *Physcomitrella patens* grouped within in the cluster of plant proteins but the branch length indicates that the *Physcomitrella* gene diverged earlier in evolution from the higher plant proteins (Figure 14). It is evident that the ADA-related sequences in plants do not belong to classic ADAs but to the novel group of ADALs.

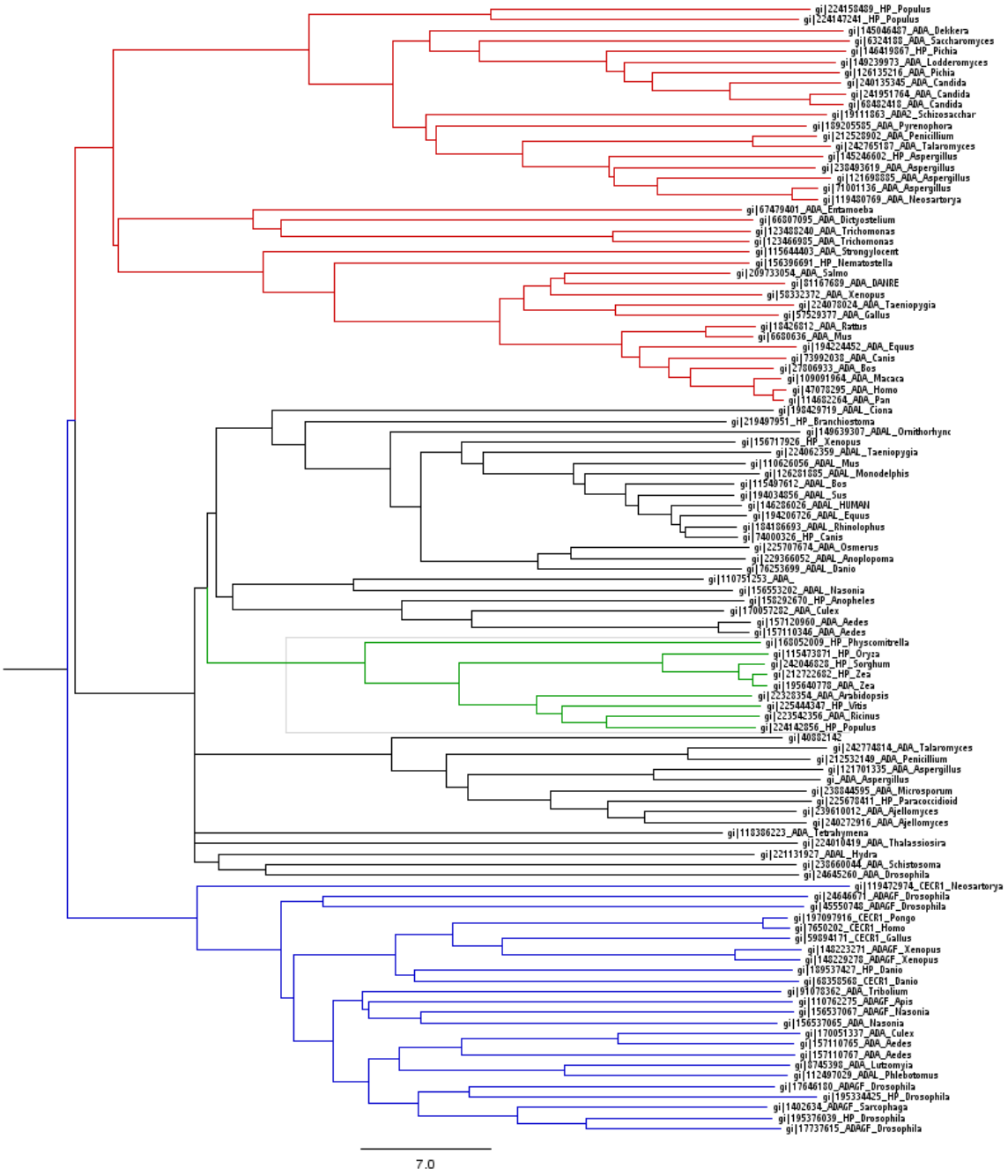

Figure 14 – Phylogenetic analysis of ADA-related proteins from eukaryotes. Rooted neighbor-joining phylogenetic tree, based on amino acid sequences showing the relationships between adenenosine deaminases (ADA, red), ADA-like genes (ADAL, black), ADA-related growth factors (ADGFs, blue) and the cluster of plant genes including *AtADA* (green). GenBank accession numbers are given along with the species name.

Another component of this research involved an additional putative Ado recycling enzyme. The genome of Arabidopsis was screened for putative ADNs using a known NH sequence from a protozoan. Candidate genes were identified, their gene products studied and their role in plant development was examined.

3.2 AT1G05620 AND AT2G36310 ENCODE PUTATIVE ADNS

ADN catalyses the irreversible hydrolysis of Ado to Ade and ribose; it may also accept CK ribosides as substrates. It contributes to purine salvage and it might be involved in the regulation of active CK levels. This enzyme activity has been demonstrated in crude extracts of several plants but no gene coding for ADN has been identified. The genome of Arabidopsis was screened for putative ADNs using a known IU-nucleoside hydrolase sequence from *Crithidia fasciculata*. Two candidate genes were selected and investigated, their gene products were studied and their role in plant development was examined using T-DNA insertion lines.

3.2.1 IDENTIFICATION OF PUTATIVE ADNS IN *ARABIDOPSIS THALIANA*

In the genome of Arabidopsis five genes have been computationally annotated as putative nucleoside hydrolases (NHs) (TAIR). The amino acid sequence of a NH that is characterized in structure and function was required to analyze the annotated genes for catalytic important residues and to screen the genome of Arabidopsis for further putative genes. NHs have been well characterized in parasitic protozoa such as *Crithidia fasciculata* (Parkin *et al.,* 1991) or *Trypanosoma vivax* (Versees *et al.,* 2001) because of their association in many human diseases i.e. trypanosomiasis (sleeping sickness) or malaria. Parasitic organisms are deficient in *de novo* synthesis of purines and are dependent on the host purine nucleosides; consequently NHs are particularly important for these organisms and are an object of intense research to find methods to cure deseases associated with parasitic organisms (Versees *et al.,* 2001). Various sequences of protozoa NH are available in genome databases and were accessible for the

screening approach of the Arabidopsis genome. The BLAST (Altschul *et al.,* 1990) on the NCBI server was used to screen the genome of Arabidopsis for putative ADNs (Section 2.17). The screen of the *Arabidopsis thaliana* proteome using the amino acid sequence of the inosine-uridine NH (IU-NH) of *C. fasciculata* led to the identification of the candidate proteins listed in Table 16; a tentative name was assigned to the genes for an easy identification in the following sections.

Table 16 – List of candidate ADN genes in *Arabidopsis thaliana*.

Gene	Annotation	*E*-value	Name (tentative)
AT2G36310.1	IU-preferring NH	$2e^{-35}$	ADN2
AT1G05620.1	IU-preferring NH	$2e^{-33}$	ADN1
AT5G18890.1	IU-preferring NH	$2e^{-05}$	ADN90
AT5G18860.1	IU-preferring NH	$4e^{-05}$	ADN60
AT5G18870.1	IU-preferring NH	0.013	ADN70

In the following, the candidate proteins retrieved by BLAST will be investigated in detail to determine their status as putative NHs. Their amino acid sequences was analyzed regarding the aspartic motif (DXDXXXDD), a highly conserved amino acid sequence in the N-terminal region of NHs that is involved in forming the nucleobase binding pocket (Versées and Steyaert, 2003). Tools provided at the TAIR and NCBI databases were used for further analysis of the candidate proteins, i.e. for gene structure, transcript abundance and protein domain structure.

Two proteins, ADN1 and ADN2 were retrieved with a very low expectation value (*E*-value) of $2e^{-33}$ and $2e^{-35}$ (Table 16); this value represents the number of expected hits with a equivalent or better alignment score than that of ADN1 or ADN2 in the database, by chance (Pevsner, 2003). These low *E*-values for the two candidate genes are a strong evidence that these proteins are very similar to IU-NH from *C. fasciculata.* Further proteins in the list shared a lower similarity with the *C. fasciculata* protein, as characterized by their higher *E*-values. Interestingly, ADN70 and ADN90 shared a very high amino acid sequence identity with ADN60

(71 % and 81 %, respectively; Table 18) but the sequence identity with each other was much lower (32 %).

ADN60 is a 100 kDa protein located in cell walls by mass-spectrometry based proteomic studies (Borderies *et al.,* 2003; Kwon *et al.,* 2005); the protein is composed of two NH domains (NCBI). The Conserved Domain Architecture Retrieval Tool (CDART, NCBI) retrieved 1770 proteins from the NCBI nonredundant protein database that contain a single NH domain but none with a double domain architecture as ADN60 (data not shown). BLAST on the NCBI server was used for finding similar double domain NH sequences in the non-redundant protein sequence databases using ADN60 amino acid sequence as query. The screen of the database led to the identification of six proteins only (Table 17) and all are derived from plants. It is evident that the double domain NH structure is unique to plants. Both domains of ADN60 have a high similarity to the inosine-adenosine-guanosine-NH from the parasitic protozoa *Trypanosoma vivax*. The amino acid alignment of ADN60, ADN70 and ADN90 (Appendix D) revealed that ADN70 aligns with an N-terminal section of ADN60 whereas ADN90 aligns with a C-terminal section of the same protein; the sections were not overlapping. These structures suggest that ADN60 was likely the common ancestor of both ADN70 and ADN90, since the longer ADN60 protein only exists in plants (data not shown). It is anticipated that ADN70 and ADN90 evolved from ADN60 by gene duplication and gene-splitting or gene fission event after *Arabidopsis thaliana* diverged from a common ancestor. The rate of gene duplications in *A. thaliana* is $2x10^{-9}$ duplicates per gene per year; the half-life to silencing and loss of a gene duplicate is estimated at $2.3x10^{-5}$ years (Moore and Purugganan, 2005). However, the average rate of fusion and fission events is lower with approximately $1x10^{-11}$ to $2\ x10^{-11}$ per gene per year (Nakamura *et al.,* 2007). The duplication event is supported by the contiguous location of ADN60 and ADN70 on chromosome five of Arabidopsis while ADN90 is separated from ADN70 by one gene only. Moreover, a recent duplication is likely since the shorter ADN90 and ADN70 proteins do not exist in other plant species. ADN60 might have evolved from

a single domain NH duplication event but if so, this event must have occurred in an ancestral plant since the duplicated gene is present in Arabidopsis and the other plant species that are listed in Table 17. This excludes the possibility that ADN60 evolved as a fusion of ADN70 and ADN90. The proposed gene fission event of ADN60 into ADN70 and ADN90 did not lead to two functional transcription units as indicated by: 1) the gene structure of ADN70 and ADN90 is incomplete (5' and 3' untranslated region (UTR) are missing) (TAIR); 2) no cDNAs or expressed sequence tags have been recovered for either gene (TAIR). In summary, ADN70 and ADN90 encode predicted NH-like proteins but it is not expected that the genes are functional. ADN70 and ADN90 were not considered as putative ADNs and were excluded from further investigations.

Table 17 – List of plant organisms carrying the gene for a double domain nucleoside hydrolase (NH). The NCBI accession number is listed for the putative double domain NH proteins recovered from the NCBI non-redundant protein sequence databases using BLAST.

NCBI protein accession	Organism name	Common name
NP_197387.1	*Arabidopsis thaliana*	Mouse-ear cress
ABD96887.1	*Cleome spinosa*	Spiderflower
EEF45449.1	*Ricinus communis*	Castor bean
CAO71050.1	*Vitis vinifera*	Grape
XP_002311814.1	*Populus trichocarpa*	Western balsam poplar
EEC79209.1	*Oryza sativa subsp. indica*	Rice
XP_002441080.1	*Sorghum bicolor*	Sorghum

The remaining candidate proteins ADN1, ADN2 and ADN60 contained the aspartic motif (DXDXXXDD), the hallmark of NHs (Figure 15) and thus were considered as putative ADNs. All three genes are functional transcription units supported by 23 to 66 cDNAs originating from different tissues (NCBI).

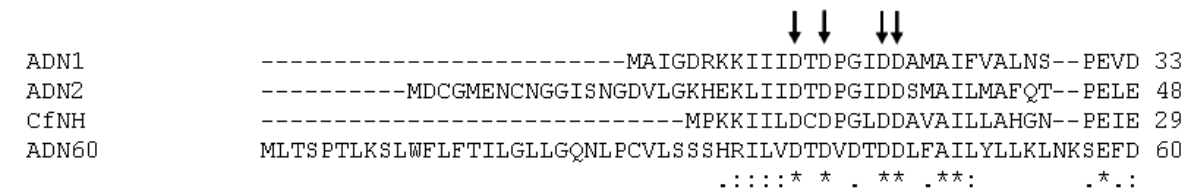

Figure 15 – N-terminal section of a multiple alignment of the amino acid sequence of candidate adenosine nucleoside hydrolases (ADNs) from *Arabidopsis thaliana* and inosine-uridine nucleoside hydrolase from *Chrithidia fasciculata* (*Cf*NH). Arrows indicate conserved amino acids of the aspartic motif, the hallmark of nucleoside hydrolases (Versées and Steyaert, 2003). The complete alignment is shown in Appendix E.

Beside the aspartic motif, additional amino acids are important for the catalytic function of nucleoside hydrolases (Versées and Steyaert, 2003). One of these, His 214 is involved in hydrogen-bonding interactions with Asp 14 and is proposed to protonate the leaving nucleobase, as demonstrated for Ino by Degano *et al.,* (1996). The protein ADN60 does not contain the His 241 residue (Figure 16). Mutagenesis experiments showed that a tryptophan (Trp260) contributes to catalysis in the IAG-NH (Versees *et al.,* 2001) but Trp 260 is absent in the amino acid sequence of ADN60 as well (data not shown). Therefore it is less likely that ADN60 possesses NH activity. Initially, five ADN candidate genes were identified in the genome of Arabidopsis. Only ADN1 and ADN2 were chosen for further investigation in this research; both genes have the highest similarity to *Cf*NH (Table 16) and contain most of the catalytic important amino acids for NH activity (data not shown).

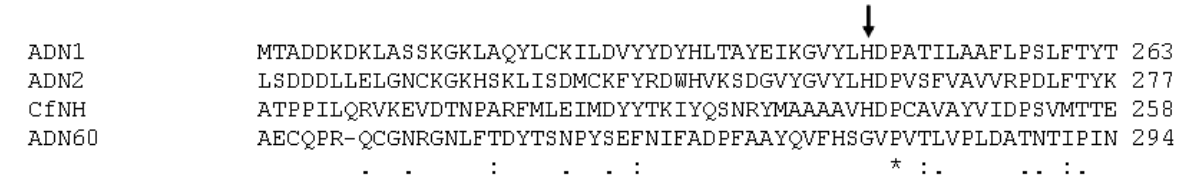

Figure 16 – Section of a multiple alignment of the amino acid sequence of candidate adenosine nucleoside hydrolases (ADNs) from *Arabidopsis thaliana* and inosine-uridine nucleoside hydrolase from *Chrithidia fasciculata* (*Cf*NH). The arrow marks a conserved histidine residue, important for the protonation of the leaving nucleobase (Versées and Steyaert, 2003). The complete alignment is shown in Appendix E.

Both, ADN1 and ADN2 share 31 % to 32 % amino acid identity with the IU-NH sequence from *C. fasciculata* (Table 18). At1g05620 and At2g36310 are currently annotated as IU-preferring NH family proteins. For the purposes of this project, the genes were tentatively designated as ADN 1 (At1g05620) and ADN 2 (At2g36310).

Table 18 – Amino acid sequence identity (percent) of putative *Arabidopsis thaliana* adenosine nucleoside hydrolases (ADNs) with the inosine-uridine nucleoside hydrolase from *Crithidia fasciculata* (*Cf*NH).

Protein	*Cf*NH	ADN1	ADN2	ADN60	ADN70
*Cf*NH	100				
ADN1	31	100			
ADN2	32	52	100		
ADN60	28	23	26	100	
ADN70	29	25	25	71	100
ADN90	27	23	24	81	32

The open reading frames of At1g05620 and At2g36310 were amplified by PCR using a cDNA template (Section 2.5.6) and cloned into *E. coli* expression vectors. Recombinant protein was used to investigate the identity of the putative plant ADNs using activity assays. Two mutant plant lines were obtained from the The Arabidopsis Stock Center containing a T-DNA insertion in At1g05620 or

At2g36310 (see Table 2); these plant lines were used to examine the role of ADN 1 and ADN 2 in plant development.

3.2.2 Purification of Recombinant ADNs

In order to characterize ADN1 and ADN2, both ORFs were cloned into expression vectors generating N-terminal 6xHis tag fusion proteins (Section 2.5.6); ADN1 was also cloned to create a N-terminal fusion with the Profinity eXact tag (2.5.5). Successful cloning of the expression constructs was verified by sequencing the complete ORF; it was confirmed that the protein coding sequence was in-frame with the affinity purification tag and the ribosome binding site was intact. The constructs were transformed into BL21(DE3) cells and protein was produced as described in Section 2.14. Cell pellets were frozen at -20 °C for up to four months prior purification on a nickel-NTA His Bind resin (Section 2.15.1) as shown in Figure 17 and Figure 19.

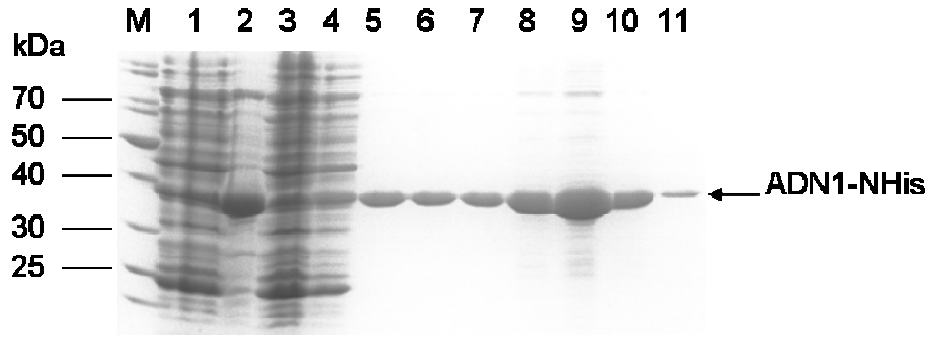

Figure 17 – Purification of His-tagged ADN1 from *E. coli* using nickel affinity chromatography. Samples of the different fractions collected during purification were separated in a 12.5 % SDS-PAGE and analyzed by Coomassie stain. Lane M: marker; 1: soluble fraction of crude lysate; 2: insoluble fraction of crude lysate; 3: flow through; 4 and 5: washes; 6 to 11: elution fractions. The masses of the marker polypeptides are shown in kDa. The purified ADN1 protein is indicated with an arrow. Protein was eluted in 3x 0.5 µl (fractions 6 to 8) and 3x 1 ml (fractions 9 to 11). A volume of 5 µl of fractions 1 to 3 was applied to the gel, for lanes 4 to 11 10 µl were applied. From the 350 ml culture 1 mg ADN1 was recovered.

Recombinant 6xHis tag ADN1 was released from the column partially in the wash fraction (Lane 5, Figure 17) but higher amounts were eluted in the third and fourth elution fractions (Lanes 7 and 8, Figure 17). A much higher amount of 6xHis tag ADN2 was eluted from the affinity column (Figure 18); most protein eluted in fractions three and four. The purified proteins were desalted and used for characterization of enzyme activity and substrate spectrum classification.

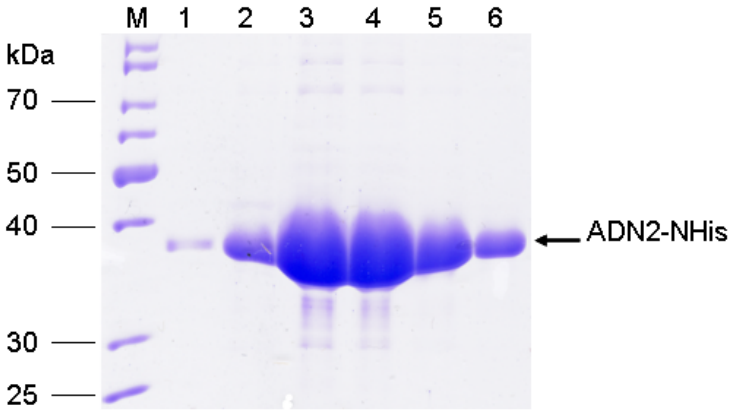

Figure 18 – Purification of His-tagged ADN2 from *E. coli* using nickel affinity chromatography. Samples of each of the six elution fraction were separated on a 12.5 % SDS-PAGE and stained with Coomassie. The masses of the marker polypeptides are shown in kDa and the purified ADN2 protein is indicated with an arrow. Five µl of the 1 ml elution fractions (1/200th) was loaded onto the SDS gel. The final yield recovered from 200 ml culture was 7.65 mg ADN2 protein.

Affinitiy chromatography was used to purify ADN1 protein from an *E. coli* culture using the Profinity eXact fusion-tag. The tag is cleaved from the fusion protein during the elution process thereby producing a highly purified ADN1 protein containing three additional amino acids on its N-terminus (Figure 19). The elution of bound protein was sufficient after 30 min incubation at RT (Figure 19), the majority of protein was eluted in this fraction. Considering the risk of loss of enzyme activity under RT conditions the shorter elution time of 30 min was used to obtain ADN1 protein for kinetic analysis.

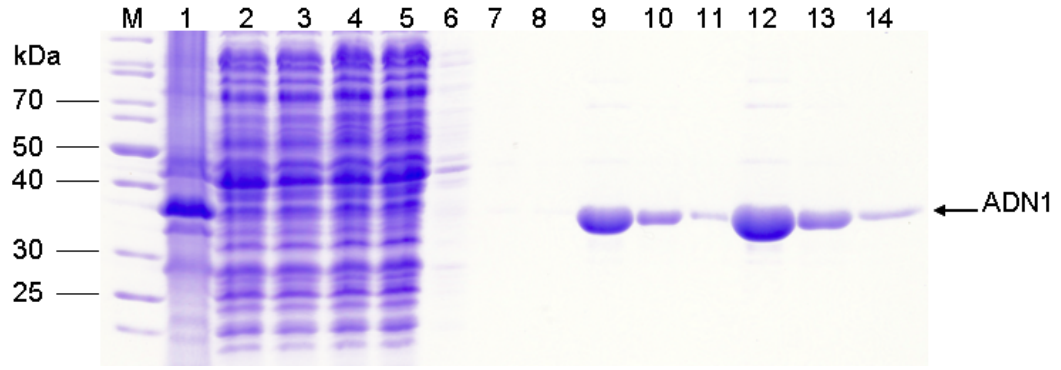

Figure 19 – Purification of ADN1 from *E. coli* by affinity chromatography using the Profinity eXact tag. Samples of the different fractions collected during purification were separated in a12.5 % SDS-PAGE and analyzed by Coomassie stain. The molecular masses of the marker proteins are indicated in kDa. Lane 1: insoluble fraction of crude lysate; 2: soluble fraction of crude lysate; 3 to 5: flow through; 6 to 8: washes; 9 and 12: elution fraction after 30 min incubation at room temperature (RT); 10 and 13: elution after 60 min incubation at RT; 11 and 14: elution fraction after 90 min incubation at RT. A volume of 5 µl of each fraction was applied to the gel, for lanes 12 to 14 10 µl were applied (1/250th of the elution fraction). From the 200 ml culture 2.5 mg purified, tagless ADN1 protein (indicated by the arrow) was recovered.

From a 200 ml culture 2.5 mg ADN1 and 7.65 mg ADN2-NHis of >95 % purity were obtained. The His-tag purification allowed the recovery of more protein than did the Profinity eXact purification, but with the latter method, a tag-free ADN1 protein was obtained, which is beneficial for the kinetic analysis.

3.2.3 Purification of "Native" ADNs

It was desirable to purify "native" ADN protein from Arabidopsis for multiple purposes: 1) to test for the presence of post-translational modifications via a shift in the migration of the protein analyzed by SDS-PAGE; 2) to investigate differences in the substrate spectrum of the "native" protein in comparison to the recombinant version; 3) to recover active ADN1 protein and 4) to investigate the detection limit of "native" ADN1 in western blot analysis using the anti-ADN2 polyclonal antibody. For these purposes, each ADN ORF was cloned into a binary vector creating an N-

terminal StrepII tag (C. P. Witte, unpublished); these constructs were stably introduced into wild-type Arabidopsis.

Both ADN-StrepII proteins expressed in *Arabidopsis thaliana* were purified to near homogeneity (Figure 20). For each transgenic plant line three replicate purifications were performed and in each case the same amount of purified protein was recovered as estimated by SDS gel analysis (compare lanes 1 to 3 and 4 to 6 in Figure 20).

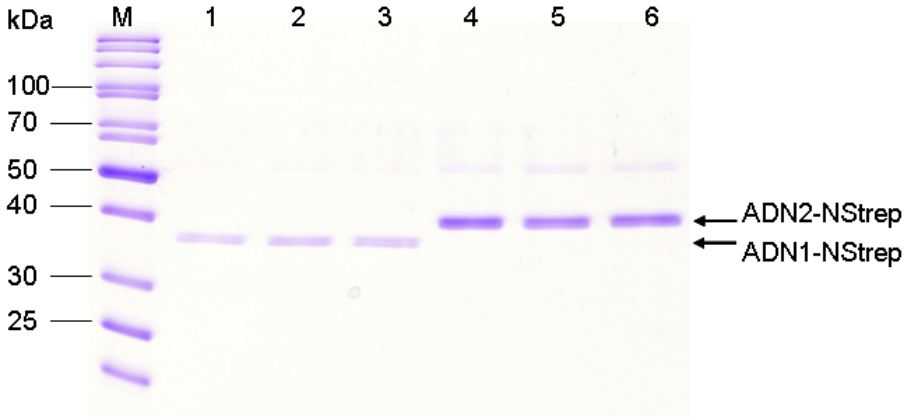

Figure 20 – Purification of ADN1 and ADN2 from *Arabidopsis thaliana* leaf tissue via StrepII tag affinity chromatography. The elution fractions were separated on a 12.5 % SDS-PAGE and analyzed by Coomassie stain. The molecular masses of the marker proteins are indicated in kDa. The arrows indicate purified ADN proteins. Each lane represents protein purified from approximately 750 mg leaf tissue. Lane 1 to 3: ADN1-NStrep, lane 4 to 6: ADN2-NStrep. Twenty µl of the 200 µl elution fractions (1/10th) were loaded onto the SDS gel.

More ADN2 than ADN1 was obtained from the plant tissue using the affinity purification. However, the yield recovered from approximately 3x 750 mg leaf tissue was low with three µg for ADN1-NStrep and eight µg for ADN2-NStrep, respectively (Table 19). This corresponds to a recovery of 1.34 µg ADN1-Nstrep from 1 g fresh weight leaf tissue and 3.8 µg for ADN2-NStrep (Table 19).

Table 19 – Results of ADN-StrepII protein purification from *Arabidopsis thaliana* leaf tissue.

	ADN1-NStrep		ADN2-NStrep	
Leaf tissue fresh weight [g]	2.2	10	2.1	10
Volume resin [ml]	3x 0.050	1	3x 0.050	1
Tissue/resin [g/ml]	14.8	10	14	10
Yield [µg]	3	20.5	8	51
Yield/tissue [µg/g]	1.34	2.05	3.8	5.1
Yield/resin [µg/ml]	20	20.5	53	51

A scaled-up purification using 10 g leaf tissue and 1 ml StrepTactin resin recovered more “native“ protein per g FW tissue (see Table 19) but the yield was still insufficient for activity assays.

3.2.4 Kinetic Properties of ADNs

ADN1 and ADN2 proteins were purified to near homogeneity from *E. coli* cells or Arabidopsis leaf tissue as described in the previous sections. The substrate spectrum and kinetic properties of these proteins was determined using a spectrophotometric assay. The colorimetric assay was used to verify the mode of reaction catalysed by ADN2 using the recombinant enzyme.

3.2.4.1 Spectrophotometric Assay

The substrate specificity of the putative ADNs was tested using a spectrophotometric assay following the decrease in absorbance of the substrate at a nucleoside-specific wavelength (Table 20). The ADN1 and ADN2 enzyme kinetics were analyzed using purified recombinant enzyme (Section 3.2.2) as the amount of “native“ protein purified was insufficient for this analysis.

The recombinant ADN2 protein can hydrolase Uri, Ino, Ado and Gua whereas no activity was detected for thymidine and cytidine (Table 20).

Table 20 – Kinetic analysis of ADN2-NHis.

Substrates	K_m [mM]	Specific activity [mM min^{-1} mg^{-1}]	k_{cat} [s^{-1}]	k_{cat}/K_m [$M^{-1}s^{-1}$]
Adenosine[a]	0.16	0.39[a]	2.31	$1.44x10^4$
Inosine	0.25±0.02	2.43±0.53	1.46±0.32	$5.86x10^3$
Uridine	0.33±0.05	23.00±5.62	13.80±3.37	$4.25x10^4$
Guanosine	Nd[b]	< 0.1	-	-
Thymidine	NDA	NDA	-	-
Cytidine	NDA	NDA	-	-

NDA: no detectable activity; Nd: not determined; a: The absorption of Ado was very high in the assay which limited the accuracy of the assay for this substrate. A deviation of the Beer's law is anticipated leading to the underestimation of K_m; b: The activity of ADN2 on Gua was too low to determine a K_m.

No nucleoside hydrolase activity was detected for ADN1 on the tested substrates. Neither the 6xHis tag fusion nor the tag-free protein (Section 2.5.5 and 2.5.6) showed NH activity in the spectrophotometric assay. Kinetic properties were determined for ADN2 only.

The kinetic constant K_m was determined by measuring the initial, constant rate of velocity for different substrate concentrations. Ado, Ino and Uri as substrates showed hyperbolic Michaelis-Menten kinetics. Example graphs for Ino and Uri are shown in Figure 21. V_{max} and K_m were determined graphically from the Michaelis-Menten plot and further kinetic constants as k_{cat} and k_{cat}/K_m were calculated based on these values.

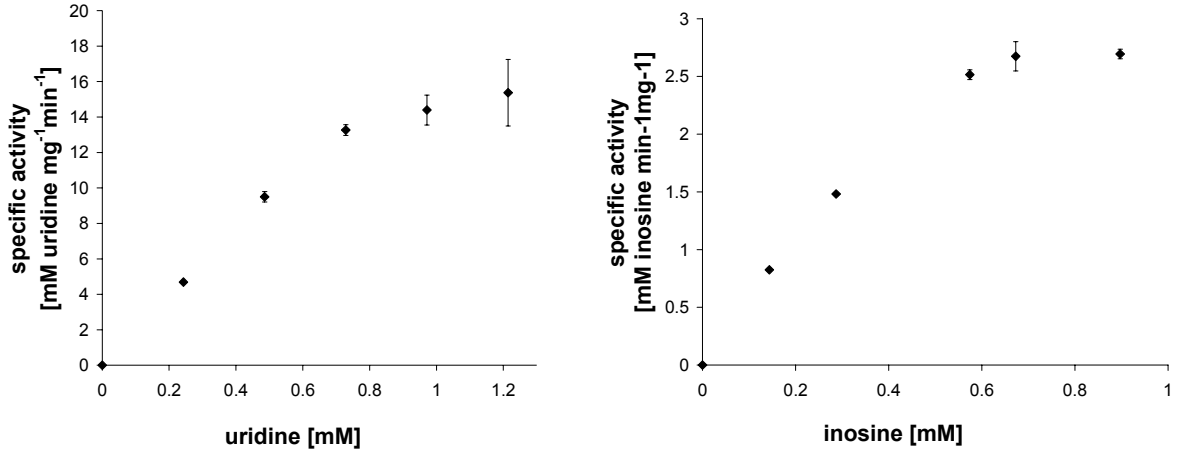

Figure 21 – Michaelis-Menten plot of ADN2 nucleoside hydrolase activity. Recombinant ADN2-NHis protein was synthesized in *E. coli* and purified to near homogeneity. The effect of substrate concentration on ADN2 hydrolysis activity is shown for uridine (left graph) and for inosine (right graph). Data given in the graphs represent experiments with 2 replicates for each substrate concentration. Bars indicate standard deviation.

As shown in Table 20, the K_m for Ino and Uri are relatively high and are in the mM range. The substrate concentrations useable in the assay were limited by the high absorption of the substrates at the desired wavelength. Approximately 1 mM Uri or Ino was the maximum concentration measurable in the spectrophotometer. Due to the high absorption of the substrates it was not possible to take measurements further into the saturation phase of the Michaelis-Menten curve. In addition, the absorption of the substrate at the highest concentration in the assay was 2 to 3. A deviation from the Beer's law is expected in this case leading to an underestimation of the V_{max} and K_m. This was particularly true for the very high absorbing substrate Ado. Even low Ado concentrations (~164 µM in contrast to 350 µM Uri and 450 µM Ino) led to an absorption of >1.0 and likely a strong deviation from Beer's law. Thus the real K_m for Ado will be much higher than that listed in Table 20. It was not possible to design the experiment for the spectrophotometric assay in order that no absorption above 1.0 was expected. The kinetic values for Ino and Uri were

expected to reflect the true values with only a minor deviation. Among the tested substrates, Uri was converted most efficiently with a 10 times higher k_{cat}/K_m than Ino mainly owing to a higher specific activity. The k_{cat}/K_m value for Ado was very high as well but once again, this was expected to be overestimated due to assay limitations.

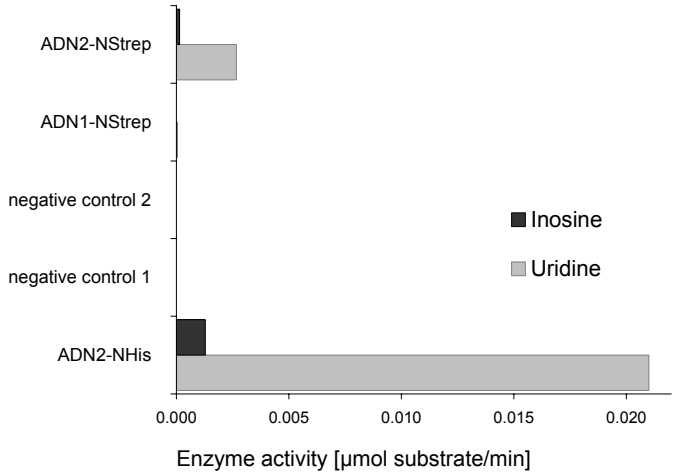

Figure 22 – Spectrophotometric assay of "native" ADN proteins. Analysis of purified plant protein (0.3 µg) on uridine and inosine as substrate using a continuous spectrophotometric assay at 280 nm detecting the decrease of substrate concentration. Both substrates were used at 150 µM. Negative control 1 represents the assay run without addition of enzyme. Negative control 2 represents the assay run with 10 µl elution buffer substituting the enzyme.

ADN1 and ADN2 StrepII tag proteins (hereafter referred to as "native" ADN1 and ADN2) were purified from Arabidopsis rosette leaves carrying the corresponding transgenes (Section 3.2.3).

The spectrophotometric assay was used to determine activity of both "native" enzymes on Ado, Ino and Uri at a concentration of 150 µM. The recombinant 6xHis tag ADN2 protein (3.2.2) was used as a positive control in this assay. Both "native" enzymes did not show detectable activity on Ado (data not shown). ADN2 utilized Uri as a substrate (Figure 22) but activity on Ino was very low. The "native" ADN1 protein did not have activity on the tested substrates. The amount of "native" protein purified from Arabidopsis leaves was not sufficient for further kinetic studies or

substrate spectrum investigations. However, these preliminary results are consistent with those obtained from the recombinant ADN protein.

3.2.4.2 COLORIMETRIC ASSAY

As described in the previous section, a spectrophotometric assay was used to analyse the enzyme kinetics of ADN2 protein (3.2.4.1). The metabolism of the tested nucleosides to bases and riboses was followed at a specific wavelength in each case and the decrease of absorbance of the substrate was observed during the enzymatic reaction. To verify that ADN2 was converting the substrates to base and ribose a second assay was used to determine the concentration of the ribose product. In this colorimetric assay the formation of the reducing sugar molecules was determined using neocuproine and subsequent colour development was measured at 450 nm (Section 2.12.2.2). Three different substrate concentrations were incubated with the recombinant 6xHis tag ADN2 protein (3.2.2) for 20 minutes. If a complete turnover of substrate to product had occurred in this period of time, a predictable amount of ribose in the sample could be calculated (white bar, Figure 23). The integrity of the assay was verified by including a reaction containing boiled enzyme or no enzyme (sample A and B, respectively, in Figure 23).

A

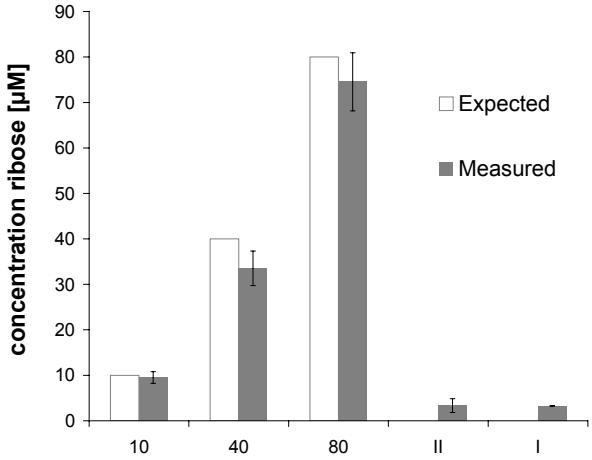

B

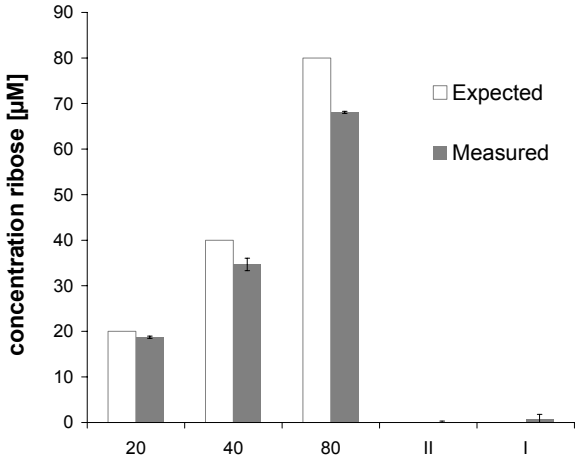

Figure 23 – Nucleoside hydrolase activity of ADN2-NHis detected by colorimetric assay. Twenty minutes after incubation of inosine (panel A) or uridine (panel B) with ADN2-NHis at 37 °C the abundance of ribose was estimated with a colorimetric assay. The expected amount of ribose by the complete turnover of substrate to base and ribose is shown as white bars and x-axis label; the amount of ribose present in the reaction mixture after incubation is shown as grey bars. Following controls were carried out: I) reaction without application of enzyme; II) reaction with 10 min boiled enzyme. Data are expressed as mean ± standard deviation (*n* = 2).

The catalysis of Ino and Uri by ADN2 resulted in ribose as a product (grey bars, Figure 23). The amount of ribose detected in the assays was lower than the expected value (white bars, Figure 22). This is likely to be caused by an incomplete turnover of substrate to product during the incubation period. The colorimetric assay verified that ADN2 catalyses a NH reaction.

3.2.4.3 TEMPERATURE AND PH DEPENDENCE OF ADN2

The spectrophotometric assay described above was used to determine the effect of temperature and pH on the velocity of ADN2. Uri was chosen as the substrate for these experiments as it was determined to be the preferred nucleoside for this enzyme (Table 20). The purified recombinant 6xHis tag ADN2 protein (3.2.2) showed an optimum pH at 7.5 and 8.0 depending on the buffer system used for the assay (Figure 24); it retained more than 40 % activity at pH 6.5 and 9.

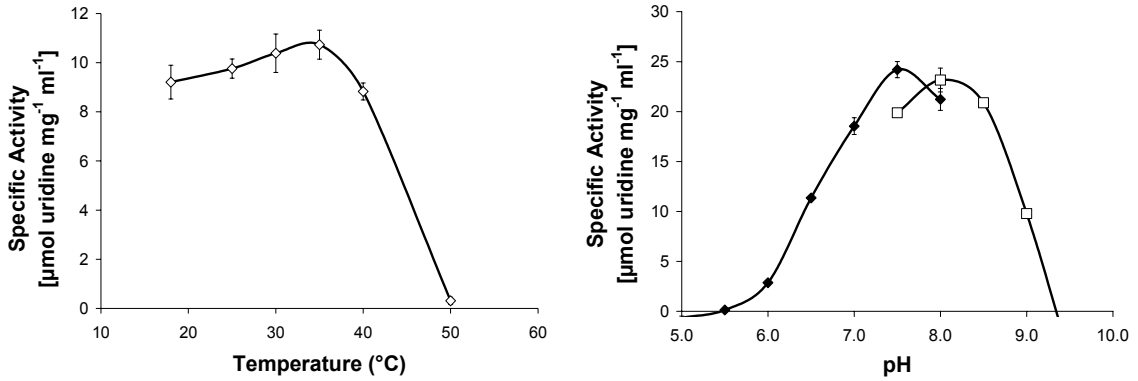

Figure 24 – Influence of temperature and pH on the catalytic efficiency of ADN2. Specific activity was determined by measuring the initial, steady rate of velocity at a constant uridine concentration but varying temperature or pH. For the temperature assay 150 µM and for pH assay 680 µM uridine was used. The temperature assay was run in standard assay buffer; pH assay was run in (◆) glycine buffer and (□) citrate-phosphate buffer at 30 °C. Bars indicate ± standard deviation (*n* = 2).

The optimum temperature for Uri hydrolase activity was at 35 °C, with the enzyme retaining 82 % activity at 40 °C but losing almost all activity at 50 °C (Figure

24). In the lower temperature range the hydrolase activity dropped slowly, retaining 85 % activity at the lowest temperature tested (18 °C).

The next stage of the research involved studying both putative ADNs *in planta*. The subcellular localization was investigated using transient expression in *Nicotiana benthamiana* leaves and T-DNA insertion lines were used to investigate the role of ADN1 and ADN2 in Arabidopsis.

3.2.5 Subcellular Localization of ADN1 and ADN2

For an analysis of the subcellular localization of ADN1 and ADN2, constructs for the expression of each ORF fused to the EGFP reporter gene and driven by the CaMV35S promoter were generated (Section 2.5.2). Transient expression was analyzed in *Nicotiana benthamiana* leaf epidermal cells and monitored under a confocal laser scanning microscope. As a positive control, *N. benthamiana* was transformed with a GFP translation construct; as expected it showed localization throughout the cell with strong signal in the cytoplasm and nucleus (Figure 25). Both ADN-GFP constructs showed clear localization in the nucleus and cytoplasmic strands (Figure 25).

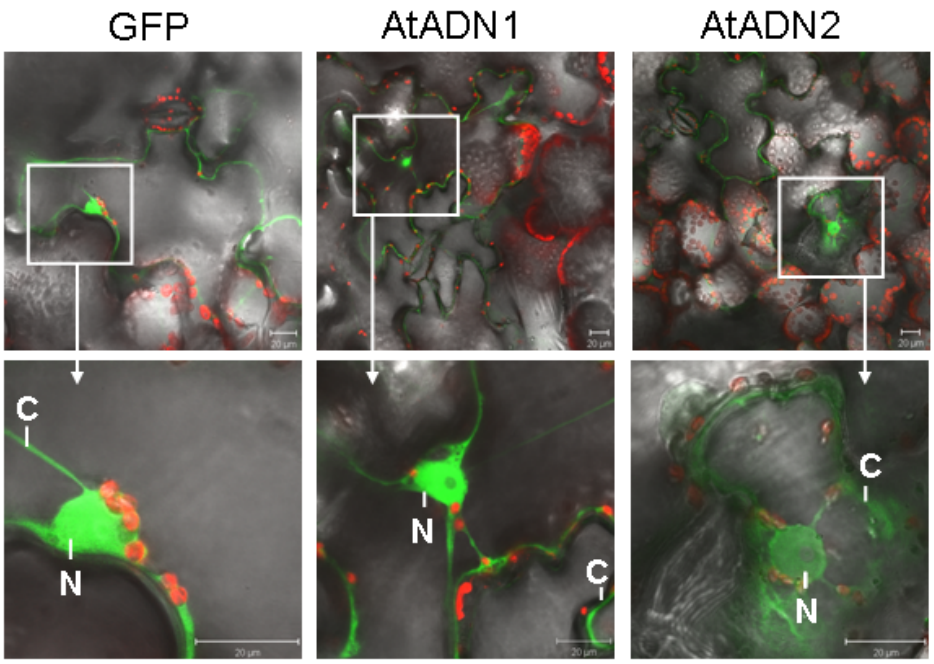

Figure 25 – Localization of transiently expressed ADN1-GFP and ADN2-GFP within tobacco *Nicotiana benthamiana* epidermal cells. Images of green fluorescent protein (GFP) and chlorophyll fluorescence were taken with a laser scanning confocal microscope. GFP signals are shown in green, chlorophyll autofluorescence in red. Both fusion proteins are approximately 67kDa. C = cytosol, N = nucleus. Scale bar represents 20 µm.

The construction of a larger double GFP fusion with ADN2 protein showed that the residence of ADN2 in the nucleus was due to diffusion; the larger ADN-2xGFP fusion protein was excluded from the nucleus (data not shown). Taken together these data showed that ADN1 and ADN2 are localized in the cytoplasm.

3.2.6 *ADN1* AND *ADN2* T-DNA INSERTION MUTANTS

The *adn1-1* and *adn1-2* T-DNA lines were obtained from The Arabidopsis Stock Center (Table 2) to examine the role of ADN 1 and ADN 2 in plant development. The mutant plants were evaluated for genotype, phenotype and ADN transcript and protein abundance.

3.2.6.1 GENOTYPING *ADN1-1* AND *ADN2-1*

DNA isolated from individual plants was screened using a primer specific for the left border of the T-DNA insertion and two flanking gene specific primers. For *adn1-1* primers 5, 6 and 22 (Table 6) and for *adn2-1* primers 4, 7 and 23 were used. The location of the T-DNA insert in the target gene was verified by sequencing (Appendix F). A *adn1-1 adn2-1* double mutant was obtained and backcrossed to wild type Columbia twice. Because no phenotype was apparent in the single and double mutant, PCR screens were performed to identify homozygous lines. DNA was isolated from backcrossed lines and analyzed in two sets of PCRs. The first PCR was designed to identify the T-DNA tagged *adn1-1* or *adn2-1* allele using the left border primer and gene specific primer as indicated in Figure 26. The second PCR used primer to identify the wild-type allele.

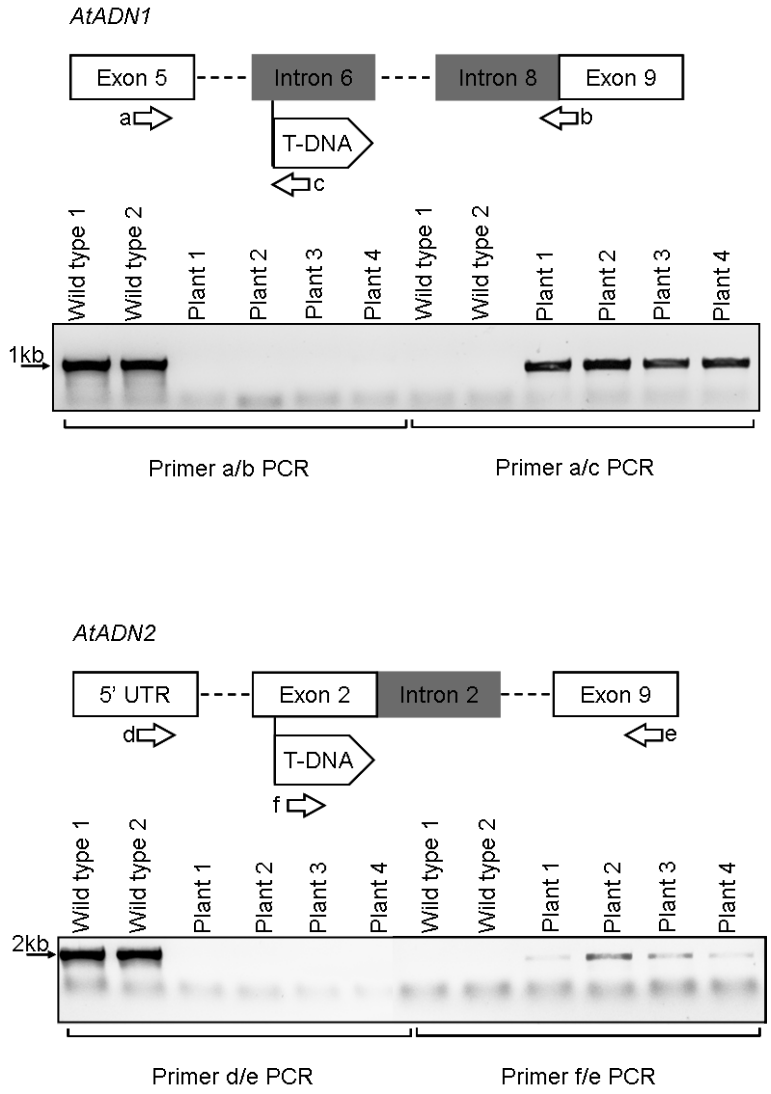

Figure 26 – Use of PCR to identify T-DNA insertion mutants *adn1-1* and *adn2-1*. Mutant plants homozygous for the T-DNA insertion were identified using two sets of primer. Primers a/b or d/e are gene specific for *Arabidopsis thaliana ADN1* or *ADN2* and flank the T-DNA insert; primers c and f bind in the T-DNA insert. Positions of the primers used for amplification are indicated below the schematic diagram. Primers used in the PCR were: a) 128723RP,b) 128723LP, c) LBa1, d) 083120LP, e) 36310R and f) LBb1.3. The exact location of the T-DNA insertion is shown in Appendix F.

A homozygous T-DNA mutant failed to amplify the wild-type allele but did amplify the T-DNA tagged *adn1-1* or *adn2-1* alleles. Homozygous mutants were investigated for ADN transcript and protein abundance as well as for phenotypic variations from wild-type Arabidopsis; the results of these investigations are presented in the following sections.

3.2.6.2 Transcript and Protein Abundance in T-DNA Insertion Lines

The expression of *ADN1* and *ADN2* was examined using reverse-transcription PCR analysis of both T-DNA insertion lines and wild type. RNA was isolated from rosette leaf tissue of homozygous plant lines (Section 2.4.3) and the presence of *ADN1* and *ADN2* transcript was examined by semi-quantitative and end-point reverse-transcription PCR (Section 2.6.4). In contrast to wild type, low *ADN1* and no *ADN2* transcript was detected in the double mutant *adn1-1adn2-1* in the linear range of amplification (Figure 27A, 30 cycles). A fragment of the ADN2 transcript can be detected at the end-point range of amplification (Figure 27A, 34 cycles), indicating that the T-DNA insertion in *adn2-1* did not lead to a complete knockout of ADN2 expression, although the decrease was stronger than that observed for ADN1 protein in *adn1-1*. The band that was observed in the RT-PCR was not a genomic DNA contamination since amplification of the corresponding genomic *ADN1* or *ADN2* regions would lead to a 1.3 kb larger product.

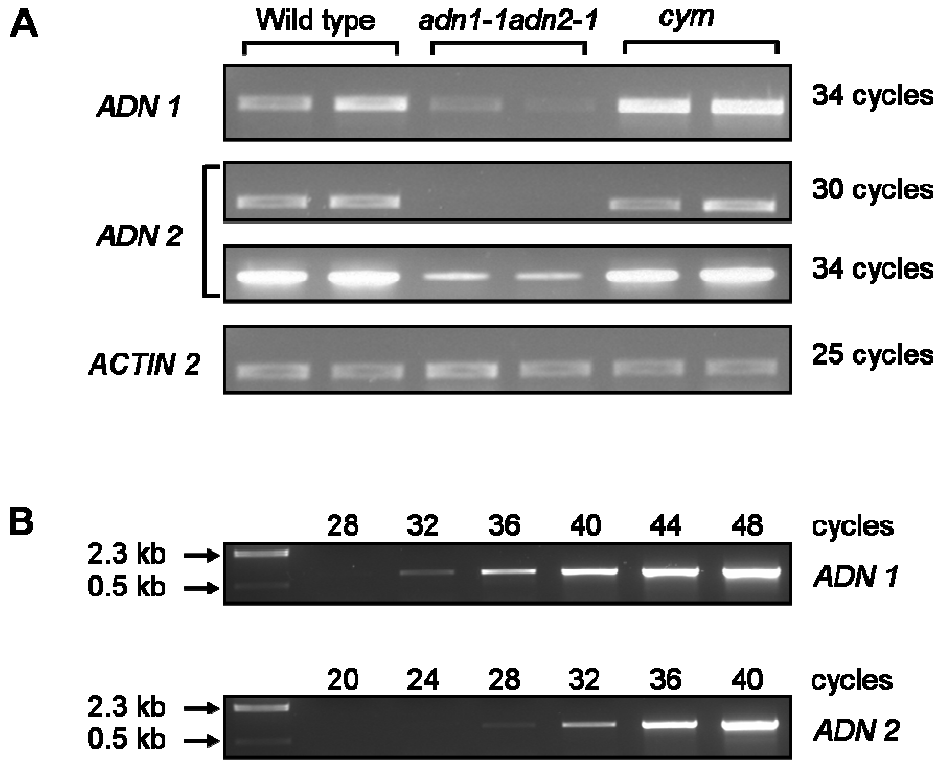

Figure 27 – Reverse-transcription-PCR analysis of *ADN1* and *ADN2* T-DNA insertion mutants. A) Reverse-transcription analysis for expression from *ADN1* and *ADN2* in rosette leaf tissue. Transcript abundance was analyzed in wild type, cytokinin metabolism mutant (*cym*) and *adn1-1adn2-1* double mutant using primer amplifying the full-length cDNA of *ADN1* and *ADN2*. *Actin 2* was used as a control. All PCRs were performed in semi-quantitative range of amplification; in addition, *ADN2* was amplified at nearly steady state level (34 cycles). B) The linear range of amplification was determined by carrying out six identical PCRs and stopping one reaction after every four cycles. Amplification products were quantified on a 1 % ethidium bromide-stained agarose gel.

ADN protein abundance was evaluated by immunoblotting. For western blot analysis a protein extract was isolated from leaf and root tips (apical 1 cm) of homozygous plant lines and separated by 12.5 % SDS PAGE. Immunoblot with polyclonal anti-ADN2 antibody showed that ADN2 protein is more abundant in root tips than in leaves (Figure 28). ADN2 is abundant at wild-type level in *adn1-1* mutant

plants but is down-regulated in *adn2-1* and in the double mutant *adn1-1adn2-1* (Figure 28). The T-DNA insertion in *adn2-1* did not result in the elimination of ADN2 protein in rosette leaves nor roots; this result is consistent with the RT-PCR that showed low ADN2 transcript abundance.

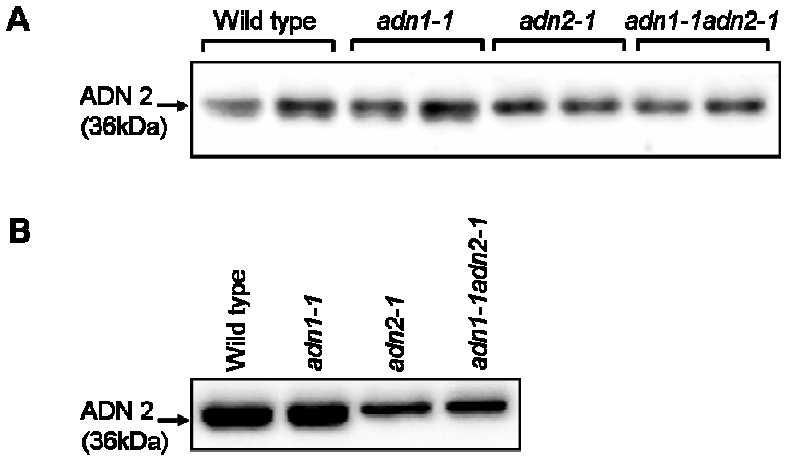

Figure 28 – Immunoblot analysis for expression of ADN2 in *ADN1* and *ADN2* T-DNA insertion mutants. A) Rosette leaf protein extracts and B) root protein extracts of wild type and mutant plant lines were probed with polyclonal antibody raised against 6x His tag ADN2 protein. Wild-type ADN2 migrates at a molecular mass of 36 kDa.

The polyclonal anti-ADN2 antibody is able to recognize both recombinant ADN1 and ADN2 proteins but is more sensitive for ADN2 (data not shown). Anti-ADN2 antibody detected a minimum of 210 ng of ADN1 but 50 ng of ADN2. No polypeptide of the expected size for ADN1 protein was detectable in root or leaf protein extracts. The abundance of ADN1 in these tissues must be below detection limits of the anti-ADN2 antibody.

Thus the T-DNA insertions in *ADN1* and *ADN2* do not eliminate either transcript, although the amount of ADN transcript is reduced compared to wild type (Figure 27). The mutant plant lines were further investigated for phenotypic deviations from wild-type Arabidopsis.

3.2.6.3 Phenotypic Investigation of ADN T-DNA Insertion Lines

Arabidopsis plants homozygous for *adn1* and/or *adn2* mutations germinated, grew, flowered and developed siliques similar to wild type when grown under normal, optimal conditions, indicating that the reduction of the proteins had no developmental effect.

I tested a range of environmental settings to reveal conditional phenotypes; preliminary result indicated differences between wild type and mutants for some conditions but the results obtained were not consistent. Since the abundance of ADN1 and ADN2 mRNA and protein was found to be higher in root tissue compared to other organs (AtGenExpress Visualization Tool, AtProteome database) most approaches concentrated on root growth of the mutants. In these experiments seeds of mutants and wild-type were germinated on vertical ½ MS media plates containing 5 µM Ino, Uri or Ado. The nucleosides did not have an effect on mutant root growth. When 7-day old seedlings were transferred onto vertical plates containing 5 µM cytokinins or cytokinin ribosides (6-benzylaminopurine, 6-benzylaminopurine-riboside, trans-zeatin or trans-zeatin riboside) a difference in root growth was observed. The growth of *adn1-1*, *adn2-1* and *adn1-1adn2-1* roots were less inhibited by these cytokinins than that of wild-type Arabidopsis seedlings. Unfortunately, these results were not consistent. Also unreliable was the result of the growth experiment under short-day light conditions; a phenotype was apparent in one set of experiments suggesting a delayed shoot development for the *adn1-1adn2-1* double mutant compared to wild type. This conditional phenotype was not observed for the single mutants. However, this result was not repeatable.

3.2.7 The Arabidopsis Mutant *cym*

The *cym* mutation was created using the chemical mutagen ethyl methanesulfonate and seeds were provided by Carol Auer (University of Connecticut, Department of Plant Science, USA). Mutant plants were identified

based on their resistance to CK riboside (6-benzylaminopurine-riboside) and their sensitivity to the free base (6-benzylaminopurine). The mutation is expected to be a single nucleotide alteration and located on chromosome 2 of Arabidopsis but a corresponding gene was not identified yet. Based on the screen for *cym* it was suspected to be a CK regulation mutant, likely a CK nucleosidase mutant. Increased anthocyanin concentration in young *cym* seedlings was reported by Carol Auer (1999) as well as stunted roots and short hypocotyls but phenotypic investigation of adult plants was not reported.

3.2.7.1 THE PHENOTYPE OF *CYM* MUTANTS

As known for juvenile seedlings, also adult *cym* plants showed increased anthocyanin concentrations in stem tissue (Figure 29). The base of primary shoots showed a dark red staining (Figure 29, panel 3 and 4) as well as juvenile secondary branches (Figure 29, panel 1). Wild-type Arabidopsis showed a reddish stem base occasionally (data not shown) but this was never as strong as *cym*.

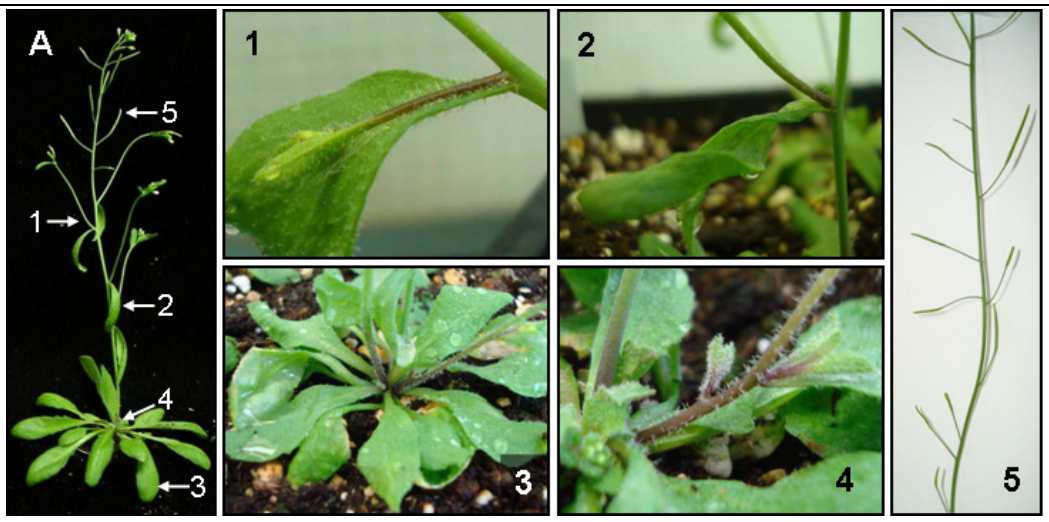

Figure 29 – Phenotypical analysis of *cym* mutants. Pictures 1 to 5 show phenotypic features of *cym* mutant plants in close-up view. The location of the close-up pictures are indicated with arrows on the overview image of wild-type *Arabidopsis thaliana* (A). 1) red secondary branch; 2) red node and curled cauline leaf; 3) pale green, flattened and slightly outwards curled rosette leaves; 4) red primary stem close to base and 5) normal sized and short siliques.

In addition to higher anthocyanin concentration in *cym*, the appearance of the rosette leaves differed compared to wild type. Rosette leaves of *cym* appeared pale green in colour, were flattened or slightly curled outwards (Figure 29, panel 3). A consistent variation in silique length was also observed. Siliques of *cym* plants were stunted and of different lengths although they contained healthy seeds (Figure 29, panel 5).

Other phenotypes observed in the *cym* line included stem fasciation and altered phyllotaxy (Figure 30). *Cym* mutants showed flattened and fasciated stems beside round wild-type stems. Fasciation was accompanied by phyllotaxy alteration as seen for siliques (Figure 30, panel 2 and 5). Fasciated stems could split into two (Figure 30, panel 5), accompanied by reversion to normal phyllotaxy and wild-type vascular pattern (Figure 30, panel 4).

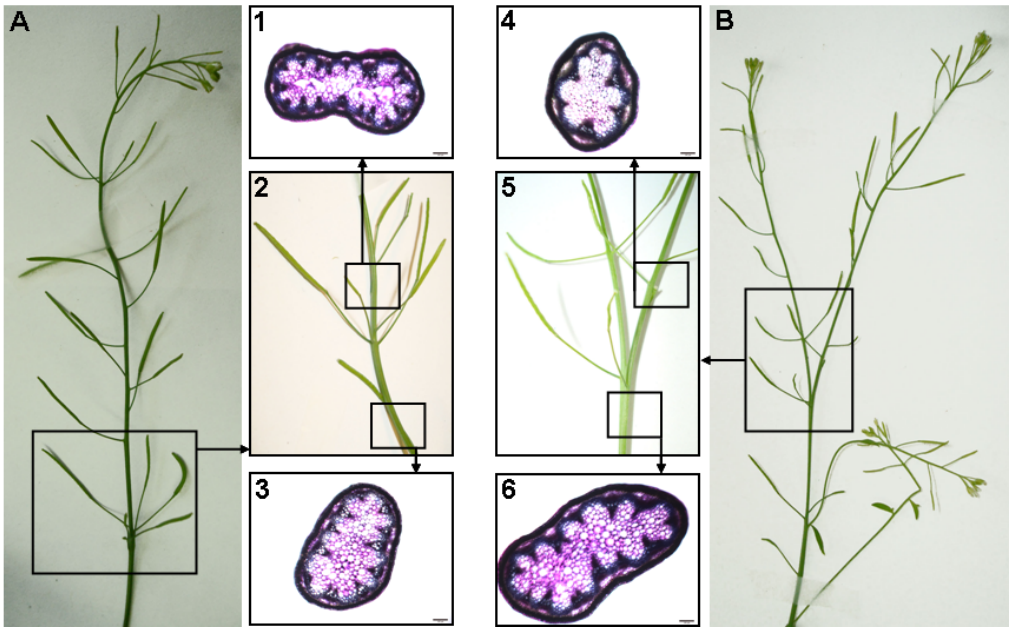

Figure 30 – Analysis of stem fasciation in *cym* mutants. *Cym* mutant plants grown under long-day conditions showed both, round wild-type appearing stems and flattened, fasciated stems often paired with altered silique phyllotaxy (A and B). Pictures 2 and 5 are magnified sections from pictures A and B. Cross sections were cut as indicated in picture 2 or 5 and stained with toluidine blue O. The scale bar in pictures 1,3,4 and 6 represents 120 µm.

3.2.7.2 Genomic Sequence of *ADN2* in *cym* Background

The *cym* mutation was mapped to chromosome 2 of Arabidopsis by Carol Auer (1999). *ADN2* was suggested as candidate gene for the location of the mutation due to close proximity to the mapped region; the proposed identity of *ADN2* as an Ado NH and a putative CK metabolizing enzyme might account for the *cym* phenotype described in the previous section. A direct sequence analysis of the *ADN2* gene was performed to test whether the *cym* mutation lay in the *ADN2* gene.

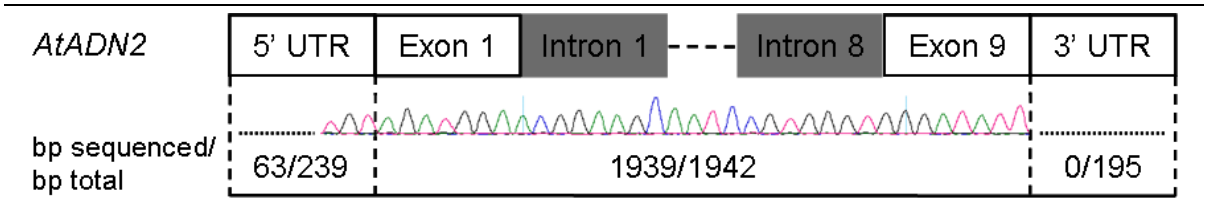

Figure 31 – Schematic of the sequencing result of *ADN2* gene in cym mutant background. The diagram shows the *Arabidopsis thaliana ADN2* gene organization (AtADN2) on top and the range of sequencing data obtained below. All exons and introns of ADN2 were sequenced completely only missing the 3 base pairs (bp) of the stop codon due to the primer used for PCR. The 5 prime untranslated region (5' UTR) was sequenced partially, the 3' UTR was not sequenced to date. The sequenced region did not show a deviation from wild-type ADN2.

To date the full-length *ADN2* sequence has been obtained except for the 3 base pairs of the stop codon due to a deletion in the primer used for amplification. In this sequence, no diversion from the wild-type allele was observed. The 5′ and 3′UTRs are incomplete or not sequenced yet.

Chapter 4

DISCUSSION

Ado recycling is an essential process in organisms. The importance of this process is illustrated by the SCID in humans which is associated with the loss of ADA enzyme activity (Fischer, 2000). The ADA deficiency causes accumulation of Ado and 2′-deoxyadenosine which is phosphorylated into deoxyATP. Immature lymphocytes are unable to convert dATP but it blocks cell division by inhibiting ribonucleotide reductase, an enzyme important for DNA synthesis (Fischer, 2000).

Higher plants also need to recycle Ado efficiently; plants depend largely on ADK activity for this process and loss of ADK has severe developmental consequences. For example, Arabidopsis *adk1 adk2* double mutants which lack ADK activity are embryonic lethal (B. Moffatt, unpublished); silencing of ADK activity causes a pleiotropic phenotype due to accumulation of Ado causing inhibition of transmethylation activities (Moffatt *et al.,* 2002).

The aim of this research was to investigate the functional significance of the putative Ado recycling enzymes ADA and ADN in *Arabidopsis thaliana*. This research sought to verify ADA identity of locus At4g04880 and ADA activity for the protein product. One further aim of this research involved the screen for ADN genes, homologs to nucleoside hydrolases from protozoa.

4.1 ATADA DOES NOT POSSESS ADA ACTIVITY

The Arabidopsis locus At4g04880 is annotated as a putative ADA/AMPD based on computational analyses (TAIR). Recombinant protein generated in *E. coli* has ADA activity based on a preliminary study using a colorimetric assay (Sherri Fry, 499 report).

I repeated the colorimetric assay but the result described by S. Fry was not obtained (3.1.2.1). Plant ADA did not show activity in the assay; reactions containing AtADA produced a signal indistinguishable from the negative control without ADA

(Figure 6). This colorimetric assay is an indirect measure of ADA activity only; the addition of ADA ensures that the reaction catalyzed by SAHH proceeds in the hydrolytic direction.

A direct test for the ADA functionality of the recombinant protein was sought next. In the selected spectrophotometric assay the enzyme activity was determined directly by the production of Ino which is detected as an increase in the absorbance at 240 nm. However, no ADA activity was detectable for purified, recombinant AtADA using this assay (Figure 10). The integrity of the spectrophotometric assay was verified by including a reaction containing recombinant ADA from the calf intestine (Roche); this enzyme preparation converted Ado to Ino effectively (graph A, Figure 10). Thus, the direct spectrophotometric assay is a valuable method to detect ADA activity and I recommend its use over the indirect colorimetric assay.

Recently, Popsiliova *et al.* (2008) demonstrated that the protein encoded by the gene At4g04880 acts with very low activity on Ade, Ado, AMP and ATP, without obvious substrate preference. These data were obtained using a spectrophotometric assay at 240 nm and a recombinant 6xHis tag protein. The activities detected by Popsiliova *et al.* (2008) were very low with k_{cat} for Ado of 0.005 and specific activity for Ade of 0.12 nkat/mg. The specific activity of the recombinant AtADA on Ado is reported to be approximately 30 % of the Ade value, which would correspond to 0.036 nkat/mg. This low catalytic activity is below the limit of detection of the spectrophotometer that I used. Despite their ability to detect these low activities, Popsiliova *et al.* (2008) concluded that it is not clear if the protein is a deaminase enzyme.

The recombinant AtADA used in colorimetric and spectrophotometric assays was purified from previously frozen *E. coli* BL21-CodonPlus(DE3)-RIPL cells using affinity chromatography; a loss of enzyme activity during the purification process is not expected but could not be excluded. Therefore, a study was done on freshly grown, quickly processed crude extracts from two different *E. coli* strains containing 6xHis tag AtADA. In addition, the spectrophotometric assay was performed at a

second wavelength (265 nm) that monitored the conversion of Ado by the decrease of the substrate concentration. The spectrophotometric assay detected K12ADA activity in BL21-CodonPlus(DE3)-RIPL and SØ3834 cell lysates (Figure 7). Thus, the assay at 265 nm is applicable to detect ADA activity in *E. coli* crude extracts although the use of SØ3834 cells is advantageous due to the absence of ADA background activity. Nevertheless, no activity for AtADA was detected (Figure 7). In IPTG-induced lysates, AtADA and K12ADA were detectable in the SDS-PAGE but the AtADA protein concentration was low due to codon usage problems (Figure 8).

The sensitivity of the spectrophotometric assay could be improved if the expression of AtADA in *E. coli* can be enhanced by either altering the rare codons in AtADA cDNA sequence or exploring an alternative expression host. In conclusion, neither the spectrophotometric nor the colorimetric assays provided any evidence that the recombinant protein encoded by At4g04880 has ADA enzyme activity.

4.2 AtADA Cannot Complement ADA or ADK Deficiency

In vivo complementation was used as a further approach to test for AtADA enzyme activity. Information relevant to AtADA overexpression in an Arabidopsis mutant can be derived from a resulting phenotype but a uniform and sensitive method to evaluate these effects was important. The complementation test involved providing the AtADA cDNA as a transgene to an ADK-deficient plant (sADK 9-1) which otherwise has a pleiotropic phenotype due to Ado accumulation. The premise of the test was if AtADA encodes a functional ADA, this activity might reduce the Ado concentration and alleviate the stunted growth, wavy leaves and reduced fertility associated with ADK deficiency. Although this *in planta* complementation test mimics the *in vivo* situation well, it was possible that the results might be inconclusive due to variability of sADK mutant phenotype or gene silencing issues.

Since ADA is a monomer and homolog to the *E. coli* enzyme, I also used a more convenient and faster approach for complementation based on the *E. coli* ADA deletion mutant strain SØ3834 (Hove-Jensen and Nygaard, 1989; Chang *et al.,*

1991). In this test, SØ3834 cannot grow on a defined medium unless provided with a functional ADA activity. Codon usage problems were apparent in earlier AtADA expressions using BL21-CodonPlus(DE3)-RIPL cells; therefore one concern with this complementation approach was that codon usage problems might reduce the expression of the AtADA transgene in SØ3834 and thus reduce the utility of the test. Fortunately, SDS-PAGE analysis of the *E. coli* crude extracts revealed detectable AtADA protein so the lack of expression was eliminated as a concern (Figure 8).

In analysing the growth promoting effect of AtADA and K12ADA on SØ3834 it was evident that K12ADA but not AtADA was able to complement ADA deficiency (Figure 11).

The final *in planta* test for ADA activity of the At4g04880 gene product was inconclusive due to gene silencing issues. sADK 9-1 35S::ADA appeared phenotypically normal but this was not due to complementation of the ADK deficiency by the At4g04880 cDNA expression. Instead the 35S promoter driving the expression of the putative AtADA was interfering with the activity of the 35S promoter expressing the ADK cDNA as verified by ADK activity assay (Figure 12). Other cases of *trans*-inactivation mediated by homology between 35S promoters on T-DNAs have been documented previously by Daxinger *et al.* (2008). These authors studied 21 SALK lines which were crossed with a line containing a 35S::GUS transgene; 11 of these lines showed silencing of the GUS gene in the F2 generation. Thus, using the 35 S promoter for the AtADA overexpression construct was not a good choice.

An alternative *in planta* complementation test was devised involving the use of an ADK-deficient line generated by artificial microRNA expression (S. Lee, unpublished results) and an AtADA cDNA expressed from the manopine synthase promoter. The preliminary results showed no complementation of ADK deficiency by AtADA.

Taken together, it is reasonable to conclude that overexpression of AtADA did not complement ADA deficiency in Arabidopsis and that the protein encoded by

locus At4g04880 does not encode a functional ADA. No further ADA-related genes have been identified in the genome of Arabidopsis, therefore it is concluded that ADA activity is not present in this plant.

4.3 Phylogenetic Analysis Reveals That At4g04880 Encodes an ADAL

Activity assays demonstrated that the recombinant AtADA does not process ADA activity; furthermore, it was demonstrated that AtADA is not able to complement ADA deficiency in *E. coli*. Concurrent phylogenetic analysis of ADA-related sequences from eukaryotes revealed that the protein encoded by At4g04880 is related to the classic ADA subfamily but in fact belongs to the ADAL family (Figure 14). The ADAL proteins are closely related to the ADA subgroup in sequence similarity and share numerous important catalytic residues. However, no ADAL subfamily member has been shown to have ADA activity (Maier *et al.*, 2005); the results presented in this thesis show that AtADA is no exception.

This raises the question of the function of AtADA but to date no answer can be given. Since Maier and colleagues published the discovery of the novel ADAL subfamily in 2005 only two additional publications were released dealing with this topic. In 2007, Rosemberg and colleagues investigated the expression profile of ADA1, ADA2 and ADAL genes in brain, gills, heart, liver, skeletal muscle and kidney tissue of zebrafish (*Danio rerio*) using RT-PCR. The results demonstrated that each protein is expressed in all tissues; ADAL transcript was more abundant in liver and kidney and less in the heart. In a second study the biochemical properties of these ADA-related proteins were investigated but no evidence about the functionality of ADAL was obtained (Rosemberg *et al.,* 2008).

In general, the knockout of At4g04880 gene product demonstrated that this locus is not essential for Arabidopsis development, when grown under normal conditions. The locus At4g04880 should be re-annotated as ADAL.

4.4 ADN1 AND ADN2 ARE POTENTIAL ADNS

ADN enzyme activity has been demonstrated in crude extracts or partially purified preparations of several plants including spinach beet (Poulton and Butt, 1976), barley (Guranowski and Schneider, 1977) and wheat (Chen and Kristopeit, 1981) but in none of the investigated plants has the gene coding for ADN been identified. The aim of this research was to screen for ADN genes in *Arabidopsis thaliana* and to investigate their enzyme activity. BLAST was used to screen the genome of Arabidopsis and the existence of five candidate genes was revealed (Table 16). I chose two genes, ADN1 and ADN2 for investigation and at the time I started my research both were computationally annotated as IU-NH. During the time of my study the genes were re-annotated as Uri ribohydrolases by Jung *et al.* (2009). The results I obtained for the characterization of both proteins are consistent with those of Jung *et al.* (2009); no substrate was found for ADN1 whereas ADN2 acts predominately on Uri. The results of my research are discussed in the following sections.

4.5 ADN2 POSSESSES NUCLEOSIDE HYDROLASE ACTIVITY

ADN2 expressed as recombinant protein in *E. coli* was purified to near homogeneity by affinity chromatography (Figure 18); this preparation had a specific activity of 23 mM Uri min^{-1} mg^{-1}. The recombinant ADN2 utilized additional substrates such as Ino, Ado and Gua but strongly preferred Uri. Its specific activity on Uri was 9.5- and 59-fold higher than on Ino or Ado, respectively (Table 20). Thus, the substrate spectrum of ADN2 includes purine and pyrimidine nucleosides, which is similar to that of the homolog from *C. fasciculata* that also prefers Uri and 5-Methyl-Uri over other substrates (Parkin *et al.,* 1991). The K_m values obtained for ADN2 on the tested substrates appeared high, being between 0.16 to 0.33 mM (Table 20) but values for the IU-NH from *Crithidia* have a similar range (0.38 to 1.2 mM). The recombinant ADN1 did not show activity on any tested substrates including Ado, cytidine, Ino, thymidine and Uri.

The precision of the kinetic values obtained for ADN2 was limited by the spectrophotometric assay used and the high absorption of the substrates at the desired concentrations. The Michaelis-Menten curve for Uri entered the saturation phase at a substrate concentration of approximately 0.9 mM and for the substrate Ino at approximately 0.7 mM (Figure 21); this corresponds to an absorbance of 2.2 and 1.5, respectively at the beginning of the assay run. The equation of the Beer's law implies that the absorption of a sample will increase linearly with the concentration. However, this linear relationship is true only over a limited range of absorption values but readings greater than 1.0 do not reflect the accurate concentration of the analyte and vice versa. Thus, a minor deviation from the Beer's law is expected for the kinetic analysis using Ino and Uri leading to a slight underestimation of the V_{max} and K_m. A strong deviation from Beer's law is expected for kinetic analysis using Ado as substrate since it is very high absorbing at the required wavelength. Even low Ado concentrations of approximately 164 µM led to an absorption of >1.0 whereas not until 350 µM Uri and 450 µM Ino this absorption value was reached. It is not recommended to obtain kinetic values for Ado with the spectrophotometric assay. Alternatively, an HPLC assay is suggested (Parkin *et al.,* 1991).

Recently it has been demonstrated that the genome of the moss *Physcomitrella patens* contains 3 sequences with 26% amino acid identity to an IU-NH sequence from *Crithidia fasciculata* (Turcinov and Schwartzenberg, unpublished). ADN1 and ADN2 share high amino acid similarity of 46 to 60% with these moss genes. Experiments to determine substrate specificity revealed that one of the moss proteins acts on purine and pyrimidine nucleosides, which is similar to the substrate profile of the ADN2 homolog from *A. thaliana.* The moss enzyme also utilizes cytokinin ribosides and a function in cytokinin homeostasis is proposed (Turcinov and Schwartzenberg, unpublished). The moss protein and ADN2 share 51 % amino acid identity and a similar substrate spectrum; the activity of ADN2 on cytokinin appears likely and should be investigated. Recombinant protein produced

from the other two moss coding sequences did not show activity on tested substrates (Turcinov and Schwartzenberg, unpublished); this fact is interesting since ADN1 did not show activity either. The function of these plant proteins with unknown substrates is yet to be revealed.

4.6 "NATIVE" ADN2 PROTEIN ACTS ON URIDINE

Affinity tagged versions of ADN1 and 2 were purified from Arabidopsis for multiple purposes; I was able to accomplish the investigation of differences in the substrate spectrum of the protein synthesized *in planta* in comparison to the recombinant version only. It was thought that some type of post-translational modification might lead to an active ADN1. Phosphorylation sites are predicted for ADN1 and ADN2 based on NetPhos 2.0 software but ADN1 and ADN2 peptides identified by mass spectrometry did not contain any modifications (AtProteome database, Baerenfaller *et al.,* 2008). Unfortunately, it was not possible to obtain a sufficient amount of protein for all experiments including a test of the detection limit of "native" ADN1 in western blots or a broad substrate spectrum analysis to reveal a substrate for ADN1.

Both ADNs were tested for their activity on Ado, Ino and Uri. The "native" ADN2 enzyme did not show detectable activity on Ado but utilized Uri and Ino (Figure 22). No ADN activity was detected on any of these substrates in reactions containing the "native" ADN1. Nevertheless, these data must be considered preliminary because it was not possible to do multiple replicates of each assay due to the low protein concentrations.

The yield of StrepII-tag protein was possibly limited by the binding capacity of the StrepTactin resin or the amount of overexpressed ADN protein per g leaf tissue (Table 19). With the current data no conclusive statement is possible but either explanation is possible. The binding capacity of StrepTactin resin is stated as 3 mg/ml by the manufacturer. These values were previously obtained when purifying recombinant protein from *E. coli*. StrepTactin resin also binds and co-purifies

biotinylated proteins along with the StrepII-tag protein. Since the cytosolic biotin level in plants has been estimated to be 3 times higher than in bacteria (Tissot *et al.,* 1997), the yield of target protein might be reduced due to this fact. However, since it was possible to purify consistently more ADN2 than ADN1 protein (Table 19) it appears that the protein expression in Arabidopsis is the most likely limiting step rather than the binding capacity of the resin. Nevertheless, both ADN-StrepII proteins were purified to near homogeneity (Figure 20). Lichty and colleagues (2005) examined two proteins and six peptide affinity tags to purify recombinant proteins from *E. coli*, yeast, *Drosophila* and HeLa cell extracts. Tags such as the His tag produced proteins with many contaminants whereas the StrepII tag produced protein almost as pure as epitope-based systems. The purification of both ADN-StrepII proteins demonstrated that this tag is very valuable to extract proteins from Arabidopsis in high purity.

4.7 Both ADNs are Subcellular Localized in the Cytosol

To study the localization of ADN, ADN1 and ADN2 GFP translational fusions were expressed in plants. The transient expression in epidermal cells of tobacco *Nicotiana benthamiana* indicated that ADN resides in the cytosol and nucleus (Figure 25). The 67 kDa fusion proteins are below the diffusion limit of nuclear pores (Pollard *et al.,* 1996) making it possible for these proteins to enter the nucleus by diffusion rather than by an active transport mechanism. To address this issue ADN2 was fused to a double GFP resulting in a 82 kDa fusion protein. Analysis of these lines showed that ADN2 resides in only the cytosol and entry to the nucleus was due to diffusion.

Immunolocalization studies using affinity-purified antibodies for ADK performed by Schoor (2007) found ADK to be present in the cytosol, nucleus and chloroplast even when fused to an 89 kDa reporter protein. To enter the nucleus an active transport of the fusion protein was presumed. The present results for localization indicate that ADN and ADK share the presence in the cytosol but not in

nucleus or chloroplasts; ADK is localized in these additional compartments. Thus ADK and ADN do not contribute to adenosine recycling activities in all the same compartments. Since the purine and pyrimidine salvage is located in the cytosolic compartment of the cell (Zrenner *et al.,* 2006), the localization of ADN in the cytosol is sufficient for this role.

4.8 FUNCTIONALITY OF ADN1 AND ADN2 IN *ARABIDOPSIS THALIANA*

The T-DNA insertion mutants *adn1-1* and *adn2-1* were chosen to investigate the role of ADN 1 and ADN 2 in plant development. The T-DNA insertions in these lines did not lead to a complete knockout of transcription of the mutated genes as demonstrated by RT-PCR analysis, although the decrease in *adn2-1* was substantial (approximately 80 %) (Figure 27). The effect of the T-DNA insertion on protein expression was investigated using a polyclonal antibody raised against ADN2. Reduced ADN2 protein in *adn2-1* could be demonstrated but the antibody did not detect ADN1 protein in crude extracts of wild type, *adn1-1* nor *adn2-1*. Thus the synthesis of ADN1 and ADN2 was not eliminated in these plant lines even though insertion in exons or introns is commonly thought to lead to knock out the target gene.

Wang (2008) studied the frequency with which insertions within the protein-coding region knocked out gene expression by reviewing 648 publications, 1084 *Arabidopsis thaliana* insertion mutants representing 755 genes. Wang (2008) revealed that in 14 % of the time insertions within the protein-coding region do not knock out gene expression; differences between the location in an intron or exon are not large with 18 % and 12 %, respectively (Wang, 2008). Since the T-DNA insertion of *adn1-1* is in an intron, a wild-type transcript may be produced in this mutant because the intron can be spliced out together with the inserted T-DNA sequence. This indeed occurs in several insertion mutants i.e. *AGL104* and *ASP2* (reviewed in Wang, 2008). However, the mechanism to explain a partial transcript for *adn1-2*,

where the T-DNA insertion is in an exon, is difficult. It is possible that the T-DNA is processed out, generating a shorter, altered transcript with a very low efficiency or only a small part of the T-DNA was inserted (Wang, 2008). Since the size of the ADN2 transcript and protein correlates with the predicted size it is unlikely that a large truncation occurred but the possibility of a very small T-DNA insertion needs to be investigated.

Although ADN1 and ADN2 transcripts were reduced in single and double mutants when compared with the wild type, all three lines do not exhibit visible phenotypic changes in standard growth conditions. Many mutants have no identifiable phenotype under standard conditions i.e. of the 17 mutants described in Krysan *et al.,* (1996) none displays an altered phenotype unless grown under specific conditions. In order to circumvent this problem, it was proposed that mutants should be tested under a wide range of environmental conditions that would reveal conditional phenotypes (Krysan *et al.,* 1999). The conditions I tested i.e. growth under short-day growth conditions, root growth on ½ MS media supplemented with nucleosides or cytokinins, did not reveal differences therefore genetic crosses to further mutants might be necessary to reveal a conditional phenotype.

The *cym* mutant was included in this research since its phenotypic description and its reported decreased adenosine nucleosidase activity (Auer, 1999) made it an interesting candidate for an ADN mutant. Since the *cym* mutation was mapped to the Arabidopsis chromosome 2 it was proposed to be an *ADN2* mutant. The sequencing of the *ADN2* gene of the *cym* mutant did not lead to the identification of a mutation (Figure 31). Changes in the 5’ or 3’UTRs have yet to be investigated.

The research in this thesis revealed that ADN2 is a purine and pyrimidine nucleoside hydrolase that acts on Ado but prefers Uri as substrate. ADN2 is proposed to be involved in the purine and pyrimidine salvage in Arabidopsis and predominantly in uridine recycling. Therefore, ADN2 might not be the ADN gene this work was aiming to identify. Nevertheless, I am confident that in the genome of Arabidopsis a gene coding for a nucleosidase exists that converts Ado and

cytokinins predominantly. Recently, an *in vivo* feeding experiment in Arabidopsis demonstrated that the conversion of tritium labeled cytokinin riboside into base was higher in an ADK deficient plant compared to wild type (K. von Schwarzenberg and H. Turcinov, personal communication). Crosses of ADK deficient plants and ADN1 and ADN2 knockout mutants could reveal if this nucleosidase activity is due to the activity of one of these loci or a different gene is coding for this activity. Further analysis is also needed to test whether ADN60 (Table 16) is the elusive functional ADN I have been seeking in this research.

Appendix A

The location of the T-DNA insertion in At4g04880 as verified by sequencing

Sequence flanking the *ada1-1* insertion allele

CCNCAGGGCCCGGCNGGGGAAAGGGCATCAGCTGTTGCCCCGTCTCACTGGTGAAAG
AAAAACCACCCCAGTACATTAAAAACGTCCGCAATGTGTTATTAAGTTGTCTAAGCGTCAATTTGT
TTACACCACAAAGACAATGATCTTCACATCACTCTTAAAGCGTCAATTTGAAATCTTCCATGTTCT
TGTAGGAGCACTTTCTTGCCTGCATTACAATATGCCAAAGACAATGATCTTCACATCACTCTTCAC
TGTGGAGAGGTATTAACTCTTGAAAATCCACTTAACCGATTTTCAAATGTTTATGTTTCAGATTGT
CTACTACTTTCTCTATCTTAGTGCTTTGTAGGTTCCCAATCCGAAAGAGATCCAAGCCATGCTTGA
TTTTAAACCGCATCGGATTGGACATGCCTGTTTCTTCAAAGACGAAGATTGGACAAAGTTGAAAT
CTTTCCGGATTCCGGTAATAGATTTGCATGTACCATTATTCTCTGTTTCTTATAATCTCTTTAACCA
ATTTCAAGAGTTTGCTATGTTTTGCAGGTTGAAATATGTTTAACATCCAACATTGTAACCAAATCG
ATATCTTCCATCGATATACACCATTTCGGTTAGATTTTCTCTTTCCGCTGCTTCGTTTTCTACATTC
CTCCTTGTTCATTTAAAATCAAAGCAATCTTGACAAGATCTTAGTCTGATCTTACCAGCTGATCTTT
ACAATGCAAAGCATCCATTGATTCTATGCACTGATGATTTTGGAGTATTCTCCACTAGCCTCTCAC
GAGNTACNCANNNNN

Location of T-DNA insertion in At4g04880

Lower letter: Intron

Upper letter: Exon

🡻: Location of T-DNA insertion in Exon 8

ATGGAATGGATACAATCACTGCCCAAAATCGAGCTTCATGCTCATCTCAACGGTTCCATT
AGAGACTCCACTCTTCTgtaaatcccccaaatttatcttctttcttacgagttttgtttccattaactctatctttcgtatctgcaactttctgca
attgcactgatcaattatgaatttacccaatttgatattttgaactgatgggtttcgtttctttttgatgaatcagAGAGCTTGCTAGGGTTCT
TGGTGAGAAAGGCGTTATAGTGTTTGCTGATGTTGAACATGTCATTCAAAAAAgtaagagtctttaatttttttg
aattcgttgttctgtattttgcttaagttttagtctactctagtgtcgcaagtagtttctaatgtttggtatgtgtgatgatgtttttttttaagATGATCGA
TCTTTGGTTGAAGTCTTCAAGTTGTTTGATTTGATCCATAAGCTCACTACTGATCACAAAACTGTG
ACAAGGATCACAAGAGAAgtaaaaccctaattctaatttccattcattagcttgattttagtaattctatagacttgactgatgatcttatctt
gacagGTTGTGGAAGATTTTGCTTTAGAGAATGTGGTGTATCTTGAGTTACGAACTACTCCAAAGgt
acacacctttggcatatttttttgcaagtggttaagttatatgaatgatggagattgtttgtttgtagAGGAGTGATTCAATAGGTATGA
GTAAACGTTCTTACATGGAAGCTGTAATCCAAGGTCTAAGATCTGTCAGTGAAGTCGATATTGAT
TTTGTTACCGCATCTGATTCTCAAAAACTGCACAATGCTGGTGATGGGATTGGAAGAAAGAAGAT

TTATGTTAGACTTCTTCTTAGTATTGATCGTAGGGAAACAACAGAGTCCGCAATGGAAACTgttagtgt
ttcaaaacaagctaagctactcagaatacttaaaagactaatgcagaaaacatttgatactctccttttttctttaaagGTTAAGCTCGCA
TTGGAAATGAGAGATGTCGGGGTAGTTGGTATCGATCTTTCGGGGAATCCTCTTGTTGGAGAAT
GgtaaactgttcttagttctcctctttatcttttgcttcgctttatgagttggttttgaaatcttccatgttcttgtagGAGCACTTTCTTGCCTGC
ATTACAATATGCCAAAGACAATGATCTTCACATCACTCTTCACTGTGGAGAGgtattaactcttgaaaatcca
cttaaccgattttcaaatgtttatgtttcagattgtctactactttctctatcttagtgctttgtagGTTCCCAATCCGAAAGA↓GATCCA
AGCCATGCTTGATTTTAAACCGCATCGGATTGGACATGCCTGTTTCTTCAAAGACGAAGATTGGA
CAAAGTTGAAATCTTTCCGGATTCCGgtaatagatttgcatgtaccattattctctgtttcttataatctctttaaccaatttcaagagt
ttgctatgttttgcagGTTGAAATATGTTTAACATCCAACATTGTAACCAAATCGATATCTTCCATCGATATA
CACCATTTCGgttagattttctctttccgctgcttcgttttctacattcctccttgttcatttaaaatcaaagcaatcttgacaagatcttagtctgat
cttaacagCTGATCTTTACAATGCAAAGCATCCATTGATTCTATGCACTGATGATTTTGGAGTATTCTC
CACTAGCCTCTCCAACGAGTACGCCCTCGCTGTTCGTTCTCTTGgtgagcttccagaacctgagctcaaatcca
acagttacagagcttttctgatttttgagaattgtgattaagtttagattcacaaagaaactacatttccaaataatctaattttgtttcttctgtgaagG
TCTTAGTAAAAGTGAAACCTTTGCATTGGCTAGAGCAGCCATAGACGCAACATTTGCAGAAGATG
AAGTTAAGCAACAACTTAGGTTCATTTTTGATTCAGCCTCGCCAGAGCACGTTTAG

Appendix B

List of ADA-related proteins retrieved from NCBI database for the phylogenetic analysis

gi|22328354_ADA_Arabidopsis thaliana	gi|145246602_HP_Aspergillus niger
gi|225444347_HP_Vitis vinifera	gi|168052009_HP_Physcomitrella patens subsp. patens
gi|195640778_ADA_Zea mays	gi|189537427_HP_Danio rerio
gi|115473871_HP_Oryza sativa	gi|8745398_ADA_Lutzomyia longipalpis
gi|125559485_HP_Oryza sativa Indica Group	gi|242765187_ADA_Talaromyces stipitatus ATCC 10500
gi|224142856_HP_Populus trichocarpa	gi|242765191_ADA_Talaromyces stipitatus ATCC 10500
gi|242046828_HP_Sorghum bicolor	gi|189205585_ADA_Pyrenophora tritici-repentis Pt-1C-BFP
gi|223542356_ADA_Ricinus communis	gi|156396691_HP_Nematostella vectensis
gi|212722682_HP_Zea mays	gi|110762275_ADAGF_Apis mellifera
gi|125601393_HP_Oryza sativa Japonica Group	gi_ADA_Aspergillus fumigatus Af293
gi|76253699_ADAL_Danio rerio	gi|212532149_ADA_Penicillium marneffei ATCC 18224
gi|194034856_ADAL_Sus scrofa	gi|209733054_ADA_Salmo salar
gi|156230101_ADAL_Danio rerio	gi|6680636_ADA_Mus musculus
gi|110626056_ADAL_Mus musculus	gi|1518868_ADA_Mus musculus
gi|74000326_HP_Canis familiaris	gi|170057282_ADA_Culex quinquefasciatus
gi|146286026_ADAL_HUMAN	gi|148229278_ADAGF_Xenopus laevis
gi|184186693_ADAL_Rhinolophus ferrumequinum	gi|121701335_ADA_Aspergillus clavatus NRRL 1
gi|194206726_ADAL_Equus caballus	gi|59894171_CECR1_Gallus gallus
gi|163781038_ADAL_Papio anubis	gi|197097916_CECR1_Pongo abelii
gi|229366052_ADAL_Anoplopoma fimbria	gi|59894169_CECR1_Xenopus laevis
gi|115497612_ADAL_Bos taurus	gi|7650202_CECR1_Homo sapiens
gi|126281885_ADAL_Monodelphis domestica	gi|156537065_ADA_Nasonia vitripennis
gi|225707674_ADA_Osmerus mordax	gi|91078362_ADA_Tribolium castaneum
gi|24645260_ADA_Drosophila melanogaster	gi|29029550_CECR1_Homo sapiens
gi|158292670_HP_Anopheles gambiae str. PEST	gi|71059839_ADA_Mus musculus
gi|219497951_HP_Branchiostoma floridae	gi|30704990_CECR1_Homo sapiens
gi|156717926_HP_Xenopus (Silurana) tropicalis	gi|114685023_CECR1_Pan troglodytes
gi|109091964_ADA_Macaca mulatta	gi|121698885_ADA_Aspergillus clavatus NRRL 1
gi|224062359_ADAL_Taeniopygia guttata	gi|112497629_ADAL_Phlebotomus duboscqi
gi|27806933_ADA_Bos taurus	gi|68358568_CECR1_Danio rerio
gi|148878089_ADA_Bos taurus	gi|212528902_ADA_Penicillium marneffei ATCC 18224
gi|58332372_ADA_Xenopus (Silurana) tropicalis	gi|148223271_ADAGF_Xenopus laevis

gi|57529377_ADA_Gallus gallus	gi|73992040_ADA_Canis familiaris
gi|114682264_ADA_Pan troglodytes	gi|55962504_CECR1_Danio rerio
gi|47078295_ADA_Homo sapiens	gi|19111863_ADA2_Schizosaccharomyces pombe
gi|224078024_ADA_Taeniopygia guttata	gi|149239973_ADA_Lodderomyces elongisporus NRRL
gi|238844595_ADA_Microsporum canis CBS 113480	gi|241951764_ADA_Candida dubliniensis CD36
gi|240272916_ADA_Ajellomyces capsulatus H143	gi|242774814_ADA_Talaromyces stipitatus ATCC 10500
gi|157110346_ADA_Aedes aegypti	gi|115644403_ADA_Strongylocentrotus purpuratus
gi|239610012_ADA_Ajellomyces dermatitidis ER-3	gi|238883594_ADA_Candida albicans WO-1
gi|1402634_ADAGF_Sarcophaga peregrina	gi|146419867_HP_Pichia guilliermondii ATCC 6260
gi|239594865_ADA_Ajellomyces dermatitidis SLH14081	gi|68482418_ADA_Candida albicans SC5314
gi|157120960_ADA_Aedes aegypti	gi|198429719_ADAL_Ciona intestinalis
gi|17737615_ADAGF_Drosophila melanogaster	gi|68482539_ADA_Candida albicans SC5314
gi|119480769_ADA_Neosartorya fischeri NRRL 181	gi|240135345_ADA_Candida tropicalis MYA-3404
gi|18426812_ADA_Rattus norvegicus	gi|149639307_ADAL_Ornithorhynchus anatinus
gi|195334425_HP_Drosophila sechellia	gi|45550748_ADAGF_Drosophila melanogaster
gi|194224452_ADA_Equus caballus	gi|126135216_ADA_Pichia stipitis CBS 6054
gi|238493619_ADA_Aspergillus flavus NRRL3357	gi|157110767_ADA_Aedes aegypti
gi|71001136_ADA_Aspergillus fumigatus Af293	gi|221131927_ADAL_Hydra magnipapillata
gi|226693318_ADAL_Homo sapiens	gi|224147241_HP_Populus trichocarpa
gi|17646180_ADAGF_Drosophila melanogaster	gi|224010419_ADA_Thalassiosira pseudonana CCMP1335
gi|19922262_ADAGF_Drosophila melanogaster	gi|18568326_ADA_Aedes aegypti
gi|24666073_ADAGF_Drosophila melanogaster	gi|67479401_ADA_Entamoeba histolytica HM-1:IMSS
gi|73992038_ADA_Canis familiaris	gi|66807095_ADA_Dictyostelium discoideum AX
gi|195376039_HP_Drosophila virilis	gi|224158489_HP_Populus trichocarpa
gi|81167689_ADA_DANRE	gi|156537067_ADAGF_Nasonia vitripennis
gi|50540360_ADA_Danio rerio	gi|118386223_ADA_Tetrahymena thermophila
gi|156553202_ADAL_Nasonia vitripennis	gi|157110765_ADA_Aedes aegypti
gi|110751253_ADA_ Apis mellifera	gi|145046487_ADA_Dekkera bruxellensis
gi|123466985_ADA_Trichomonas vaginalis G3	gi|24646671_ADAGF_Drosophila melanogaster
gi|225557937_ADA_Ajellomyces capsulatus G186AR	gi|238660044_ADA_Schistosoma mansoni
gi|123488240_ADA_Trichomonas vaginalis G3	gi|56417438_ADA_Aedes albopictus
gi|40882142 _ADA_Neurospora crassa	gi|6324188_ADA_Saccharomyces cerevisiae
gi|112497029_ADAL_Phlebotomus duboscqi	gi|170051337_ADA_Culex quinquefasciatus
gi|225678411_HP_Paracoccidioides brasiliensis Pb03	gi|119472974_CECR1_Neosartorya fischeri NRRL 181

Appendix C

SDS-PAGE analysis of *E. coli* lysates carrying the ADA complementation constructs

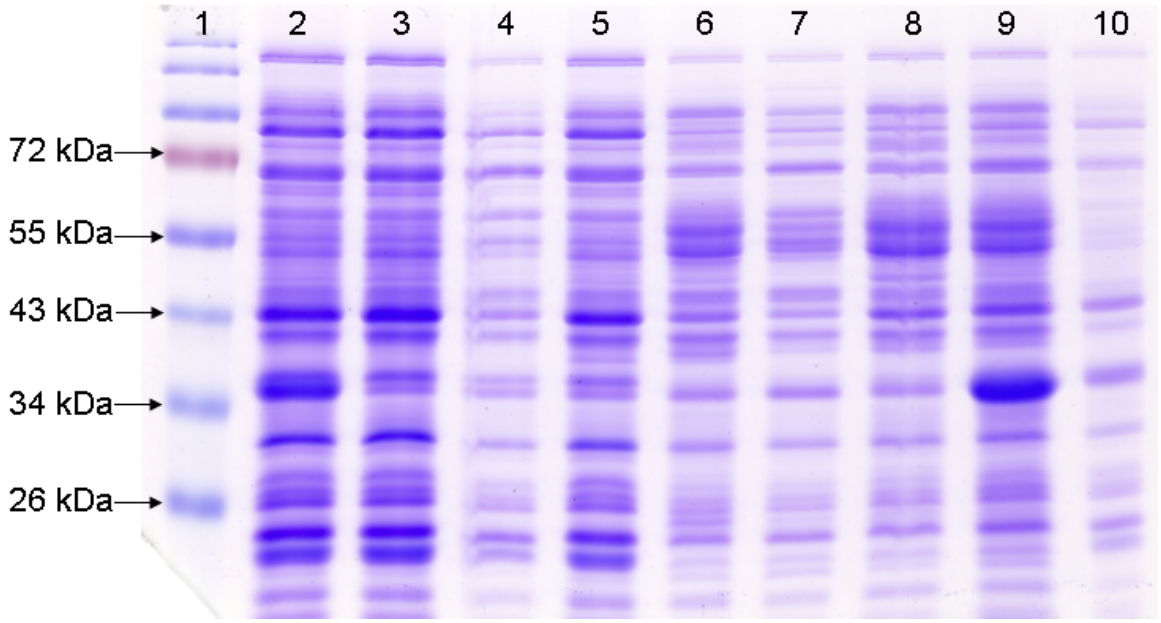

SDS-PAGE of SØ3834 (lane 6 to 9) and BL21-CodonPlus(DE3)-RIPL (lane 1 to 5, lane 10) lysates grown without IPTG (lane 3 and 8) or 100 µM IPTG (lane 2, 4 to 7, 9 and 10) harboring the ADA complementation constructs as follows: lane 2, 3, 8 to 10: pK12ADA; lane 5, 6: pAtADA; lane 4: pMBP. For SØ3834 lysates 25 µl were loaded onto the SDS-gel and 20 µl for BL21-CodonPlus(DE3)-RIPL lysates except in lane 10 only 5 µl was loaded.

Appendix D

Amino acid alignment of ADN70 with a N-terminal section of ADN60 and of ADN90 with a C-terminal section of ADN60

Amino acid sequence alignment of ADN70 with the N-terminal section of ADN60 from *Arabidopsis thaliana*. Identical amino acids are highlighted in a dark grey color and marked with a star symbol (*).

Amino acid sequence alignment of ADN90 with the C-terminal section of ADN60 from *Arabidopsis thaliana*. Identical amino acids are highlighted in a dark grey color and marked with a star symbol (*).

Appendix E

Multiple amino acid alignment of ADN candidate genes from *Arabidopsis thaliana*

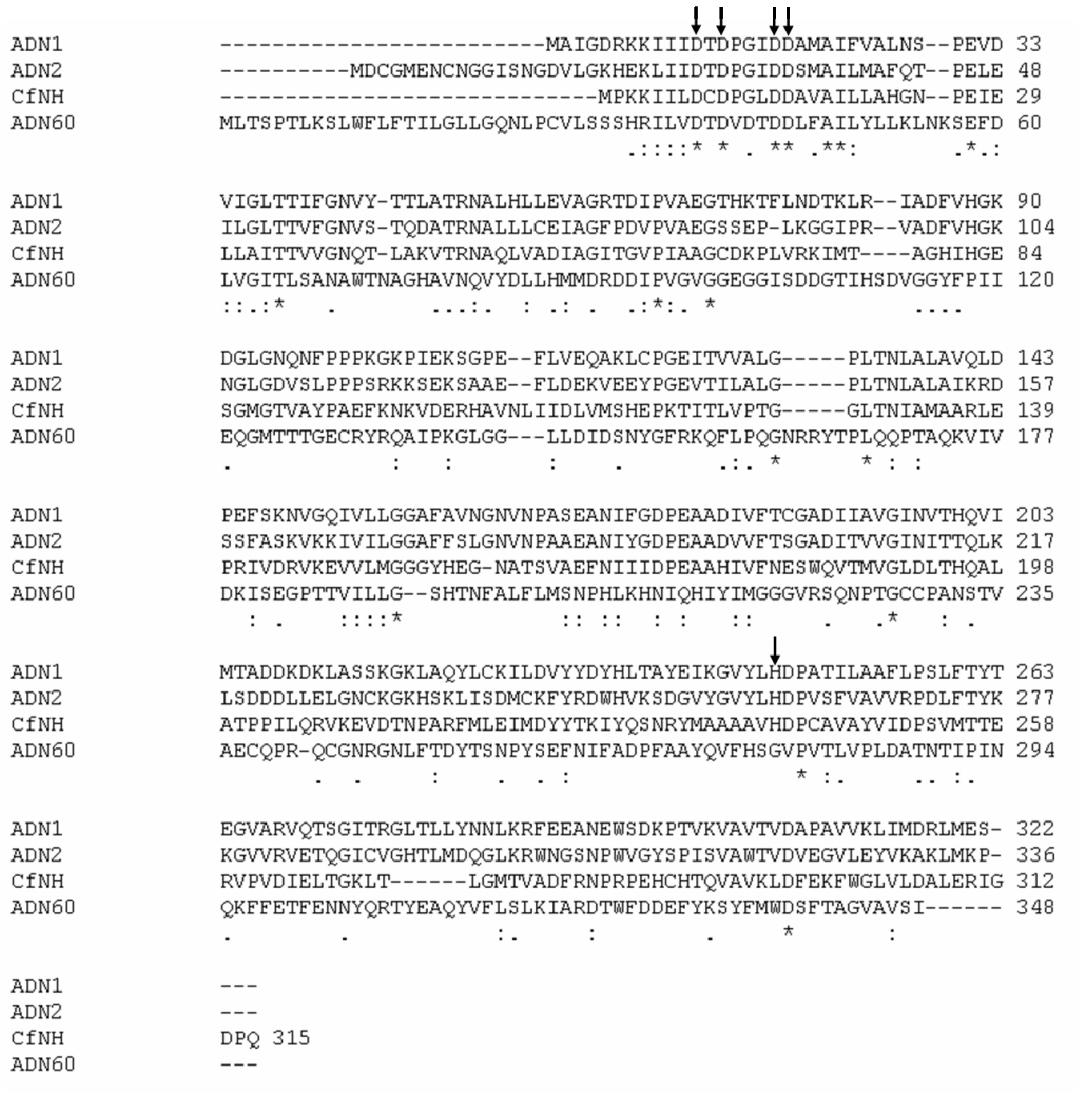

Multiple alignment of the amino acid sequence of candidate adenosine nucleoside hydrolases (ADNs) from *Arabidopsis thaliana* and inosine-uridine nucleoside hydrolase from *Chrithidia fasciculata* (CfNH). The arrows mark conserved amino acids of the aspartic motif (DXDXXXDD, the hallmark of nucleoside hydrolases and a conserved histidine residue, important for the protonation of the leaving nucleobase (Versees and Steyaert, 2003).

Appendix F

The location of the T-DNA insert in the At1g05620 and At2g36310 gene as verified by sequencing

Sequence flanking the *adn1-1* insertion allele

NNNNNNNNNNNNNNCNTNGNNNTGGANTCCNCGTTCTTTATAGTGGANTCTTGTTCCAA
ACTGGANCNNCNCTCAACCCTATCTCGGGCTATTCTTTTGATTTATAAGGGATTTTGCCGATTTC
GGAACCACCATCAAACAGGATTTTCGCCTGCTGGGGCAAACCAGCGTGGACCGCTTGCTGCAA
CTCTCTCAGGGCCAGGCGGTGAAGGGCAATCAGCTGTTGCCCGTCTCACTGGTGAAAAGAAAA
ACCACCCCAGTACATTAAAAACGTCCGCAATGTGTTATTAAGTTGTCTAAGCGTCAATTTGTTTAC
ACCACAATATATTGACGCTTAATTTGTGTTATTAAGTAATGAAAACCTCGAGCCATAAAGGCAACA
ATCAGGATCATCACGGTTCTGTTGACAGCATTTGTATATTTTCAATATAAAACATCAAATAAGGAA
AAAAGATTATCCAAGATAACCTGTCATAATAACTTGATGGGTCACATTGATTCCCACAGCAATTAT
ATCGGCCCCACATGTGAACACAATATCTGCAGCTTCGGGATCGCCAAAAATCTACCCTAACCAAA
AAATTGGTTAAACAGATGTGAAAACTAAAAGAAGAGTTTTTGATAGAAAGTGATGTGTTATGTGTA
TGAATATCACATTACTTTTA

Location of the *adn1-1* T-DNA insertion in At1g05620

Lower letter: Intron

Upper letter: Exon

🡻: location of T-DNA insertion in Intron 6

ATGGCGATAGGAGACCGCAAGAAGATTATCATCGATACTGATCCTGGAATCGgtatatacttat
ctccttttcattggattcgatttggatctctgtttctctactgtcattgcccaatatctttgaatcttctcggatttagaaaattttgggttttactggattctctc
cacttagtggaactacttggttttactgaatcttggtttacgaaaactctgggaaattagagatctgagttttttttttaagcgtttgactttacttaagaga
gctatcatgagtttattctcactggatttgatgatgttgtagATGATGCAATGGCGATATTCGTAGCTTTAAATTCACCTG
AAGTTGATGTCATTGGCCTCACTACTATCTTTGGAAACGTGTATACCACTCTCGCCACTCGAAAC
GCCTTGCATTTGgtaccatttctacaccatttttctcatatggatctcattacgaaaatgaagtcaataacatttcttggttgatctaatcatca
ttgttctatatgcatatctactagTTGGAGGTTGCGGGTAGGACCGATATTCCGGTGGCTGAAGGAACACATA
AAACCTTCTTGgtatgtttccactttatggcctttgatatgtttttgtgagaaagatggatgctatgtaatgtgtttgagattcaatatatgttttcta
gatctttagtaagaataataattcacacaaatgtgtttagttccaatctgtgttataaatcaaatggtaagttatattgtgtctttttcacatgtcatacca
cttagatttttttagcattgataacttgttgtctttttcttctctaaagAACGATACGAAGCTTCGAATAGCTGACTTTGTTCATG
GAAAAGATGGGCTTGGCAACCAAAACTTCCCTCCACCTAAAGGAAAACCAATTGAAAAGTCTGG
ACCTGAGTTTTTAGTTGAACAAGCAAAGCTTTGCCCTGGTGAAATCACGGTTGTTGCTTTGGGAC

CACTAACAAATCTCGCGTTGgtaagactttctcatccgcaatttttatattccggttcttacttatctctgttcctatcatcttatcggagatt
tcattaccttgataatgcagGCTGTTCAGCTTGATCCAGAGTTTTCGAAAAATGTCGGACAAATTGTTCTTC
TTGGTGGAGCATTTGCAGTAAACGGAAATGTAAATCCAGCTTCGGAAGCTAATgtaagttccttcacccgtt
aaagtaatgtgatattcatacacataacacatcactttctatcaaaaactcttcttttagttttcacatctgtttaaccaatttttttggttagggtagATT
TTTGGCGATCCCGAAGCTGCAGATATTGTGTTCACATGTGGGGCCGATATAATTGCTGTGGGAA
TCAATGTGACCCATCAAGTTATTATGACAGgttatcttggataatctttttttccttatttgatgttttatattgaaaatatacaaatgc
tgtcaacagaaccgtgatgatcctgattgttgcctttatggctcgaggttttcattactt⬇gttgcgaccaagaacataatttagttaaacagagctt
tctaatggctttttttcccggtgtttctgctggatttagCTGATGACAAGGACAAACTAGCATCATCGAAGGGGAAATTAG
CTCAATATCTCTGTAAAATCCTTGATGTGTACTATGATTATCATCTCACGGCTTACGAAATCAAAG
gtacgataatgataatcatttgtatgtgtgtttatttcatttggtaataagttcagttgtacacaaaattatataacaagaatttccacgactacgtatttttt
atcttaacctcttctttttttgtgtgtgtgtggggcagGTGTGTACCTTCATGATCCTGCGACGATCCTTGCGGCTTTCC
TTCCTTCTCTATTCACTTATACAGAAGGAGTTGCTAGAGTGCAGACAAGTGGTATCACTAGGGGA
CTCACTTTACTGTACAACAATCTTAAGAGgtaagttttttttcatacatacaatacaaacattcaaaatagacagttgtgttatat
ataatagaggatgtaaatgtcatgtgtggtgatggaaaaaaacttgttgttgtgatgtgaaccagGTTTGAGGAAGCGAACGAGT
GGTCAGACAAACCAACGGTAAAAGTGGCAGTGACGGTTGATGCTCCTGCAGTCGTGAAGCTCAT
AATGGATAGGCTTATGGAGTCTTAA

Sequence flanking the *adn2-1* insertion allele

NNNNNNNNNNNNNNNCNTTNNNNNGGNNTCCACGTTCTTTATAGTGGANTCTTGTTCCA
AACTGGNNNNNNNNNNNNNCNTATCTCGGGCTATTCTTTTGATTTANNNNGNANTTTNCCGATTTC
GGAACCACCATCAAACAGGATTTTCGCCTGCTGGGGCAAACCAGCGTGGACCGCTTGCTGCAA
CTCTCTCAGGGCCAGGCGGTGAAGGGCAATCAGCTGTTGCCCGTCTCACTGGTGAAAAGAAAA
ACCACCCCAGTACATTAAAAACGTCCGCAATGTGTTATTAAGTTGTCTAAGCGTCAAGTTGTAGA
AACATTACCAAACACAGTAGTTAATCCTAATATCTCCAGCTCCGGTGTTTGAAACGCCATCAATAT
CGCCATGCTATCATCTAATCATACACTAATGTTAGAACTGATCCTATTGAACAGTCATTTGGAAAA
AAGTCAACACACAAAAAAGAACAATTTCCCCTGAATCTTTCTATTAAGCAAAGCATTGAACTTTAC
AAGTAAATGAGCACACAAAAACAGATTCAAGAGATAACCATCTAAATATTTCTATTCAAATTAAAC
AAAGTTGGAAGCTTTCTGAGGTTAAATCCTACTCTGCCTGAAGATCCATTTACTAAAAGACGTAAT
CNAAACAGGGGAAGAAGAAGCTCACCAANTNNN

Location of the *adn2-1* T-DNA insertion in At2g36310

Lower letter: Intron

Upper letter: Exon

🡻: location of T-DNA insertion in Exon 2

ATGGATTGTGGTATGGAGAATTGTAATGGTGGGATCTCAAACGGTGACGTTTTGGGTAA
GCATGAGAAGCTCATTATCGATACAGACCCAGGAATTGgtgagcttcttcttcccctgttttgattacgtcttttagtaaat
ggatcttcaggcagagtaggatttaacctcagaaagcttccaactttgtttaatttgaatagaaatatttagatggttatctcttgaatctgtttttgtgtg
ctcatttacttgtaaagttcaatgctttgcttaatagaaagattcaggggaaattgttctttttgtgtgttgacttttttccaaatgactgttcaataggatc
agttctaacattagtgtatgattagATGATAGCATGGCGATATTGATGGCGTTTCAAACACCGGAGCTGGAGA
TATTAGGATTAACTACTGTGTTTGGTAATGTTTCTACA🡻CAAGATGCTACTCGCAACGCTTTACT
CTTGgtatgtacagtacaatgcatcagtttactctgtcactacaacttttggaatgcgtctgtgatctctttctctttgttcattttgcaaaagaatagT
GTGAGATTGCTGGCTTCCCTGATGTTCCCGTTGCAGAAGGAAGTTCCGAACCTTTAAAGgtaccatct
ttctctcctctcataaggattgaaactttagtttatgccatgaagatttttcagatctttgctatgagacaaaaagccaaaccgttgtgactttagcttg
aattctggctttggtgtgttgattcagGGTGGAATTCCGCGTGTTGCTGATTTTGTGCATGGTAAAAACGGACTA
GGAGATGTCTCTCTTCCTCCTCCGAGTAGAAAGAAATCTGAGAAAAGTGCAGCTGAGTTTCTAGA
TGAGAAGGTCGAAGAATATCCGGGTGAAGTCACCATTCTCGCCCTCGGACCTCTAACCAACCTG
GCATTAgtaagaatcatgaatcccctcctttaatcttcttaaaatccgatttgtgtactgacgatgaccgggttttttcgttatagGCCATCAA
ACGCGATAGTTCATTTGCGAGCAAGGTGAAGAAAATTGTTATTCTTGGTGGAGCTTTCTTTTCTTT
GGGAAATGTCAATCCTGCAGCTGAGGCTAATgtaacccctccttgtaacctcatcttaatcttctgttaatgaaaaaggaaa
tgctggtttcattttgttggtctctgttctatatgcagATATATGGTGACCCGGAAGCAGCTGATGTTGTTTTCACATCT
GGAGCGGATATCACTGTTGTCGGTATAAACATCACAACCCAACTTAAACTATCAGgtgaagaagcttctc

ccctcatctcctttagcattctggatatcacaatatagcctgctaaaagaatgtgtctgtttttgatctatttcagATGATGACCTCTTGGA
GCTTGGTAACTGCAAGGGGAAACACTCTAAATTGATAAGCGATATGTGCAAATTTTATAGAGATT
GGCACGTCAAATCTGATGGTGTTTACGgtaagcaagaatctgtgatcaatcaaacatgcttagaaattgcagttttgattctca
agagtttgttgttactggtttcagGAGTGTACCTCCATGACCCAGTCAGCTTTGTGGCTGTAGTACGGCCTGA
TTTATTCACATATAAGAAAGGCGTTGTTCGGGTGGAGACTCAAGGGATATGTGTTGGCCACACG
CTCATGGATCAAGGCCTCAAGAGgtttataacttgtttttcaccaaaaaataacactctttgaatctttagacctttcactaagtaatg
gtttggttcggattgtagATGGAACGGAAGCAATCCGTGGGTGGGATATTCACCGATATCAGTTGCTTGGA
CGGTTGACGTAGAAGGAGTTTTGGAATATGTCAAAGCAAAGCTGATGAAGCCATAA

BIBLIOGRAPHY

Alberts, B., Bray, D., Hopkin, K., Johnson, A., Lewis, J., Raff, M., Roberts, K., Walter, P. 2005. Lehrbuch der molekularen zellbiologie. 3. Auflage ed. Wiley-VCH, .

Alonso, J. M., Stepanova, A. N., Leisse, T. J., Kim, C. J., Chen, H., Shinn, P., Stevenson, D. K., Zimmerman, J., Barajas, P., Cheuk, R., Gadrinab, C., Heller, C., Jeske, A., Koesema, E., Meyers, C. C., Parker, H., Prednis, L., Ansari, Y., Choy, N., Deen, H., Geralt, M., Hazari, N., Hom, E., Karnes, M., Mulholland, C., Ndubaku, R., Schmidt, I., Guzman, P., Aguilar-Henonin, L., Schmid, M., Weigel, D., Carter, D. E., Marchand, T., Risseeuw, E., Brogden, D., Zeko, A., Crosby, W. L., Berry, C. C., Ecker, J. R. 2003. Genome-wide insertional mutagenesis of *Arabidopsis thaliana*. Science **301**(5633): 653-657.

Altschul, S. F., Gish, W., Miller, W., Myers, E. W., Lipman, D. J. 1990. Basic local alignment search tool. J. Mol. Biol. **215**(3): 403-410.

Arabidopsis Genome Initiative. 2000. Analysis of the genome sequence of the flowering plant *Arabidopsis thaliana*. Nature **408**(6814): 796-815.

Arredondo-Vega, F. X., Santisteban, I., Daniels, S., Toutain, S., Hershfield, M. S. 1998. Adenosine deaminase deficiency: Genotype-phenotype correlations based on expressed activity of 29 mutant alleles. The American Journal of Human Genetics **63**(4): 1049-1059.

Auer C. A. 1999. The Arabidopsis mutation *cym* changes cytokinin metabolism, adenosine nucleosidase activity and plant phenotype. Biol Plant 42:S3

Auer, C. A. 2002. Discoveries and dilemmas concerning cytokinin metabolism. J. Plant Growth Regul. **21**(1): 24-31.

Baerenfaller, K., Grossmann, J., Grobei, M. A., Hull, R., Hirsch-Hoffmann, M., Yalovsky, S., Zimmermann, P., Grossniklaus, U., Gruissem, W., Baginsky, S. 2008. Genome-scale proteomics reveals *Arabidopsis thaliana* gene models and proteome dynamics. Science **320**(5878): 938-941.

Borderies, G., Jamet, E., Lafitte, C., Rossignol, M., Jauneau, A., Boudart, G., Monsarrat, B., Esquerre-Tugaye, M. T., Boudet, A., Pont-Lezica, R. 2003. Proteomics of loosely bound cell wall proteins of *Arabidopsis thaliana* cell suspension cultures: A critical analysis. Electrophoresis **24**(19-20): 3421-3432.

Cantoni, G. L. 1975. Biological methylation: Selected aspects. Annu. Rev. Biochem. **44**(1): 435-451.

Chang, Z. Y., Nygaard, P., Chinault, A. C., Kellems, R. E. 1991. Deduced amino acid sequence of escherichia coli adenosine deaminase reveals evolutionarily conserved amino acid residues: Implications for catalytic function. Biochemistry **30**(8): 2273-2280.

Chen, C. M. and Kristopeit, S. M. 1981. Metabolism of cytokinin: Deribosylation of cytokinin ribonucleoside by adenosine nucleosidase from wheat germ cells. Plant Physiol. **68**(5): 1020-1023.

Chung, S., Frankman, E. L., Tzfira, T. 2005. A versatile vector system for multiple gene expression in plants. Trends Plant Sci. **10**(8): 357-361.

Clough, S. J. and Bent, A. F. 1998. Floral dip: A simplified method for agrobacterium-mediated transformation of *Arabidopsis thaliana.* The Plant Journal **16**(6): 735-743.

Cristalli, G., Costanzi, S., Lambertucci, C., Lupidi, G., Vittori, S., Volpini, R., Camaioni, E. 2001. Adenosine deaminase: Functional implications and different classes of inhibitors. Med. Res. Rev. **21**(2): 105-128.

Dancer, J. E., Hughes, R. G., Lindell, S. D. 1997. Adenosine-5[prime]-phosphate deaminase (A novel herbicide target). Plant Physiol. **114**(1): 119-129.

Daxinger, L., Hunter, B., Sheikh, M., Jauvion, V., Gasciolli, V., Vaucheret, H., Matzke, M., Furner, I. 2008. Unexpected silencing effects from T-DNA tags in arabidopsis. Trends in. Plant. Science **13**(1): 4-6.

de Boer, H. A., Comstock, L. J., Vasser, M. 1983. The tac promoter: A functional hybrid derived from the trp and lac promoters. Proc. Natl. Acad. Sci. U. S. A. **80**(1): 21-25.

Degano, M., Gopaul, D. N., Scapin, G., Schramm, V. L., Sacchettini, J. C. 1996. Three-dimensional structure of the inosine-uridine nucleoside N-ribohydrolase from crithidia fasciculata. Biochemistry **35**(19): 5971-5981.

Edwards, K., Johnstone, C., Thompson, C. 1991. A simple and rapid method for the preparation of plant genomic DNA for PCR analysis. Nucleic Acids Res. **19**(6): 1349.

Engel, K. 2006. Functional Analysis of Adenosine Kinase and Adenosine Deaminase in *Arabidopsis thaliana*. Diploma thesis, unpublished data, University of Applied Sciences Berlin, Berlin, Germany.

Fischer, A. 2000. Severe combined immunodeficiencies (SCID). Clinical & Experimental Immunology **122**(2): 143-149.

Frick, L., Mac Neela, J. P., Wolfenden, R. 1987. Transition state stabilization by deaminases: Rates of nonenzymatic hydrolysis of adenosine and cytidine, Bioorganic Chemistry, **15 (**2): 100-108, ISSN 0045-2068, DOI: 10.1016/0045-2068(87)90011-3.

Fry, S. 2005. Unravelling the identity of locus At4g04880 in *Arabidopsis thaliana*. 499 report, unpublished data, University of Waterloo, Ontario, Canada.

Gamborg, O. L., Miller, R. A., Ojima, K. 1968. Nutrient requirements of suspension cultures of soybean root cells. Exp. Cell Res. **50**(1): 151-158.

Gopaul, D. N., Meyer, S. L., Degano, M., Sacchettini, J. C., Schramm, V. L. 1996. Inosine-uridine nucleoside hydrolase from crithidia fasciculata. genetic characterization, crystallization, and identification of histidine 241 as a catalytic site residue. Biochemistry **35**(19): 5963-5970.

Guranowski, A. and Schneider, Z. 1977. Purification and characterization of adenosine nucleosidase from barley leaves. BBA - Enzymology **482**(1): 145-158.

Haan, C. and Behrmann, I. 2007. A cost effective non-commercial ECL-solution for western blot detections yielding strong signals and low background. J. Immunol. Methods **318**(1-2): 11-19.

Hanahan, D. 1985. DNA Cloning, Volume 1, D. Glover, ed., IRL Press, Ltd., London, 109

Hansen, M. R. and Dandanell, G. 2005. Purification and characterization of RihC, a xanthosine-inosine-uridine-adenosine-preferring hydrolase from salmonella enterica serovar typhimurium. Biochim. Biophys. Acta **1723**(1-3): 55-62.

Hirose, N., Takei, K., Kuroha, T., Kamada-Nobusada, T., Hayashi, H., Sakakibara, H. 2008. Regulation of cytokinin biosynthesis, compartmentalization and translocation. J. Exp. Bot. **59**(1): 75-83.

Hove-Jensen, B. and Nygaard, P. 1989. Role of guanosine kinase in the utilization of guanosine for nucleotide synthesis in escherichia coli. J. Gen. Microbiol. **135**(5): 1263-1273.

Islam, M. R., Kim, H., Kang, S. W., Kim, J. S., Jeong, Y. M., Hwang, H. J., Lee, S. Y., Woo, J. C., Kim, S. G. 2007. Functional characterization of a gene encoding a dual domain for uridine kinase and uracil phosphoribosyltransferase in *Arabidopsis thaliana*. Plant Mol. Biol. **63**(4): 465-477.

Jung, B., Florchinger, M., Kunz, H. H., Traub, M., Wartenberg, R., Jeblick, W., Neuhaus, H. E., Mohlmann, T. 2009. Uridine-ribohydrolase is a key regulator in the uridine degradation pathway of arabidopsis. Plant Cell **21**(3): 876-891.

Kaplan, N. 1955 Specific Adenosine Deaminase from Intestine, Methods in Enzymology Vol. **2**: 473-80.

Katahira, R. and Ashihara, H. 2006. Role of adenosine salvage in wound-induced adenylate biosynthesis in potato tuber slices. PLANT PHYSIOLOGY AND BIOCHEMISTRY **44**(10): 551-555.

Kurakawa, T., Ueda, N., Maekawa, M., Kobayashi, K., Kojima, M., Nagato, Y., Sakakibara, H., Kyozuka, J. 2007. Direct control of shoot meristem activity by a cytokinin-activating enzyme. Nature **445**(7128): 652-655.

Kwon, H. K., Yokoyama, R., Nishitani, K. 2005. A proteomic approach to apoplastic proteins involved in cell wall regeneration in protoplasts of arabidopsis suspension-cultured cells. Plant Cell Physiol. **46**(6): 843-857.

Liang, L., He, X., Liu, G., Tan, H. 2008. The role of a purine-specific nucleoside hydrolase in spore germination of bacillus thuringiensis. Microbiology **154**(Pt 5): 1333-1340.

Lichty, J. J., Malecki, J. L., Agnew, H. D., Michelson-Horowitz, D. J., Tan, S. 2005. Comparison of affinity tags for protein purification. Protein Expr. Purif. **41**(1): 98-105.

Maier, S. A., Galellis, J. R., McDermid, H. E. 2005. Phylogenetic analysis reveals a novel protein family closely related to adenosine deaminase. J. Mol. Evol. **61**(6): 776-794.

Moffatt B. A. and Ashihara, H. 2002. Purine and pyrimidine nucleotide synthesis and metabolism. In The Arabidopsis Book, CT Somerville and EM Meyerowitz, eds, American Society of Plant Biologists, Rockville, MD, pp DOI: 10.1199/tab.0018

Moffatt, B. A. and Weretilnyk, E. A. 2001. Sustaining S-adenosyl-L-methionine-dependent methyltransferase activity in plant cells. Physiol. Plantarum **113**(4): 435-442.

Moffatt, B. A., McWhinnie, E. A., Agarwal, S. K., Schaff, D. A. 1994. The adenine phosphoribosyltransferase-encoding gene of *Arabidopsis thaliana*. Gene **143**(2): 211-216.

Moffatt, B. A., Wang, L., Allen, M. S., Stevens, Y. Y., Qin, W., Snider, J., Von Schwartzenberg, K. 2000. Adenosine kinase of arabidopsis. kinetic properties and gene expression. Plant Physiol. **124**(4): 1775-1785.

Moffatt, B. A., Stevens, Y. Y., Allen, M. S., Snider, J. D., Pereira, L. A., Todorova, M. I., Summers, P. S., Weretilnyk, E. A., Martin-McCaffrey, L., Wagner, C. 2002. Adenosine kinase deficiency is associated with developmental abnormalities and reduced transmethylation. Plant Physiol. **128**(3): 812-821.

Moore, R. C. and Purugganan, M. D. 2005. The evolutionary dynamics of plant duplicate genes. Curr. Opin. Plant Biol. **8**(2): 122-128.

Murashige, T. and Skoog, F. 1962. A revised medium for rapid growth and bioassays with tobacco tissue cultures. Physiol. Plant. **15**: 473-497.

Nakamura, Y., Itoh, T., Martin, W. 2007. Rate and polarity of gene fusion and fission in oryza sativa and *Arabidopsis thaliana*. Mol. Biol. Evol. **24**(1): 110-121.

Parkin, D. W. 1996. Purine-specific nucleoside N-ribohydrolase from trypanosoma brucei brucei. PURIFICATION, SPECIFICITY, AND KINETIC MECHANISM. J. Biol. Chem. **271**(36): 21713-21719.

Parkin, D., Horenstein, B., Abdulah, D., Estupinan, B., Schramm, V. 1991. Nucleoside hydrolase from crithidia fasciculata. metabolic role, purification, specificity, and kinetic mechanism. J. Biol. Chem. **266**(31): 20658-20665.

Pereira, L. A. R., Todorova, M., Cai, X., Makaroff, C. A., Emery, R. J. N., Moffatt, B. A. 2007. Methyl recycling activities are co-ordinately regulated during plant development. J. Exp. Bot. **58**(5): 1083-1098.

Petersen, C. and Moller, L. B. 2001. The RihA, RihB, and RihC ribonucleoside hydrolases of escherichia coli. substrate specificity, gene expression, and regulation. J. Biol. Chem. **276**(2): 884-894.

Pevsner, J. 2003. Bioinformatics and functional genomics. 2nd edition. Wiley-Blackwell, Hoboken, New York, 753 p., ISBN:. 0471210048

Pollard, V. W., Michael, W. M., Nakielny, S., Siomi, M. C., Wang, F., Dreyfuss, G. 1996. A novel receptor-mediated nuclear protein import pathway. Cell **86**(6): 985-994.

Pospisilova, H., Sebela, M., Novak, O., Frebort, I. 2008. Hydrolytic cleavage of N6-substituted adenine derivatives by eukaryotic adenine and adenosine deaminases. Biosci. Rep. **28**(6): 335-347.

Poulton, J. E. and Butt, V. S. 1976. Partial purification and properties of adenosine nucleosidase from leaves of spinach beet (*beta vulgaris* L.). Planta **131**(2): 185.

Radhamony, R. N., Mohan Prasad, A., Srinivasan, R. 2005. T-DNA insertional mutagenesis in arabidopsis: A tool for functional genomics. EJB **8**(1): 82-106.

Rosemberg, D. B., Rico, E. P., Senger, M. R., Dias, R. D., Bogo, M. R., Bonan, C. D., Souza, D. O. 2008. Kinetic characterization of adenosine deaminase activity in zebrafish (danio rerio) brain. Comp. Biochem. Physiol. B. Biochem. Mol. Biol. **151**(1): 96-101.

Rosemberg, D. B., Rico, E. P., Guidoti, M. R., Dias, R. D., Souza, D. O., Bonan, C. D., Bogo, M. R. 2007. Adenosine deaminase-related genes: Molecular identification, tissue expression pattern and truncated alternative splice isoform in adult zebrafish (danio rerio). Life Sci. **81**(21-22): 1526-1534.

Saitou, N. and Nei, M. 1987. The neighbor-joining method: A new method for reconstructing phylogenetic trees. Mol. Biol. Evol. **4**(4): 406-425.

Schinzel, A., Schmid, W., Fraccaro, M., Tiepolo, L., Zuffardi, O., Opitz, J. M., Lindsten, J., Zetterqvist, P., Enell, H., Baccichetti, C., Tenconi, R., Pagon, R. A. 1981. The "cat eye syndrome": Dicentric small marker chromosome probably derived from a no.22 (tetrasomy 22pter to q11) associated with a

characteristic phenotype. report of 11 patients and delineation of the clinical picture. Hum. Genet. **57**(2): 148-158.

Schmülling, T. 2004. Cytokinin. In Encyclopedia of Biological Chemistry (Eds. Lennarz, W., Lane, M.D.) Academic Press/Elsevier Science.

Schoor, S. M. 2007. Determining the subcellular localization of adenosine kinase and SAH hydrolase and their roles in adenosine metabolism. Masters Thesis, University of Waterloo, Ontario, Canada.

Tissot, G., Douce, R., Alban, C. 1997. Evidence for multiple forms of biotin holocarboxylase synthetase in pea (pisum sativum) and in *Arabidopsis thaliana*: Subcellular fractionation studies and isolation of a cDNA clone. Biochem. J. **323 (Pt 1)**(Pt 1): 179-188.

Tzfira, T., Tian, G., Lacroix, B., Vyas, S., Li, J., Leitner-Dagan, Y., Krichevsky, A., Taylor, T., Vainstein, A., Citovsky, V. 2005. pSAT vectors: A modular series of plasmids for autofluorescent protein tagging and expression of multiple genes in plants. Plant Molecular Biology **57**(4): 503.

Versees, W., Decanniere, K., Pelle, R., Depoorter, J., Brosens, E., Parkin, D. W., Steyaert, J. 2001. Structure and function of a novel purine specific nucleoside hydrolase from trypanosoma vivax. J. Mol. Biol. **307**(5): 1363-1379.

Versées, W. and Steyaert, J. 2003. Catalysis by nucleoside hydrolases. Current Opinion in Structural Biology, **13**(6): 731-738.

Vogt, C. 1999. Creating Long Documents using Microsoft Word. Published on the Web at the University of Waterloo.

Voinnet, O., Rivas, S., Mestre, P., Baulcombe, D. 2003. An enhanced transient expression system in plants based on suppression of gene silencing by the p19 protein of tomato bushy stunt virus. Plant Journal **33**(5): 949-956.

Von Schwartzenberg, K., Kruse, S., Reski, R., Moffatt, B., Laloue, M. 1998. Cloning and characterization of an adenosine kinase from *Physcomitrella* involved in cytokinin metabolism. Plant Journal **13**(2): 249-257.

Wang, Y. H. 2008. How effective is T-DNA insertional mutagenesis in Arabidopsis? J Biochem Tech **1**(1): 11-20

Waterhouse, A. M., Procter, J. B., Martin, D. M., Clamp, M., Barton, G. J. 2009. Jalview version 2--a multiple sequence alignment editor and analysis workbench. Bioinformatics **25**(9): 1189-1191.

Werner, T., Motyka, V., Laucou, V., Smets, R., Van Onckelen, H., Schmulling, T. 2003. Cytokinin-deficient transgenic arabidopsis plants show multiple developmental alterations indicating opposite functions of cytokinins in the regulation of shoot and root meristem activity. Plant Cell **15**(11): 2532-2550.

Wilson, D. K., Rudolph, F. B., Quiocho, F. A. 1991. Atomic structure of adenosine deaminase complexed with a transition-state analog: Understanding catalysis and immunodeficiency mutations. Science **252**(5010): 1278-1284.

Wilson, D. K. and Quiocho, F. A. 1993. A pre-transition-state mimic of an enzyme: X-ray structure of adenosine deaminase with bound 1-deazaadenosine and zinc-activated water. Biochemistry **32**(7): 1689-1694.

Wolfson, G., Chisholm, J., Tashjian, A.,Jr, Fish, S., Abeles, R. 1986. Neplanocin A. actions on S-adenosylhomocysteine hydrolase and on hormone synthesis by GH4C1 cells. J. Biol. Chem. **261**(10): 4492-4498.

Yabuki, N. and Ashihara, H. 1991. Catabolism of adenine nucleotides in suspension-cultured plant cells. Biochim. Biophys. Acta **1073**(3): 474-480.

Zrenner, R., Stitt, M., Sonnewald, U., Boldt, R. 2006. Pyrimidine and purine biosynthesis and degradation in plants. Annu. Rev. Plant. Biol. **57**: 805-836.

Zurovec, M., Dolezal, T., Gazi, M., Pavlova, E., Bryant, P. J. 2002. Adenosine deaminase-related growth factors stimulate cell proliferation in drosophila by depleting extracellular adenosine. Proc. Natl. Acad. Sci. U. S. A. **99**(7): 4403-4408.